A biomechanics approach to sensorimotor control of insect walking

Chris J. Dallmann

A dissertation submitted in partial fulfillment of the
requirements for the degree of
Doctor rerum naturalium

Department of Biological Cybernetics, Faculty of Biology
Cluster of Excellence Cognitive Interaction Technology (CITEC)
Bielefeld University, Germany

2018

Abstract

Walking is an everyday motor control task that most of us take for granted. Although seemingly trivial, the underlying control comprises a highly complex interplay between the nervous system, the musculoskeletal system and the environment. Due to their accessible nervous and musculoskeletal systems, insects have served as important model systems for studying walking control. However, it has been difficult to understand the specific mechanisms at work during natural locomotion—when the body mechanically interacts with the environment. One reason is that the comparatively small size of insect legs has hampered a detailed understanding of the mechanical output at the leg joints (joint kinematics, joint torques) and its relation to leg muscle activity during natural locomotion. The present thesis is an attempt to tackle this issue by providing the first combination of 3D motion capture, ground reaction force measurements and electromyography in a freely walking insect, the stick insect *Carausius morosus*.

In Chapter 1, I introduce the complexity of walking and our current understanding of how insects control it. I argue that detailed biomechanical analyses of freely walking insects are an important next step, because knowledge of joint kinematics, joint torques and leg muscle activity can help identify behaviorally relevant sensory signals for control and probe specific control mechanisms studied in tethered or reduced preparations. Due to their comparatively large size and well-studied anatomy and physiology, stick insects are an attractive model system for these biomechanical analyses.

In Chapter 2, I combine 3D motion capture and ground reaction force measurements to determine the kinematics and torques of all leg joints during level walking. The results provide new insights into how stick insect leg joints interact to propel and stabilize the body during the stance phase. All legs were retracted and flexed/extended around the thorax-coxa (ThC) and femur-tibia (FTi) joints as expected for propulsion. However, the torques at these joints were often directed opposite to joint movements, indicating that they serve a stabilizing rather than a propulsive function. Unexpectedly,

much of the propulsion resulted from strong torques at the coxa-trochanter (CTr) joint, which pressed the leg down on the ground. The ThC and FTi joints appeared to "steer" these strong torques to control both body height and propulsion. Because this propulsive mechanism is not predicted from kinematics, it had been overlooked in the past. It conceptually resembles propulsive mechanisms in other walking, jumping and flying insects and challenges current control models of insect walking.

In Chapter 3, I combine 3D motion capture, ground reaction force measurements and electromyography to show that the strong torques at the CTr joint can aid in the control of inter-leg coordination. I show that the decrease in torque toward the end of the stance phase—the unloading of the leg—is well suited to reverse the activation of two groups of load sensors (campaniform sensilla) near the CTr joint. Consistent with the known motor effects of these sensors, the unloading of the leg coincided with a switch from stance to swing muscle activity, suggesting that load feedback promoted the stance-to-swing transition. Moreover, a mechanical simulation revealed that the unloading of the leg can be specifically ascribed to the touch-down and load acceptance of the posterior neighboring leg. These findings indicate that legs can be coordinated in a back-to-front sequence during walking based on "mechanical communication" of legs through the ground and feedback from load sensors local to each leg. This decentralized coordination mechanism might be used across insects analogously to mammals, and it could provide a useful complementary control strategy for multi-legged robots.

In Chapter 4, I combine 3D motion capture, ground reaction force measurements and electromyography in hind legs to show how leg muscle activity is adjusted to different mechanical demands during uphill (+45°) and downhill (-45°) walking. Kinematic parameters varied little across walking conditions, although leg forces and joint torques revealed substantial changes in mechanical demand. At the ThC joint, the altered mechanical demand was met by characteristic adjustments in timing and magnitude of antagonistic muscle activity. Adjustments occurred primarily in the first half of stance and with the first step of the leg on the incline. These findings suggest that stick insects do not use distinct, inclination-specific motor programs during walking, but instead adjust leg muscle activity on a step-by-step basis so as to maintain the same kinematic pattern under different mechanical demands. The underlying control might rely primarily on feedback from leg proprioceptors signaling leg position and movement.

Chapter 5 concludes with a general discussion on the significance of the results for walking control, limitations of the biomechanics approach, and possible future directions. Overall, the present thesis demonstrates that detailed biomechanical analyses of freely walking insects are a powerful complementary tool to study sensorimotor control of natural locomotion.

Acknowledgements

There are many people I would like to thank for helping me to complete this thesis. I am particularly grateful to my advisors, Josef Schmitz and Volker Dürr, for providing the freedom to pursue my research interests and for essential guidance and support at every stage of this work. Josef's knowledge and experience were invaluable, from developing the experimental setup to interpreting the results in the context of sensorimotor control. This work benefited greatly from inspiring collaborations with Thierry Hoinville and Sasha Zill, and from many insightful discussions with Holk Cruse, Jan Ache, Leslie Theunissen, Gaetan Lepreux, Arne Gollin, Malte Schilling, Stephan Haupt and Nalin Harischandra. I would like to thank Vijay Korat and Stefan Meyer for assistance in collecting kinematic and force data for Chapter 2, Thierry Hoinville for contributing simulation data to Chapter 3 (Figures 3.5 and 3.7), Yannick Günzel for collecting example data on the transition from level to incline walking for Chapter 4 (Figure 4.5), Leslie Theunissen for providing many of the kinematic analysis scripts, and Alessandro Moscatelli for advice on linear mixed models. I am grateful to Gitta Otte-Eustergerling, Annelie Exter and Florian Paul Schmidt for insect care and technical assistance. I would also like to thank Robert Full, Jean-Michel Mongeau, Kaushik Jayaram and Talia Moore for introducing me to insect biomechanics during my undergraduate studies, and for supporting me ever since. Finally, I would like to thank my family and friends, in particular my wonderful wife Eva. Their unconditional love and support for everything I do were essential to the completion of this thesis.

This work was generously supported by the Cluster of Excellence Cognitive Interaction Technology (CITEC) at Bielefeld University based on funding from the German Research Foundation (DFG).

Contents

List of figures

List of tables

Chapter 1

General introduction

1.1 Walking, a complex motor control task

In a recent science campaign[1], the Natural History Museum of Bielefeld titled "Machines fly to the moon, but they cannot walk through the Teutoburg Forest"—a powerful reminder that engineering a robot that is capable of walking in the real world is a true challenge. Some of the most impressive legged robots, like Honda's *Asimo* or Boston Dynamics' *BigDog* and *Atlas*, are beginning to deliver the long sought animal-like motility. However, the flexibility and efficiency of modern walking robots is still far from that of their biological counterparts (Buschmann et al. 2015; Ijspeert 2014). Why is that? Following Richard Feynman's provocative standard "What I cannot create, I do not understand," I would argue that this reflects our still incomplete understanding of how we and other animals solve this complex motor control task.

At first sight, walking might seem rather trivial. Most of us do it each and every day without having to think about it. During walking, each leg moves in two major phases (Figure 1.1A). During the stance phase, the leg is in ground contact and moves backward to exert a force on the ground, which, according to Newton's laws, moves the body forward. In the subsequent swing phase, the leg moves forward through the air to a position from which to start the next stance phase. Legs typically alternate between stance and swing phases in a rhythmic fashion. This rhythmicity makes walking appear to be a stereotyped behavior that is easy to control. However, it is not as trivial as it

[1] Natural History Museum of Bielefeld (2017). Wert der Vielfalt der Insekten [The value of insect diversity]. www.namu-ev.de.

might appear at first sight. Legs must not only propel the body but also stabilize[2] it above ground against gravity-induced collapse (Figure 1.1A). One complication is that the mechanical demand acting at individual leg joints is not constant but dependent on the phase of the step cycle, the actions of the other leg(s), and the specific walking situation. For example, the mechanical demands during uphill or downhill walking are quite different from those during level walking because the orientation of the body with respect to gravity differs (e.g., Gregor et al. 2006; Lay et al. 2006; Wöhrl et al. 2017; see Chapter 4). As a consequence, the mechanical output at the leg joints must be continuously monitored, adjusted and coordinated within and across legs in a context-dependent manner. Studying how animals solve this complex control task provides important general insights into sensorimotor control for neuroscientists and roboticists alike (Buschmann et al. 2015; Ijspeert 2014).

1.2 Insights from insects

We have a good understanding of many basic mechanisms involved in walking control. This understanding is based on decades of research on various animals, from tiny insects to humans. Although there are obvious differences between insects and humans, ultimately both have to solve the same tasks during walking: propel the body and stabilize it above ground against gravity (Figure 1.1A). Insects are attractive model systems for studying the underlying control, because compared with higher vertebrates, insects have central and peripheral nervous systems with many fewer neurons that are easier to access and the musculoskeletal structure of their leg joints is often simpler. For example, the femur-tibia or "knee" joint of a stick insect leg is controlled by only two muscles, a flexor and an extensor, the latter of which is innervated by only two excitatory motor neurons (reviewed in Bässler 1993). In comparison, the human knee is controlled by more than ten muscles, each of which is innervated by hundreds of motor neurons. This comparison does not imply that insects are particularly simple. But it illustrates that insects offer an opportunity to study motor control mechanisms in detail, for example by linking the activity of individual, identified neurons directly to behavior. Some of these control mechanisms might be unique to insects with no parallels in vertebrates (see Section 1.3.3 for an example). However, the basic components involved in walking control are strikingly similar between insects and vertebrates (Figure 1.1B). Like in vertebrates, walking in insects results from complex interactions between the brain (head ganglia), the lower central nervous system (ventral nerve cord, similar to the spinal cord), the leg

[2]Here, the term "stabilize" refers to all actions that counteract the effects of gravity, including those that control body height and balance.

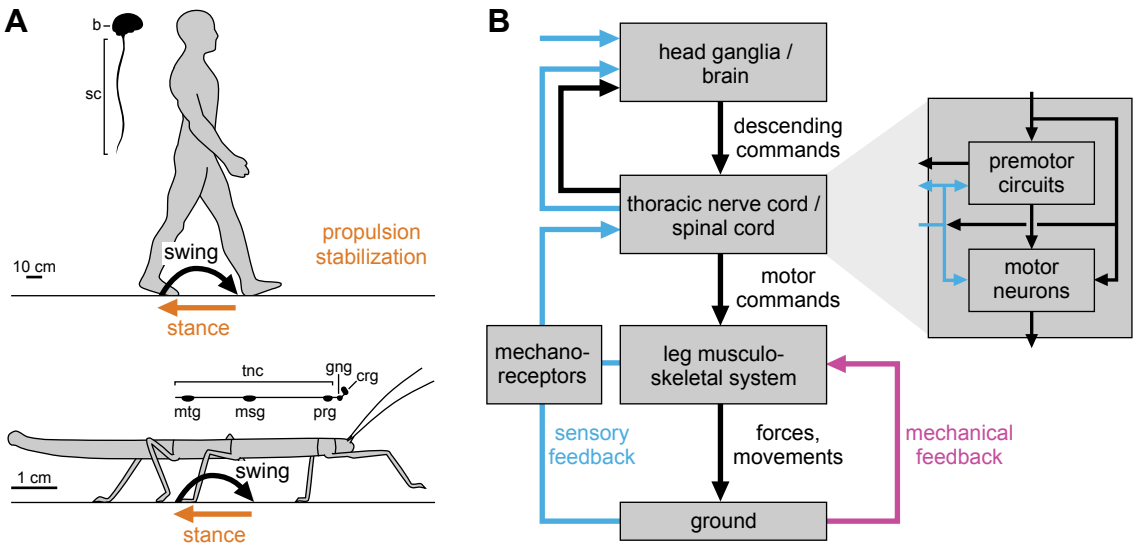

Figure 1.1: Walking control in insects and vertebrates
(**A**) In both humans and stick insects the movement cycle of a leg during walking consists of two major phases: the stance phase, in which the leg is on the ground and exerts forces to propel and stabilize the body, and the swing phase, in which the leg is moved through the air to a position from which to start the next stance phase. Insets show side view schematics of the nervous systems. Top: b, brain; sc, spinal cord. Bottom: crg, cerebral ganglion; gng, gnathal ganglion; tnc, thoracic nerve cord (thoracic part of the ventral nerve cord); prg, prothoracic ganglion; msg, mesothoracic ganglion; mtg, metathoracic ganglion. Abdominal ganglia are not shown. (**B**) Diagram illustrating the basic components involved in walking control in insects and vertebrates. Once internal or external cues trigger the decision to walk, the head ganglia/brain send information about speed and direction to the thoracic part of the ventral nerve cord/spinal cord. There, premotor circuits activate motor neurons, which send motor commands to the leg musculoskeletal system. The latter produces forces and movements and interacts with the ground during stance. Many leg mechanoreceptors provide sensory feedback about the body and its interaction with the ground (blue arrows). The nervous system processes this information and adjusts the descending and motor commands accordingly. In parallel, the viscoelastic properties of the musculoskeletal system can provide mechanical feedback to stabilize fast movements and resist rapid perturbations (magenta arrow). **B** adapted from Dickinson et al. (2000).

musculoskeletal system, and sensory feedback from leg mechanoreceptors. This suggests that the fundamental control strategies discovered in insects will be relevant to control in other animals, including humans (Duysens et al. 2000; Hooper and Büschges 2017; Orlovsky et al. 1999; Pearson 1995; Prochazka 1996; see the leg coordination mechanism described in Chapter 3 for an example).

Much is known about walking control in insects (more on this below). Many insights came from restrained animals or reduced preparations, which permit detailed neurophysiological investigations. However, the specific mechanisms at work during natural locomotion—when the body mechanically interacts with the environment—remain poorly understood. One reason is that little is known about the actual mechanical output at the leg joints (joint kinematics, joint torques) and its relation to leg muscle activity during walking. The present thesis is an attempt to tackle this issue using a biomechanics approach in a freely walking insect, the stick insect *Carausius morosus* (Figure

1.1A). Specifically, I combine 3D motion capture, ground reaction force measurements and electromyography in stick insects walking on level ground (Chapters 2 and 3) and up and down inclines (Chapter 4). The following sections are intended to provide a background for these studies by introducing our current understanding of walking control in insects (Section 1.3), the value of the biomechanics approach taken in this thesis (Section 1.4), and stick insects as model systems (Section 1.5).

1.3 Walking control in insects

Insects like cockroaches and ants often alternate two tripods of support, each of which is composed of the front leg and the hind leg on one side of the body and the middle leg on the opposite side (Full and Tu 1991; Reinhardt and Blickhan 2014; Wahl et al. 2015; Zollikofer 1994). This might evoke the impression that insect walking is a repetition of stereotyped patterns of leg movements. However, already the earliest careful observations have shown that insect walking is in fact remarkably flexible and adaptive (reviewed in Graham 1985). The tripod pattern only falls at one end of a large, speed-dependent continuum of patterns. At intermediate walking speeds, four legs will be in stance at any one time (tetrapod patterns). At low walking speeds, five legs will be in stance (metachronal or wave pattern). Unlike larger vertebrates, which switch between distinct coordination patterns (e.g., horses switching from walk to trot to gallop), insects transition seamlessly from one pattern into another (Dürr et al. 2018; Graham 1985; Hughes 1952; Mendes et al. 2013; Wendler 1964; Wosnitza et al. 2013). The head ganglia, the thoracic nerve cord (thoracic part of the ventral nerve cord), the leg musculoskeletal system and sensory feedback from leg mechanoreceptors all play important roles in walking control (Figure 1.1B).

1.3.1 Descending regulation by head ganglia

The two ganglia in the head, the cerebral (supraesophageal) ganglion and the gnathal (subesophageal) ganglion, are thought to initiate, maintain and terminate normal walking and determine walking direction and speed (Figure 1.1B; for a schematic of the nervous system see Figure 1.1A, inset). These "higher-level" regulatory functions are comparable to those of the vertebrate brain (reviewed in Orlovsky et al. 1999; Pflüger et al. 2017). A brain region that seems to be of particular importance is the central complex in the cerebral ganglion (Strauss 2002). If this brain region is damaged, animals have difficulty walking (Strauss 2002), while stimulation of neurons in this brain region evokes changes in stepping frequency and turning (Bender et al. 2010; Guo and Ritzmann 2013; Martin et al. 2015). These findings are in line with lesion experiments

showing that insects with a disconnected cerebral ganglion can walk for some time, but with little ability to adjust movements (Gal and Libersat 2006; Graham 1979; Ridgel and Ritzmann 2005; Roeder 1937). Some descending neurons mediating such information from the brain to the motor circuits in the thoracic nerve cord have been identified (Bidaye et al. 2014; Böhm and Schildberger 1992; Kien 1990; Staudacher 1998). Overall, several hundred neurons descend from the head ganglia (Hsu and Bhandawat 2016; Kien et al. 1990; Okada et al. 2003; Staudacher 1998). How exactly they direct leg movements is only beginning to be understood. They might recruit interneurons in the thoracic nerve cord that encode motor synergies (Ting et al. 2015) and modulate leg reflex circuits (Martin et al. 2015; Mu and Ritzmann 2008). Compared to the cerebral ganglion, the role of the gnathal ganglion in walking control is less clear. Lesion experiments indicate that it is necessary for normal walking. When the gnathal ganglion is disconnected from the thoracic nerve cord, insects rarely walk at all (Gal and Libersat 2006; Graham 1979; Ridgel and Ritzmann 2005; Roeder 1937). The gnathal ganglion may thus exert a continuous excitatory effect required to maintain walking, although its regulatory functions are likely more complex (Kien and Altman 1984).

1.3.2 Pattern generation in the thoracic nerve cord

In insects, the neural circuits that are responsible for activating the leg muscles are located in the thoracic part of the ventral nerve cord, which is similar to the spinal cord in vertebrates (Figure 1.1). These circuits comprise a complex network of interneurons located in the segmental ganglia close to the legs. For example, the neural circuits controlling the right middle leg are located in the right half of the mesothoracic ganglion (Figure 1.1A, inset). Because these circuits generate motor patterns that activate the motor neurons of the leg muscles, they are collectively referred to as pattern generating or premotor circuits (Figure 1.1B, inset).

Since the seminal work of T. G. Brown in the early twentieth century (Brown 1911; Brown 1914), part of the motor pattern is believed to arise from so-called central pattern generators, interneurons capable of producing rhythmic motor patterns in the absence of phasic or rhythmic input. Circuits capable of producing rhythmic activity have been reported in several invertebrate and vertebrate species (Bidaye et al. 2018; Guertin 2013; Marder and Bucher 2001; Orlovsky et al. 1999). Brown originally proposed that a single, central rhythm-generating module per leg drives pattern generation. A competing concept is that multiple, distributed rhythm-generating modules per leg drive pattern generation in coordination with each other (Grillner 1975; Grillner 1981). Data from stick insects support the idea of multiple modules per leg. After stimulating the isolated thoracic nerve cord pharmacologically, Büschges et al. (1995) observed

alternating activity in the antagonistic motor neuron pools of each leg joint, but only weak coordination across motor neuron pools of different leg joints. This suggests a functional (not necessarily anatomical) pattern generator for each leg joint. However, the anatomical organization of central pattern generators is largely unknown—only few candidate neurons have been identified in insects (Büschges 1995; Pearson and Fourtner 1975). In addition, the relevance of central pattern generators for walking control is still debated. Recall that the mechanical output at the leg joints must be continuously adjusted to the current mechanical demand acting on the body (see Section 1.1). With this consideration in mind, one could argue that a centrally generated rhythm—while possibly appropriate for flight or swimming—is not very helpful for walking. Indeed, it seems clear that motor patterns during walking are strongly shaped by sensory feedback from leg mechanoreceptors acting onto premotor circuits or directly onto motor neurons (Figure 1.1B, inset; reviewed in Büschges and Gruhn 2007; Duysens et al. 2000; Pearson 1995; Prochazka 1996; see Section 1.3.4). It has been argued that the influence of sensory feedback is so strong that it should be viewed as an integral and necessary part of a distributed pattern generating circuit (Prochazka 1996). Along these lines, simulation studies have shown that central oscillators are not necessary to generate insect-like walking (Cruse et al. 1998; Dürr et al. 2004; Dürr et al. 2018; Schilling et al. 2013). That said, processing sensory information and modulating the mechanical output accordingly is associated with inevitable time delays. Therefore, one hypothesis is that motor patterns during very rapid walking are indeed primarily shaped by central pattern generators in a feed-forward manner. In support of this hypothesis, Zill and Moran (1981b) showed that sensory feedback from load receptors is too slow for appropriately coordinating muscle activity on a step-by-step basis in rapidly walking cockroaches (above seven steps per second). Moreover, partial leg amputations disrupt leg use in slow walking but have little effect on the motor pattern during rapid walking (Delcomyn 1991). Thus, sensory feedback might be suppressed or attenuated during rapid walking in favor of centrally generated motor patterns. Importantly for this thesis, stick insects walk comparatively slowly (below two steps per second; see Chapters 2-4), which should provide sufficient time for sensory feedback to shape motor patterns on a step-by-step basis (Büschges and Gruhn 2007; Zill et al. 2004).

1.3.3 Movement generation in the leg musculoskeletal system

Once the motor neurons in the thoracic nerve cord are activated, they send motor commands to the musculoskeletal system of the leg, which translates the motor pattern into movement (Figure 1.1B). However, predicting movement from motor neuron activity or vice versa is complicated. Like in vertebrates, the translation is non-linear and depends

on complex intrinsic muscle properties and behavioral context (reviewed in Hooper and Weaver 2000; Ting and Chiel 2017). In turn, a single muscle may serve multiple functions during locomotion: it may generate joint movement, stabilize joint movement, transmit forces, or act as a spring (Dickinson et al. 2000). Therefore, it might be more appropriate to view the musculoskeletal system as a collaborating partner rather than a mere mediator of motor commands (Chiel and Beer 1997; Chiel et al. 2009).

Two characteristics of the insect leg musculoskeletal system are of particular interest for this thesis. First, unlike vertebrate muscles, which are controlled by several hundred motor neurons, insect muscles are controlled by only few motor neurons (less than 20, often only three; reviewed in Wolf 2014). A typical insect muscle is innervated by one or few excitatory motor neurons, a common inhibitory motor neuron, and a modulatory neuron. Excitatory motor neurons can be grouped into slow motor neurons, which generate gradual contractions, fast motor neurons, where a single action potential causes a powerful twitch, and intermediate motor neurons with intermediate effects. An inhibitory motor neuron often innervates several muscles; it facilitates faster movements by inhibiting slow muscle fibers. For example, its activity may peak at the end of the stance phase to facilitate the transition to the subsequent swing phase (Burns and Usherwood 1979; Graham and Wendler 1981; Wolf 1990). Finally, neuromodulatory neurons can alter a muscle's response to excitation (e.g., octopaminergic DUM neurons; Burrows 1996). The motor neurons innervate the muscle at multiple sites (multiterminal innervation), so several types of motor neurons may innervate a single muscle fiber (polyneuronal innervation). This kind of innervation allows insect muscle to function as flexibly as vertebrate muscle (Belanger 2005; Pflüger and Duch 2011; Wolf 2014). It also has important implications for recording muscle activity. For example, the few innervating motor neurons can often be individually identified in electromyographic recordings (e.g., Burns and Usherwood 1979; Watson and Ritzmann 1998; see also Chapter 3). Moreover, the multiterminal innervation urges caution when recording the activity of large muscles. For example, the proximal and distal parts of the flexor muscle in the locust femur show quite different patterns of activity that can only be recorded when using multiple recording sites (Page et al. 2008).

A second important characteristic of the insect leg musculoskeletal system is its small mass. As a consequence, insect leg movements are dominated by passive, viscoelastic forces—with important implications for neural control (Hooper et al. 2009; Hooper 2012). For example, a stick insect swinging its legs forward cannot rely on inertial forces to complete the movement. Rather, swing muscles need to be continuously activated during the swing phase to overcome passive forces (Hooper et al. 2009; see also Chapter 4). At the same time, the comparatively strong passive forces from muscles

and skeletal structures can help stabilize leg joints (Ache and Matheson 2013; Hooper et al. 2009; Yox et al. 1982; Zakotnik et al. 2006) and resist rapid perturbations (Jindrich and Full 2002; Sponberg and Full 2008). This mechanical feedback (Figure 1.1B) can act more quickly than sensory feedback and seems to be particularly useful during very rapid walking when the step-to-step influence of sensory feedback on motor pattern generation is limited (see Section 1.3.2). The contribution of passive forces is another important aspect to keep in mind when interpreting electromyographic recordings.

1.3.4 Sensory feedback from leg mechanoreceptors

While the musculoskeletal system can contribute to walking control with passive forces, adaptive and efficient walking relies on the modulation of active muscle force through sensory feedback (Figure 1.1B). To this end, insect legs are equipped with many mechanoreceptors that detect forces and movements of the leg and its interactions with the ground (reviewed in Burrows 1996; Büschges and Gruhn 2007; Tuthill and Wilson 2016). Most leg mechanoreceptors have their cell bodies in the leg and send axonal projections to distinct regions of the central nervous system, typically within their segmental ganglion (Schmitz et al. 1991; Tsubouchi et al. 2017). There, mechanosensory signals are integrated by premotor circuits, act directly onto motor neurons, or are relayed to other ganglia including the brain (Figure 1.1B, inset). In this way, local feedback from leg mechanoreceptors can contribute to coordinating movements within and across legs during walking (reviewed in Büschges and Gruhn 2007; Dürr et al. 2004). One important prerequisite is that the effects of a mechanoreceptor are not fixed but modulated depending on the task, for example by afferent input from other mechanoreceptors or descending input from the brain (Martin et al. 2015; Schmitz and Stein 2000; reviewed in Tuthill and Wilson 2016). Among other things, this allows sensory signals that resist leg movements in a quiescent animal to assist leg movements in an actively walking animal ("reflex reversal"; Bässler 1976; reviewed in Bässler and Büschges 1998).

The various types of leg mechanoreceptors can be divided into two functional categories: receptors primarily detecting the position and movement of leg segments and those primarily detecting forces and loads. Like in vertebrates, position/movement signals and force/load signals are thought to adjust motor patterns during stance and swing phases and regulate the timing of stance and swing phase transitions (reviewed in Büschges and Gruhn 2007; Duysens et al. 2000; Pearson 1995; Pearson 2008; Prochazka 1996). For example, in both insects and mammals the leg appears to transition from stance to swing once it is sufficiently extended and unloaded (e.g., Bässler 1977b; Cruse 1985; Duysens and Pearson 1980; Newland and Emptage 1996; Whelan et al. 1995; Zill et al. 2009).

Below, I introduce the position/movement sensors and force/load sensors of insect legs and their potential function during walking in more detail. This is particularly relevant for interpreting the results of Chapters 3 and 4. Note that although not every type of mechanoreceptor needs to be present in every insect, the locations of receptors on the leg and their projections in the central nervous system are overall quite similar across species (Bräunig 1982a; Field and Matheson 1998; Matheson and Field 1995; Pflüger et al. 1981; Zill et al. 2004).

Position and movement sensors

The most visible and abundant of the types of mechanoreceptors are the tactile hairs on the surface of the cuticle. Each hair is composed of a hollow shaft whose base is articulated with the cuticle in a flexible socket, where it is linked to the dendrites of a bipolar sensory neuron (Figure 1.2A). When the shaft is deflected, the dendrites are mechanically distorted, which leads to the opening of mechanotransduction channels and activates the neuron. Solitary tactile hairs cover the entire leg. They detect local contact with external objects and can drive and modulate many different motor behaviors, including avoidance movements (Pflüger 1980). Close to the leg joints, on the other hand, tactile hairs are often clustered into **hair rows** or **hair plates** and function as proprioceptors (Figure 1.2B). These hairs are deflected by flexible membranes linking the leg segments, which roll and fold during movement of the joint. On legs, hair rows and hair plates are located at proximal joints (Pflüger et al. 1981; Wendler 1964). During walking, their sensory signals contribute to controlling the movement ranges of the leg segments (Bässler 1977b; Cruse et al. 1984; Markl 1962; Schmitz 1986b; Theunissen et al. 2014; Wendler 1964; Wong and Pearson 1976). In stick insects, for example, the leg oversteps and collides with the leg in front after ablation of a hair plate on the coxa, indicating that proprioceptive signals from the hair plate limit the forward movement of the leg (Wendler 1964).

Several other types of position and movement sensors are located internally to the cuticle. The best studied among them are the **chordotonal organs**, which are found at nearly every leg joint (Figure 1.2C; reviewed in Field and Matheson 1998). A chordotonal organ is a cluster of several scolopidia—elaborate mechanical transducers that contain one or more bipolar sensory neurons. The scolopidia are attached to one or more strands of connective tissue, which are stretched between the cuticle and an apodeme (tendon) or a part of the next leg segment. When this attachment site moves, the strand is stretched and each stimulated sensory neuron sends a signal to the central nervous system. The encoding properties of the sensory neurons are quite diverse. In the femoral chordotonal organ, for example, sensory neurons may encode vibrations of the tibia

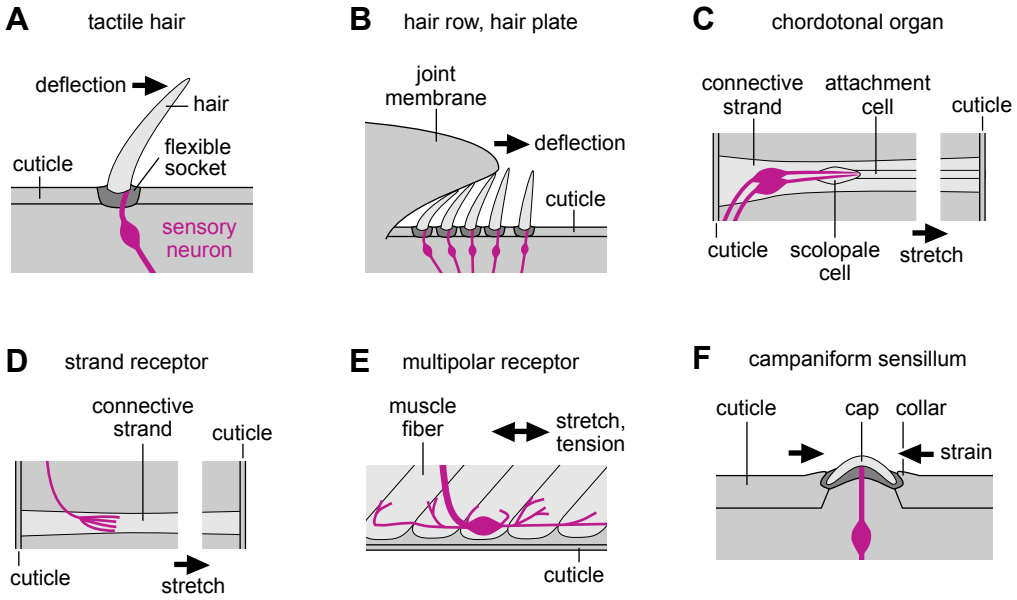

Figure 1.2: Mechanoreceptors of insect legs
(**A**) Single tactile hairs on the surface of the cuticle function as the primary exteroceptive organs by detecting contact with external objects. Each hair is innervated by a sensory neuron, which is activated when the hair shaft is deflected. Adapted from Tuthill and Wilson (2016). (**B**) Close to leg joints, tactile hairs are often arranged in hair rows or hair plates, so that they can be deflected by the joint's membrane during leg movement. Hair rows and hair plates are proprioceptors that signal the movement between two adjacent body segments. Adapted from Tuthill and Wilson (2016). (**C**) Chordotonal organs are complex, stretch-sensitive mechanoreceptors embedded in connective tissue strands. Each organ consists of many scolopidia, elaborate mechanical transducers that are formed by sensory neurons enveloped by a scolopale cell and an attachment cell. Chordotonal organs are proprioceptors that signal the position, movement and vibration of a leg segment. Adapted from Field and Matheson (1998). (**D**) Strand receptors are stretch-sensitive mechanoreceptors embedded in connective tissue strands. Each receptor consists of a single sensory neuron, whose dendrite branches widely in the strand, and whose cell body is located in the central nervous system (not shown) instead of the periphery. Strand receptors likely function as proprioceptive position/movement sensors. (**E**) Multipolar receptors are single sensory neurons that extend complex dendrites into a structure that is linked to a moveable part of the leg. Some multipolar receptors, like the tension receptors, are directly embedded in muscle tissue and are sensitive to active muscle contraction (tension) and passive muscle stretch. Multipolar receptors may function as proprioceptive position/movement sensors. Based on Theophilidis and Burns (1979). (**F**) Campaniform sensilla are embedded in cuticular sockets and function as the primary load sensors. Each sensillum is innervated by a single sensory neuron, which is activated when strain in the cuticle deforms the socket edges (collar) and indents the cuticular cap. Adapted from Sane and McHenry (2009).

(Stein and Sauer 1999) or else its position, velocity, acceleration or a combination of these parameters (Burns 1974; Büschges 1994; Hofmann et al. 1985; Kittmann and Schmitz 1992; Mamiya et al. 2018; Matheson 1992; Zill 1985). Due to this complexity, the exact role of chordotonal organs in walking control has yet to be fully understood. In actively moving animals, chordotonal organs can serve to stabilize joint velocity and are thought to be involved in coordinating transitions between stance and swing phases (reviewed in Bässler and Büschges 1998). Recent studies on freely walking fruit flies, in which chordotonal organs could be ablated genetically, indicate that their feedback

is important for overall walking performance (Mendes et al. 2013) and the ability to compensate for additional load (Mendes et al. 2014) or the loss of a leg (Isakov et al. 2016).

The other types of internal position and movement sensors are less well studied. They are typically single-cell sense organs, such as the **strand receptors**. A strand receptor consists of a sensory neuron innervating a connective tissue strand with widely branching dendrites (Figure 1.2D). In contrast to other types of mechanoreceptors, the cell body of a strand receptor is located in the central nervous system instead of the periphery (Bräunig and Hustert 1980). Strand receptors are found in different leg segments, most notably in the coxa of many insects (Bräunig 1982a; Schöwerling 1992). In addition, there are several types of **multipolar receptors**. A multipolar receptor consists of a sensory neuron that extends complex dendrites into a structure that is linked to a moveable part of the leg (Figure 1.2E). In one type of multipolar receptor, often referred to as stretch receptor, the sensory neuron is associated with the membrane and cuticle of a leg joint and is sensitive to joint position and movement (Bässler 1977a; Coillot and Boistel 1968; Guthrie 1967; Williamson and Burns 1978). In the muscle receptor organ, the sensory neuron is associated with a modified muscle, the receptor muscle (Bräunig 1982b), and signals the muscle's tensions as well as passive muscle stretch by movement of the adjacent leg segment (Bräunig and Hustert 1985a). This is similar in the tension receptor, where the sensory neuron is embedded in muscle tissue and also sensitive to muscle tension and passive muscle stretch (Figure 1.2E; Bässler 1977a; Matheson and Field 1995; Theophilidis and Burns 1979). Finally, in the apodeme receptor, the sensory neuron is associated with an apodeme and signals movement of the adjacent leg segment (Bässler 1977a). By signaling changes in joint position, movement or muscle tension, strand receptors and multipolar receptors can contribute to controlling leg joints (Bräunig and Hustert 1985b). However, to which extent they contribute to control during walking is largely unknown.

Load sensors

The primary load sensors of insects are **campaniform sensilla** (Figure 1.2F; reviewed in Zill et al. 2004). While the position and movement sensors described above can indirectly detect the effects of load, for example when gravitational forces induce joint movements, campaniform sensilla can provide detailed information about the direction, magnitude and rate of loads (Duysens et al. 2000; Zill et al. 2004). Each campaniform sensillum consists of a bipolar sensory neuron whose dendrite inserts into a convex cuticular cap embedded in a small socket in the cuticle (Figure 1.2F). When the cuticle is compressed, the socket edges (collar) indent the cap, which squeezes the dendritic tip

and thereby activates the neuron (Spinola and Chapman 1975). In this way, campaniform sensilla encode load as strain in the cuticle (Pringle 1938a). Many campaniform sensilla are oval-shaped, which endows them with directional selectivity[3]. Based on mechanical rubber-and-paper models, J. W. S. Pringle was the first to realize that the cap is specifically indented when compressed along its short axis (Pringle 1938b). Therefore, differently oriented sensilla can signal bending or twisting of the leg in different directions (Zill and Moran 1981a). Figure 1.3 illustrates this mechanism for two groups of campaniform sensilla located on the dorsal side of the stick insect trochanter. Sensilla of the more proximal group are oriented perpendicularly to the long axis of the trochanter (Figure 1.3A, top view, magenta). These sensilla are excited by upward bending of the leg, because upward bending induces compressive strain in parallel to the long axis of the trochanter. Sensilla of the more distal group are oriented in parallel to the long axis of the trochanter (Figure 1.3A, top view, blue). These sensilla are excited by downward bending of the leg, because downward bending induces compressive strain perpendicularly to the long axis of the trochanter. Sensilla with similar orientations are often grouped together in regions where stress is likely to be high, typically near the leg joints (Pringle 1938b). Importantly, campaniform sensilla signal both the magnitude of load and the rate of load change (Figure 1.3B; e.g., Zill et al. 2012). During walking, they will be excited whenever leg muscle contractions are resisted, for example when the leg is pressed against the ground during stance or when an obstacle impedes leg movements during swing. Excitation of campaniform sensilla can trigger local and inter-joint motor effects. During stance, they are thought to adjust motor patterns to the current mechanical demand acting on the body by reinforcing muscle activity (Figure 1.3C; Burrows and Pflüger 1988; Pearson 1972; Zill et al. 2012; Zill et al. 2015). Toward the end of stance, campaniform sensilla are thought to promote the stance-to-swing transition by signaling the unloading of the leg (Bässler 1977b; Newland and Emptage 1996; Zill et al. 2009; see also Chapter 4). In addition, campaniform sensilla could be involved in more complex mechanisms, such as changing the overall gain of sensorimotor pathways (Macmillan and Kien 1983). Their role in walking control remains to be fully understood.

It is noteworthy that campaniform sensilla are functionally similar to load sensors in other animals (reviewed in Duysens et al. 2000). Campaniform sensilla closely resemble cuticular mechanoreceptors of other arthropods, like lyriform slit sense organs of spiders (Barth 2004; Blickhan and Barth 1985) or cuticular stress detectors of crus-

[3]Note that campaniform sensilla with round caps are not necessarily omnidirectional. On the stick insect tibia, for example, a group with round caps is directionally selective, presumably due to an asymmetrical coupling of the caps with the surrounding collars (Zill et al. 2011; Zill et al. 2013).

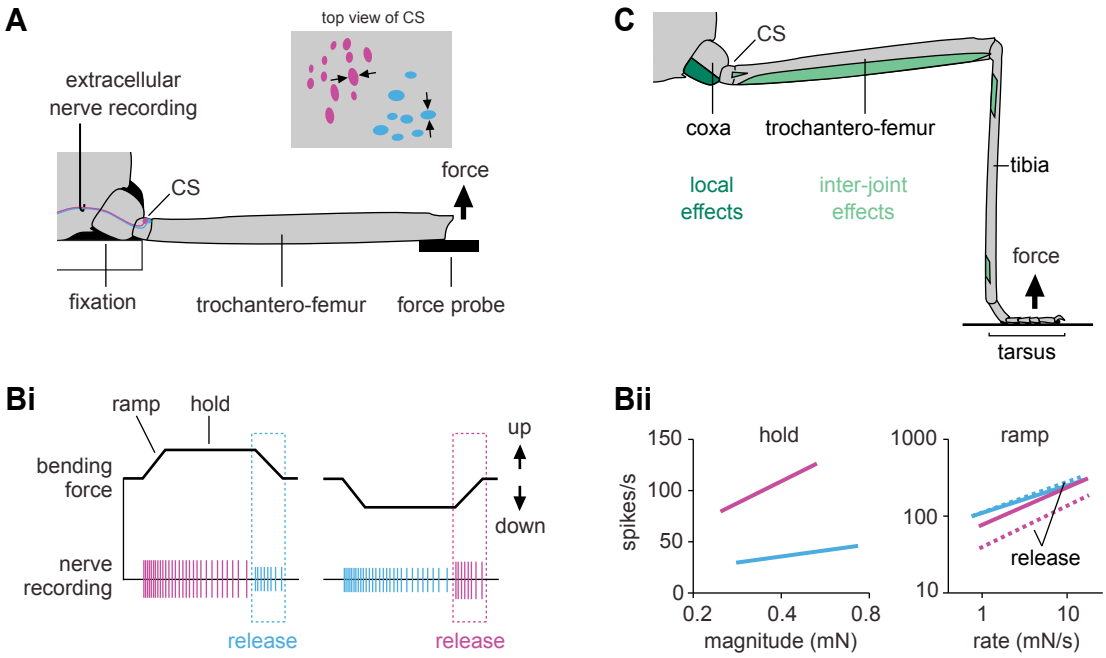

Figure 1.3: Encoding properties and motor effects of campaniform sensilla
(**A**) Schematic of preparation used to record activity of campaniform sensilla (CS) located on the dorsal side of the stick insect trochanter (Zill et al. 2012). The insect is fixated on a platform and the proximal leg joints are immobilized by glue. The leg is cut at the distal trochantero-femur (trochanter and femur are fused in stick insects). The segment is bent upward or downward via a force probe. Activity of CS afferents is recorded extracellularly from the main leg nerve using a hook electrode. Other afferents are ablated. Inset shows a top view of the two dorsal CS groups. The proximal group (magenta) is oriented perpendicularly to the long axis of the trochanter. The distal group (blue) is oriented in parallel to the long axis. Both are excited by compression along their short axes (arrows). (**Bi**) Schematic activity of CS groups to bending forces applied as ramp and hold stimuli. Upward bending excites the proximal group (magenta), whereas downward bending excites the distal group (blue). Responses are phasic-tonic. Importantly, the release from bending is always signaled by the opposite group, presumably because the cuticle is deformed to a new starting point after the hold phase so that the release from bending is detected as bending in the opposite direction (Zill et al. 2011). (**Bii**) CS groups encode both the magnitude and the rate of applied bending force. Data from Zill et al. (2012). (**C**) Campaniform sensilla can have local and inter-joint motor effects. For example, during the stance phase of walking, resisted depression of the leg can excite the proximal CS group (magenta in **A**), which can provide short-latency positive feedback to motor neurons of the depressor muscle (dark green; Zill et al. 2012) and long-latency positive feedback to motor neurons of the tibial and tarsal flexors (light green; Zill et al. 2015). This reinforces body weight support and substrate grip.

taceans (Clarac 2002; Libersat et al. 1987; Marchand et al. 1995). They might also serve a function similar to vertebrate Golgi tendon organs (Duysens et al. 2000). However, unlike tendon organs, campaniform sensilla do not signal the tension of any one muscle but rather the integrated effects of all forces causing strain in the cuticle, whether they are generated by muscle contractions or by external loads.

1.4 A biomechanics approach to walking control

As outlined in the previous section, we have a good understanding of many mechanisms involved in the control of insect walking. However, it is important to keep in mind that much of our understanding is based on experiments on restrained animals or reduced preparations. These experiments are necessary, because they permit detailed neurophysiological investigations of a given control mechanism in isolation. For example, studying the encoding properties and reflex effects of campaniform sensilla requires a reduced leg preparation where mechanical stimuli can be precisely controlled and sensory and motor responses can be precisely recorded (see Figure 1.3 for an example). Ultimately, however, a control mechanism can only be fully understood in a behaviorally-relevant, biomechanical context (Chiel and Beer 1997; Chiel et al. 2009; Nishikawa et al. 2007). One reason is that a freely walking insect may require a considerably different mechanical output than a restrained or reduced preparation, simply because a freely walking insect has to actively propel and stabilize its body. In turn, the actual timing, magnitude and variability of joint kinematics and joint torques affects the sensory feedback available for control. Therefore, the mechanical output at the leg joints can provide a window into sensorimotor control during natural locomotion (Winter and Eng 1995; Zernicke and Smith 1996).

The mechanical output at the leg joints can be determined using a combination of biomechanical techniques (Figure 1.4). 3D motion capture can be used to determine joint kinematics, and simultaneous measurements of ground reaction forces can be used to determine net joint torques. In addition, electromyography can be used to determine muscle activity, which is indicative of the motor commands sent by the nervous system. These techniques are particularly powerful when used in combination. Consider, for example, an insect leg extending around the femur-tibia (FTi) joint during stance (Figure 1.4B). Naively, one might assume that the extension is caused at the FTi joint by activity of the extensor muscle. However, in multi-joint movements, the cause of a movement cannot be inferred from kinematics alone due to mechanical coupling with other leg segments (Zernicke and Smith 1996). In our example, the FTi joint could also resist (stabilize) an extension induced by other legs or simply by gravity acting on the body. This can be resolved by determining the net joint torque, which represents the net magnitude and direction of all forces acting at the joint (Figure 1.4C; Winter 1990). If the FTi joint indeed stabilizes an extension, the net torque will point toward flexion rather than extension. Naively, one might then assume that a net flexion torque is generated by contraction of the flexor muscle. However, it could also be generated by co-contraction of the flexor and extensor muscles or—again due to mechanical coupling

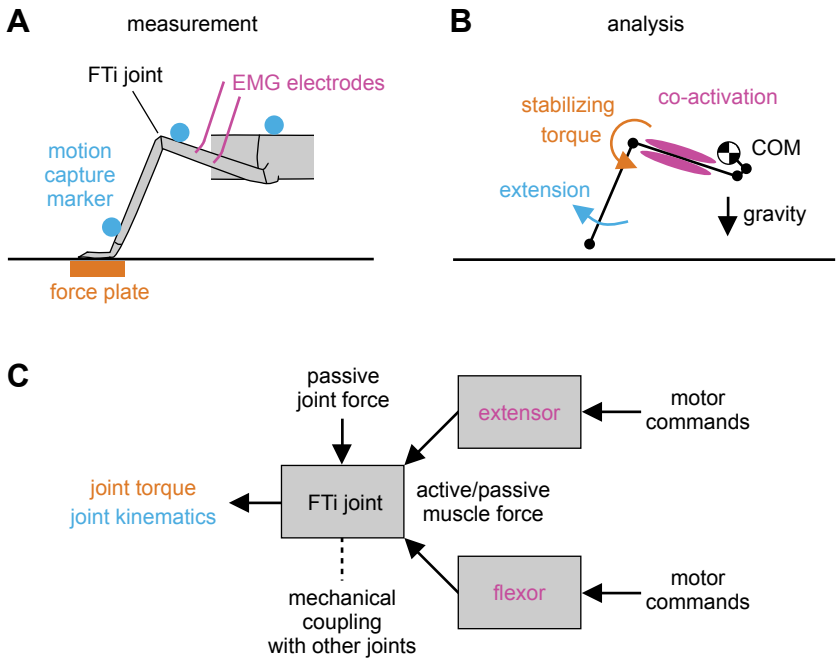

Figure 1.4: A biomechanics approach to walking control
(**A**,**B**) Schematic of combined marker-based motion capture (blue), single leg ground reaction force measurements (orange) and electromyography (EMG; magenta) in a stick insect hind leg for analyzing joint kinematics (blue), joint torques (orange) and muscle activity (magenta). FTi, femur-tibia joint; COM, center of mass. **B** shows a rigid link model used for kinematic and dynamic calculations. In this example, gravity-induced leg extension is counteracted by a stabilizing torque at the FTi joint, which is accompanied by co-contraction (here due to co-activation) of flexor and extensor muscles. (**C**) Diagram illustrating the transformation of motor commands into kinematics and torques at the FTi joint. Torques represent the net effect of all forces acting at the joint, i.e., active forces from muscle contractions, passive forces from muscles and skeletal structures, and forces induced by other joints due to mechanical coupling.

with other leg segments—by other leg muscles (Zajac 1993). This can be resolved by recording antagonistic muscle activity at the joint. As this example illustrates, a biomechanics approach can help reveal which of the many possible control strategies underlies a given movement by resolving often nonintuitive relations between muscle activity and mechanical output. At the same time, knowing the timing, magnitude and variability of joint kinematics and joint torques helps identify behaviorally-relevant movement and load signals for control. In addition, monitoring muscle activity helps determine whether the observed motor patterns agree with those predicted from a specific control mechanism studied in reduced preparations.

In larger vertebrates like cats and humans, combined biomechanical analyses have been used successfully to study sensorimotor control of walking (e.g., Donelan et al. 2009; Gregor et al. 2006; Lay et al. 2006; Lay et al. 2007; Winter and Eng 1995). In insects, the required measurements are generally complicated by the comparatively small size of the legs. Nevertheless, several studies have examined joint kinematics (e.g., Bender et al. 2010; Kram et al. 1997; Theunissen et al. 2015), ground reaction

forces of single legs (e.g., Cruse 1976; Full and Tu 1991; Harris and Ghiradella 1980; Reinhardt and Blickhan 2014), or leg muscle activity (e.g., Delcomyn and Usherwood 1973; Duch and Pflüger 1995; Watson and Ritzmann 1998). However, no study to date has combined all measurements and analyses in a freely walking insect. For example, no study has resolved the magnitude, timing and variability of joint torques in detail. As a consequence, our understanding of the mechanical output during natural walking and its potential consequences for sensorimotor control is quite simplistic. The aim of the present thesis was to tackle this issue by providing the first combination of 3D motion capture, ground reaction force measurements and electromyography in a freely walking insect, the stick insect *Carausius morosus*.

1.5 Stick insects as a model system for walking control

Stick insects have served as an important model system for studying sensorimotor control of walking since the 1960s (reviewed in Bässler 1983; Büschges and Gruhn 2007; Dürr et al. 2018; Graham 1985). Studies on stick insects have contributed important insights into almost all aspects of control discussed above (see Section 1.3). This is in part attributable to their relatively long and accessible legs, which also offer several advantages for detailed biomechanical analyses. First, stick insects hold their legs out to the side of the body and move them in a plane of action that is almost perpendicular to the ground. This facilitates marker-based motion capture (Theunissen and Dürr 2013) and measurements of single leg ground reaction forces (Cruse 1976). Second, all legs are rather unspecialized walking legs. This is different from locusts, where the large hind legs are specialized for jumping (Burns 1973), or cockroaches, where the hind legs move in a plane of action parallel to the ground (Kram et al. 1997). Finally, stick insect leg movements are comparatively slow. Stick insects take less than two steps per second during walking (Chapters 2-4). This should provide sufficient time for sensory feedback to shape motor patterns on a step-by-step basis (see Section 1.3 above).

So far, I have focused on general control mechanisms rather than species-specific details. However, applying a biomechanics approach as described above requires an understanding of the specific leg musculoskeletal system and the leg mechanoreceptors in question. Below, I introduce the musculoskeletal system (Section 1.5.1) and the mechanoreceptors (Section 1.5.2) of stick insect legs in more detail. This information is important for the electromyographic recordings, kinematic and dynamic analyses, and inferences about sensory control in the next chapters.

1.5.1 Leg musculoskeletal system

As is typical for insect legs, stick insect legs contain five segments: coxa, trochanter, femur, tibia, and tarsus (with pretarsus) (Figure 1.5A). The musculoskeletal structure is similar in all legs. For front legs, the muscle system in the thorax is considerably compressed due to the short length of the prothorax. Details of these deviations can be found in Marquardt (1939). All leg muscles are composed of slow, fast, and intermediate fiber types, reflecting their innervation by at least one slow motor neuron, one fast motor neuron, or both. Details of the motor neuron innervation and fiber-type distribution can be found in Goldammer et al. (2012) and Godlewska-Hammel et al. (2017), respectively.

Thorax-coxa joint

The thorax-coxa (ThC) joint or subcoxal joint connects the leg to the thorax and orients the leg plane, the plane in which all leg segments move (except for tarsus and pretarsus) (Figure 1.5A). Like in other insects, the ThC joint is the most complex leg joint. It is controlled by several muscles in the thorax (Figure 1.5B). The dorsal rim of the coxa has a typical articulation with the side wall of the thorax (pleuron), similarly to a ball joint (Figure 1.5B, arrow). The ventral rim of the coxa is attached to the pleuron by a short strut, the trochantin (Figure 1.5B, tn, arrow). The trochantin is a sclerite embedded in the soft cuticle that links the coxa anteriorly with the thorax. It points anteriorly and is flexibly joined to the pleuron. Therefore, the ventral pivot of the coxa is relatively mobile. However, during walking, coxal movements can be described well by rotations around a single rotational axis that is slanted outward with respect to the thorax (Figure 1.5A; see Theunissen et al. 2015 and Chapter 2). Around this axis, the protractor coxae and the retractor coxae muscles move the leg forward and backward, respectively.

The **protractor** muscle ($_1$p-cx) originates anteriorly of the ThC joint from the pleuron (Graham 1985; Marquardt 1939). It attaches to the soft cuticle at the anterior rim of the coxa (Figure 1.5B). $_1$p-cx is innervated by 6-9 excitatory motor neurons (Goldammer et al. 2012). The **retractor** muscles ($_1$t-cx, $_1$at-cx, $_2$t-cx, from anterior to posterior) originate anteriorly of the ThC joint from the tergum (Graham 1985). They insert at the posterior-dorsal side of the coxa (Figure 1.5B). $_1$t-cx is innervated by 7 excitatory motor neurons; $_1$at-cx and $_2$t-cx are innervated by 16-17 motor neurons (Goldammer et al. 2012). Activity of the protractor and retractor muscles during walking is investigated in Chapter 4.

It is noteworthy that at least four other muscles can move the coxa (Figure 1.5B, gray). One muscle ($_2$p-cx) originates from the pleuron and inserts at the posterior side of the coxa. It can assist in the retraction of the leg. Two other muscles ($_1$st-cx, $_2$st-cx)

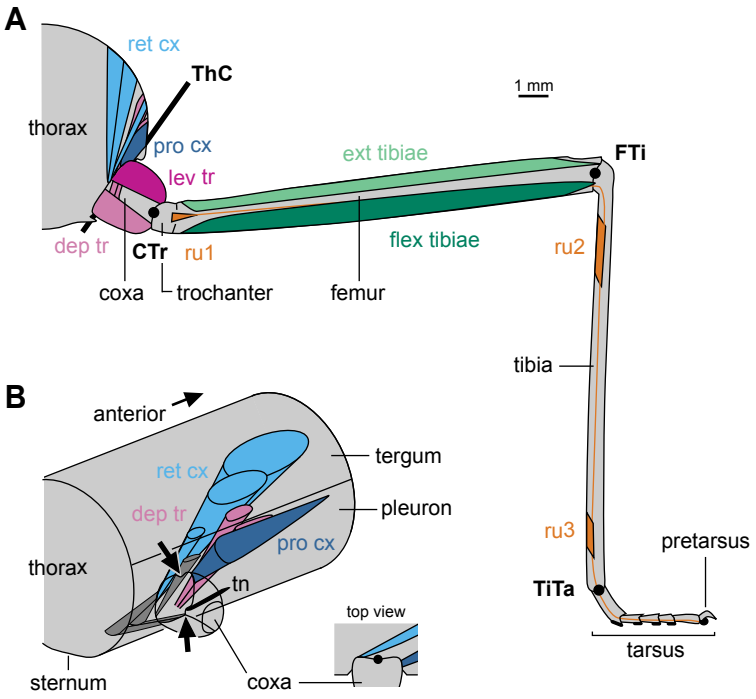

Figure 1.5: Musculoskeletal system of a stick insect leg
(**A**) Schematic cross section of a right stick insect leg (posterior side) showing approximate locations of the leg muscles. The thorax-coxa (ThC) joint can be modelled as a hinge with a slanted rotational axis (bold black line). Around this axis, the protractor coxae (pro cx, dark blue) and the retractor coxae (ret cx, light blue) muscles move the leg forward and backward, respectively. The coxa-trochanter (CTr) joint and the femur-tibia (FTi) joint are hinges with parallel rotational axes (filled black circles). The levator trochanteris (lev tr, dark magenta) and the depressor trochanteris (dep tr, light magenta) muscles lift and lower the fused trochantero-femur segment, respectively. The flexor tibiae (flex tibiae, dark green) and the extensor tibiae (ext tibiae, light green) muscles flex and extend the tibia, respectively. The tibia-tarsus (TiTa) joint is a ball-and-socket joint (filled black circle). The three parts of the retractor unguis (ru1-ru3, orange) attach to a common apodeme that flexes the tarsus. (**B**) Schematic of leg muscles originating from the thorax and inserting at the coxa and trochanter (based on two-dimensional drawings of the metathorax in Graham 1985). The protractor coxae (pro cx, dark blue) muscle originates from the pleuron, the retractor coxae (ret cx, light blue) muscles originate from the tergum, and two depressor trochanteris (dep tr, light magenta) muscles originate from the tergum and pleuron. Additional coxal muscles (gray) originate from the sternum and pleuron. The coxa articulates dorsally with the pleuron (upper arrow) and ventrally with the trochantin (tn, black, lower arrow). The top view illustrates the attachment sites of the retractor and protractor coxae relative to the rotational axis (filled black circle) of the coxa.

originate from the ventral side of the thorax (sternum) and insert at the ventral side of the coxa. These muscles pull the coxa closer to the thorax; hence, they are referred to as sternal adductors (Marquardt 1939) or sternal depressors (Graham 1985). A fourth muscle ($_3$st-cx) originates from the sternum and inserts at the posterior side of the coxa with the retractors. It might retract (Marquardt 1939) or levate (Graham 1985) the coxa. The activity of these muscles during walking is unknown, but they might aid in stabilizing the ThC joint as described in the locust (Duch and Pflüger 1995).

Coxa-trochanter joint

The coxa-trochanter (CTr) joint is a hinge connecting the coxa with the trochanter (Figure 1.5A). Its rotational axis is orthogonal to that of the ThC joint (Cruse 1976). Around this axis, the levator trochanteris and the depressor trochanteris muscles move the leg up and down, respectively. Note that in stick insects the short trochanter is rigidly linked to the long femur. This is not necessarily the case in other insects (Frantsevich and Wang 2009). In cockroaches, for example, the mobile trochanter-femur joint permits small posterior movements of the femur (Watson et al. 2002; Zill et al. 2017b).

The **levator** muscles ($_3$cx-tr, $_{3a}$cx-tr, $_4$cx-tr, $_{4a}$cx-tr) originate from the coxa and insert at the dorsal trochanter (Figure 1.5A; Marquardt 1939). The innervation of the levator muscles is not fully described, but $_3$cx-tr is innervated by 9-11 motor neurons (Goldammer et al. 2012). The **depressor** muscles insert at the ventral trochanter. Two muscles ($_1$cx-tr, $_2$cx-tr) originate from the coxa, one muscle (t-tr) originates from the tergum, and one muscle (p-tr) originates from the pleuron (Graham 1985; Marquardt 1939) (Figure 1.5B). The tergal and pleural depressors are innervated by 8-9 excitatory motor neurons (Goldammer et al. 2012). The coxal depressors are innervated by only two excitatory motor neurons, the slow depressor trochanteris (SDTr) and the fast depressor trochanteris (FDTr) (Goldammer et al. 2012; Schmitz 1986b). Activity of the levator and depressor muscles during walking is investigated in Chapter 3.

Femur-tibia joint

The femur-tibia (FTi) joint is a hinge connecting the fused trochantero-femur with the tibia (Figure 1.5A). Its rotational axis is parallel to that of the CTr joint. Around this axis, the flexor tibiae and the extensor tibiae muscles move the tibia inward and outward, respectively.

The **flexor** muscle is a pinnate muscle with relatively short fibers (Guschlbauer et al. 2007). The fibers originate from the side wall of the femur and insert obliquely on an apodeme that spans the length of the femur. The oblique arrangement of the fibers increases the effective cross-sectional area of the muscle and hence its ability to produce force in a confined space (Full 1997). The flexor is innervated by more than 20 excitatory motor neurons (Goldammer et al. 2012). In all legs, the flexor is considerably larger than the extensor (Bässler 1983). The **extensor** muscle is also a pinnate muscle with short fibers (Guschlbauer et al. 2007). The fibers originate from the dorsal wall of the femur and insert obliquely on a common apodeme. Similar to the coxal parts of the depressor, the extensor is innervated by just two excitatory motor neurons, the slow extensor tibiae (SETi) and the fast extensor tibiae (FETi) (Bässler and Storrer 1980; Goldammer et al. 2012). This comparatively simple innervation is also found in other

insects like the cockroach (Atwood et al. 1969) and locust (Hoyle and Burrows 1973).

Tibia-tarsus joint

The tibia-tarsus (TiTa) joint is a ball joint connecting the tibia with the flexibly linked segments of the tarsus (Figure 1.5A). The tarsus is moveable in all directions. The first four tarsal segments each bear a pair of soft "friction" pads (euplantulae) on their ventral side; the pretarsus bears an adhesive pad (arolium) between the claws (Labonte and Federle 2013). The retractor unguis muscle can bend the tarsal segments ventrally to bring the pretarsus in contact with the ground (Radnikow and Bässler 1991).

The **retractor unguis** muscle is a tripartite muscle (Bässler 1983). One part (ru1) resides in the proximal femur, the others in the proximal (ru2) and distal (ru3) tibia. All parts attach to a common apodeme that terminates on a sclerotized plate, the unguitractor. The retractor unguis muscle has no antagonist. Like in cockroaches, it works against elastic bands in the tarsus (Frazier et al. 1999; Radnikow and Bässler 1991).

1.5.2 Leg mechanoreceptors

Stick insect legs are equipped with mechanoreceptors of all types described above (Section 1.3.4). These mechanoreceptors can monitor the movements of individual leg segments and the mechanical loads acting on them (Figure 1.6).

Thorax-coxa joint

The relatively high mobility of the coxa (see above) is mirrored in the number of sensors monitoring its movements. On its anterior side, the coxa bears two hair plates (Figure 1.6, hp_2 and hp_3). One is located ventrally near the articulation with the trochantin. It contains 20-30 hairs that are excited when the coxa moves forward (Wendler 1964). The other is located dorsally near the articulation with the pleuron. It contains 15-30 hairs that are excited when the coxa moves forward and upward (Wendler 1964). On its ventral and posterior sides, the coxa carries four hair rows that are oriented approximately perpendicularly to the slanted ThC joint axis (Figure 1.6). The rows contain 4-13 hairs each (Bässler 1965). Conversely to the hair plates, the hair rows are excited when the coxa moves backward and downward (Bässler 1965; Cruse et al. 1984). Both hair plates and hair rows contribute to controlling leg movements about the ThC joint. For example, the leg moves further forward after ablation of the hair plates (Wendler 1964) and further backward after ablation of the hair rows (Bässler 1977b). Finally, it is likely that a set of chordotonal organs in the ventral thorax (Figure 1.6, co) is associated with measuring movements of the coxa as described in the locust (reviewed in Field and

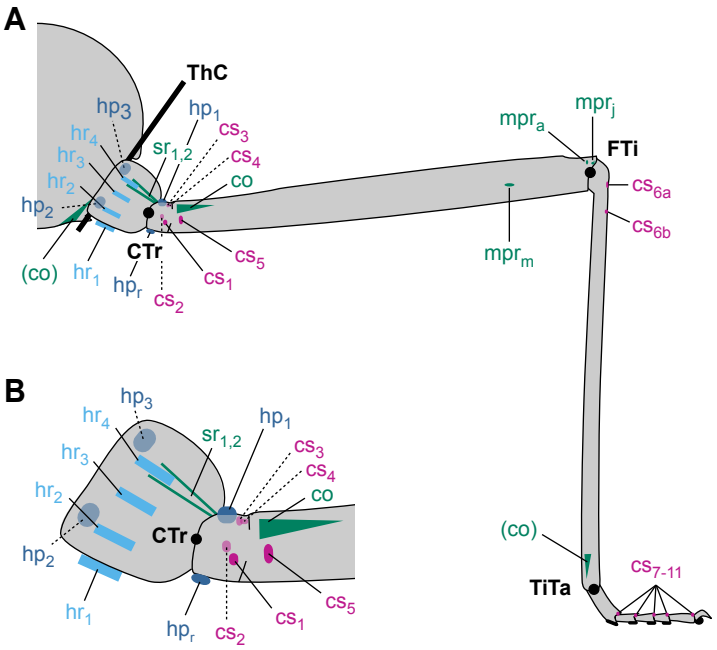

Figure 1.6: Mechanoreceptors of a stick insect leg
(**A**) Schematic cross section of a right stick insect leg (posterior side) showing approximate locations of the main leg mechanoreceptors. External movement sensors are colored in blue, internal movement sensors in green, and cuticular load sensors in magenta. Dotted lines indicate sensors on the anterior side. co, chordotonal organ; cs, campaniform sensilla; hp, hair plate; hr, hair row; mpr, multipolar receptor associated with apodeme (a), joint (j) or muscle (m); sr, strand receptor. Note that this schematic does not represent the full complement of mechanoreceptors; solitary tactile hairs, for example, are not shown. Note also that the locations of mechanoreceptors in parentheses are based on descriptions in other insects. (**B**) Close-up of mechanoreceptors on the coxa, trochanter and proximal femur.

Matheson 1998). The role of hair plates, hair rows and chordotonal organs at the ThC during walking is discussed in Chapter 4.

Loads applied to the leg in the forward and backward direction are primarily monitored by two groups of campaniform sensilla on the trochanter. One is located on the posterior side of the trochanter, the other one on its anterior side (Figure 1.6, cs_1 and cs_2; Hofmann and Bässler 1982; Tatar 1976). The caps of both groups are oriented perpendicularly to the long axis of the trochanter. Therefore, the campaniform sensilla are preferentially excited when the trochantero-femur is bent forward (anterior group cs_2) or backward (posterior group cs_1) (Schmitz 1993). The sensory signals of these groups can reset and entrain rhythmic activity of motor neurons of the protractor and retractor muscles (Akay et al. 2007). Hence, they can contribute to controlling leg movements about the ThC joint. Their role during walking is discussed in Chapter 4. In addition, a group of diversely oriented campaniform sensilla on the posterior femur is excited by backward bending of the trochantero-femur (Figure 1.6, cs_5; Zill et al. 2017b). However, its influence on controlling the ThC joint seems weak (Akay et al. 2007).

Coxa-trochanter joint

Levation of the trochantero-femur is monitored by a dorsal hair plate close to the CTr joint (Figure 1.6, hp_1; Wendler 1964). It is involved in controlling the CTr joint angle (Schmitz 1986a; Wendler 1964). Ablation of the hair plate impairs searching and swing movements and affects coordination between legs (Berg et al. 2013; Cruse et al. 1984; Theunissen et al. 2014; Wendler 1964). Depression of the trochantero-femur can be monitored by a ventral, rhomboid-shaped hair plate close to the CTr joint (Figure 1.6, hp_r; Tatar 1976), but its exact function is unclear (Schmitz 1986a). Depression is additionally monitored by two internal strand receptors in the dorsal coxa (Figure 1.6, sr_1 and sr_2; Schöwerling 1992), similarly to other insects (Bräunig 1982a). Their sensory signals can affect the activity of the motor neurons of the levator (Schöwerling 1992), but their function during walking is unknown. The role of these mechanoreceptors during walking is discussed in Chapter 3.

Loads applied to the leg in the upward and downward direction are primarily monitored by two groups of campaniform sensilla on the dorsal trochanter (Figure 1.6, cs_3 and cs_4; Zill et al. 2012; see also Figure 1.3). The caps of one group (cs_3) are oriented perpendicularly to the long axis of the trochanter. These campaniform sensilla are preferentially excited when the trochantero-femur is bent upward. The caps of the other group (cs_4) are oriented in parallel to the long axis of the trochanter. These campaniform sensilla are preferentially excited when the trochantero-femur is bent downward. Both groups affect the activity of the levator and depressor muscles (Zill et al. 2012; Zill et al. 2017a). Their role during walking is studied in more detail in Chapter 3. In addition, the aforementioned group of campaniform sensilla on the femur is excited by upward/downward bending of the trochantero-femur. However, its motor effects are primarily associated with the FTi joint (Akay et al. 2001; Zill et al. 2017b; see below). Moreover, activity of the depressor muscle is affected by campaniform sensilla on the tibia and tarsus (Zill et al. 2011; Zill et al. 2015; see below). Finally, a subgroup of the campaniform sensilla on the anterior trochanter is oriented in parallel to the long axis of the trochanter, so that it could respond to upward/downward bending of the trochantero-femur. The encoding properties and actions of this subgroup are unknown.

Femur-tibia joint

The position and movement of the FTi joint is primarily monitored by the femoral chordotonal organ (Figure 1.6, co; Bässler 1965). In stick insects, the femoral chordotonal organ is located in the proximal femur and connected to the tibia by a long apodeme. During walking, it is thought to assist ongoing stance phase motor activity and contribute to initiating the swing phase of the leg at a specific FTi joint position (reviewed

in Bässler and Büschges 1998). The position and movement of the FTi joint can also be signaled to some extent by different types of multipolar receptors near the joint (Figure 1.6, mpr_a, mpr_j and mpr_m; Bässler 1977a). Two stretch receptors associated with the joint articulation respond to joint extension, an apodeme receptor responds to both joint extension and flexion, and a tension receptor signals tension in the flexor tibiae (Bässler 1977a). As noted above (Section 1.3.4), the functions of these multipolar receptors during walking is largely unknown.

Loads applied to the leg in the inward and outward direction are monitored by two groups of campaniform sensilla on the proximal, dorsal tibia (Figure 1.6, cs_{6a} and cs_{6b}; Zill et al. 2011). The caps of one group (cs_{6a}) are oriented in parallel to the long axis of the tibia. These campaniform sensilla are preferentially excited when the tibia is bent inward. The caps of the other group (cs_{6b}) are round. These campaniform sensilla are preferentially excited when the tibia is bent outward, presumably due to an asymmetrical coupling of the cap with the surrounding cuticle (Zill et al. 2013). Both groups affect the activity of motor neurons of the flexor and extensor muscles as well as the depressor muscle (Zill et al. 2011). In addition, motor neurons of the flexor muscle are affected by the aforementioned group of campaniform sensilla on the femur (Akay et al. 2001). Ablation of this group affects the magnitude (Akay et al. 2001) and the timing (Schmitz et al. 2015) of flexor muscle activity. Finally, flexor muscle activity is also influenced by campaniform sensilla on the tarsus (see below; Zill et al. 2014; Zill et al. 2015).

Tibia-tarsus joint

The position and movement of the TiTa joint is likely monitored by a chordotonal organ in the distal tibia (Figure 1.6, co) as described in the locust (reviewed in Field and Matheson 1998).

Loads acting on the tarsus are monitored by campaniform sensilla located on the distal end of each of the tarsal segments close to the intrinsic tarsal joints (Figure 1.6, $cs_{7\text{-}11}$; Zill et al. 2014). These campaniform sensilla can activate motor neurons of the retractor unguis, flexor tibiae and depressor trochanteris muscles (Zill et al. 2014; Zill et al. 2015).

1.6 Aim and objectives

The aim of the present thesis was to study sensorimotor control in freely walking stick insects using a combination of 3D motion capture, ground reaction force measurements and electromyography (Figure 1.4). Stick insects are one of the best-studied model systems for walking control. The combination of biomechanical techniques should reveal

the mechanical output at their leg joints (joint kinematics, joint torques) and its relation to leg muscle activity during natural locomotion. As outlined above, this information might help identify behaviorally relevant sensory signals for control and probe specific control mechanisms studied in tethered or reduced preparations.

The objectives of the present thesis were:

1. To develop a setup for simultaneously analyzing joint kinematics, joint torques and muscle activity in stick insects walking freely on level ground and up and down inclines (see Chapters 2-4).

2. To develop a rigid link model of a stick insect leg for torque calculations and evaluate potential simplifying assumptions (see Chapter 2).

3. To determine kinematics and torques of all leg joints during walking and identify the role of individual joints in propulsion and stabilization of the body (see Chapter 2).

4. To determine the correlations between joint torques and antagonistic muscle activity during walking and identify the potential contribution of local load reflexes to the control of the stance phase (see Chapter 3).

5. To determine how leg muscle activity is adjusted to changing mechanical demands during incline walking (see Chapter 4).

1.7 References

Ache, J. M. and Matheson, T. (2013). Passive joint forces are tuned to limb use in insects and drive movements without motor activity. *Curr. Biol.* 23, 1418–1426.

Akay, T., Bässler, U., Gerharz, P., and Büschges, A. (2001). The role of sensory signals from the insect coxa-trochanteral joint in controlling motor activity of the femur-tibia joint. *J. Neurophysiol.* 85, 594–604.

Akay, T., Ludwar, B. C., Göritz, M. L., Schmitz, J., and Büschges, A. (2007). Segment specificity of load signal processing depends on walking direction in the stick insect leg muscle control system. *J. Neurosci.* 27, 3285–3294.

Atwood, H. L., Smyth Jr., T., and Johnston, H. S. (1969). Neuromuscular synapses in the cockroach extensor tibiae muscle. *J. Insect Physiol.* 15, 529–532.

Barth, F. G. (2004). Spider mechanoreceptors. *Curr. Opin. Neurobiol.* 14, 415–422.

Bässler, U. (1965). Proprioreceptoren am Subcoxal- und Femur-Tibia-Gelenk der Stabheuschrecke *Carausius morosus* und ihre Rolle bei der Wahrnehmung der Schwerkraftrichtung. *Kybernetik* 2, 168–193.

Bässler, U. (1976). Reversal of a reflex to a single motoneuron in the stick insect *Carausius morosus*. *Biol. Cybern.* 24, 47–49.

Bässler, U. (1977a). Sense organs in the femur of the stick insect and their relevance to the control of position of the femur-tibia-joint. *J. Comp. Physiol. A* 121, 99–113.

Bässler, U. (1977b). Sensory control of leg movement in the stick insect *Carausius morosus*. *Biol. Cybern.* 25, 61–72.

Bässler, U. (1983). *Neural Basis of Elementary Behavior in Stick Insects*. Berlin: Springer.

Bässler, U. (1993). The femur-tibia control system of stick insects - a model system for the study of the neural basis of joint control. *Brain Res. Rev.* 18, 207–226.

Bässler, U. and Büschges, A. (1998). Pattern generation for stick insect walking movements - multisensory control of a locomotor program. *Brain Res. Rev.* 27, 65–88.

Bässler, U. and Storrer, J. (1980). The neural basis of the femur-tibia-control-system in the stick insect *Carausius morosus*. I. Motoneurons of the extensor tibiae muscle. *Biol. Cybern.* 38, 107–114.

Belanger, J. H. (2005). Contrasting tactics in motor control by vertebrates and arthropods. *Integr. Comp. Biol.* 45, 672–678.

Bender, J. A., Simpson, E. M., and Ritzmann, R. E. (2010). Computer-assisted 3D kinematic analysis of all leg joints in walking insects. *PLoS One* 5, e13617.

Berg, E., Büschges, A., and Schmidt, J. (2013). Single perturbations cause sustained changes in searching behavior in stick insects. *J. Exp. Biol.* 216, 1064–1074.

Bidaye, S. S., Machacek, C., Wu, Y., and Dickson, B. J. (2014). Neuronal control of *Drosophila* walking direction. *Science* 344, 97–101.

Bidaye, S. S., Bockemühl, T., and Büschges, A. (2018). Six-legged walking in insects: how CPGs, peripheral feedback, and descending signals generate coordinated and adaptive motor rhythms. *J. Neurophysiol.* 119, 459–475.

Blickhan, R. and Barth, F. G. (1985). Strains in the exoskeleton of spiders. *J. Comp. Physiol. A* 157, 115–147.

Böhm, H. and Schildberger, K. (1992). Brain neurones involved in the control of walking in the cricket *Gryllus bimaculatus*. *J. Exp. Biol.* 166, 113–130.

Bräunig, P. (1982a). Strand receptors with central cell bodies in the proximal leg joints of orthopterous insects. *Cell Tissue Res.* 222, 647–654.

Bräunig, P. (1982b). The peripheral and central nervous organization of the locust coxotrochanteral joint. *J. Neurobiol.* 13, 413–433.

Bräunig, P. and Hustert, R. (1980). Proprioceptors with central cell bodies in insects. *Nature* 283, 768–770.

Bräunig, P. and Hustert, R. (1985a). Actions and interactions of proprioceptors of the locust hind leg coxo-trochanteral joint. I. Afferent responses in relation to joint position and movement. *J. Comp. Physiol. A.* 157, 73–82.

Bräunig, P. and Hustert, R. (1985b). Actions and interactions of proprioceptors of the locust hind leg coxo-trochanteral joint. II. Influence on the motor system. *J. Comp. Physiol. A.* 157, 83–89.

Brown, T. G. (1911). The intrinsic factors in the act of progression in the mammal. *Proc. R. Soc. B* 84, 308–319.

Brown, T. G. (1914). On the nature of the fundamental activity of the nervous centres; together with an analysis of the conditioning of rhythmic activity in progression, and a theory of the evolution of function in the nervous system. *J. Physiol.* 48, 18–46.

Burns, M. D. (1973). The control of walking in Orthoptera. I. Leg movements in normal walking. *J. Exp. Biol.* 58, 45–58.

Burns, M. D. (1974). Structure and physiology of the locust femoral chordotonal organ. *J. Insect Physiol.* 20, 1319–1339.

Burns, M. D. and Usherwood, P. N. R. (1979). The control of walking in Orthoptera. II. Motor neuron activity in normal free-walking animals. *J. Exp. Biol.* 79, 69–98.

Burrows, M. and Pflüger, H. J. (1988). Positive feedback loops from proprioceptors involved in leg movements of the locust. *J. Comp. Physiol. A* 163, 425–440.

Burrows, M. (1996). *The Neurobiology of an Insect Brain*. Oxford: Oxford University Press.

Büschges, A. (1994). The physiology of sensory cells in the ventral scoloparium of the stick insect femoral chordotonal organ. *J. Exp. Biol.* 189, 285–292.

Büschges, A. (1995). Role of local nonspiking interneurons in the generation of rhythmic motor activity in the stick insect. *J. Neurobiol.* 27, 488–512.

Büschges, A. and Gruhn, M. (2007). Mechanosensory feedback in walking: from joint control to locomotor patterns. *Adv. In Insect Phys.* 34, 193–230.

Büschges, A., Schmitz, J., and Bässler, U. (1995). Rhythmic patterns in the thoracic nerve cord of the stick insect induced by pilocarpine. *J. Exp. Biol.* 198, 435–456.

Buschmann, T., Ewald, A., Twickel, A. von, and Büschges, A. (2015). Controlling legs for locomotion - insights from robotics and neurobiology. *Bioinspir. Biomim.* 10, 041001.

Chiel, H. J. and Beer, R. D. (1997). The brain has a body: adaptive behavior emerges from interactions of nervous system, body and environment. *Trends Neurosci.* 20, 553–557.

Chiel, H. J., Ting, L. H., Ekeberg, O., and Hartmann, M. J. Z. (2009). The brain in its body: motor control and sensing in a biomechanical context. *J. Neurosci.* 29, 12807–12814.

Clarac, F. (2002). Neurobiology of crustacean walking: from past to future. *Crustacean Experimental Systems in Neurobiology*. Ed. by Wiese, K. Berlin: Springer, 119–137.

Coillot, J. P. and Boistel, J. (1968). Localisation et description des récepteurs à l'étirement au niveau de l'articulation tibio-fémorale de la patte sauteuse du criquet *Schistocerca gregaria*. *J. Insect Physiol.* 14, 1661–1667.

Cruse, H. (1976). The function of the legs in the free walking stick insect, *Carausius morosus*. *J. Comp. Physiol. A* 112, 235–262.

Cruse, H. (1985). Which parameters control the leg movement of a walking insect? II. The start of the swing phase. *J. Exp. Biol.* 116, 357–362.

Cruse, H., Dean, J., and Suilmann, M. (1984). The contributions of diverse sense organs to the control of leg movement by a walking insect. *J. Comp. Physiol. A* 154, 695–705.

Cruse, H., Kindermann, T., Schumm, M., Dean, J., and Schmitz, J. (1998). Walknet - a biologically inspired network to control six-legged walking. *Neural Netw.* 11, 1435–1447.

Delcomyn, F. (1991). Perturbation of the motor system in freely walking cockroaches. I. Rear leg amputation and the timing of motor activity in leg muscles. *J. Exp. Biol.* 156, 483–502.

Delcomyn, F. and Usherwood, P. N. R. (1973). Motor activity during walking in the cockroach *Periplaneta americana*. I. Free walking. *J. Exp. Biol.* 59, 629–642.

Dickinson, M. H., Farley, C. T., Full, R. J., Koehl, M. A. R., Kram, R., and Lehman, S. (2000). How animals move: an integrative view. *Science* 288, 100–106.

Donelan, J. M., McVea, D. A., and Pearson, K. G. (2009). Force regulation of ankle extensor muscle activity in freely walking cats. *J. Neurophysiol.* 101, 360–371.

Duch, C. and Pflüger, H. J. (1995). Motor patterns for horizontal and upside down walking and vertical climbing in the locust. *J. Exp. Biol.* 198, 1963–1976.

Dürr, V., Schmitz, J., and Cruse, H. (2004). Behaviour-based modelling of hexapod locomotion: linking biology and technical application. *Arthropod Struct. Dev.* 33, 237–250.

Dürr, V., Theunissen, L. M., Dallmann, C. J., Hoinville, T., and Schmitz, J. (2018). Motor flexibility in insects: adaptive coordination of limbs in locomotion and near-range exploration. *Behav. Ecol. Sociobiol.* 72, 15.

Duysens, J., Clarac, F., and Cruse, H. (2000). Load-regulating mechanisms in gait and posture: comparative aspects. *Physiol. Rev.* 80, 83–133.

Duysens, J. and Pearson, K. G. (1980). Inhibition of flexor burst generation by loading ankle extensor muscles in walking cats. *Brain Res.* 187, 321–332.

Field, L. H. and Matheson, T. (1998). Chordotonal organs of insects. *Adv. In Insect Phys.* 27, 1–228.

Frantsevich, L. and Wang, W. (2009). Gimbals in the insect leg. *Arthropod Struct. Dev.* 38, 16–30.

Frazier, S. F., Larsen, G. S., Neff, D., Quimby, L., Carney, M., DiCaprio, R. A., and Zill, S. N. (1999). Elasticity and movements of the cockroach tarsus in walking. *J. Comp. Physiol. A.* 185, 157–172.

Full, R. J. (1997). Invertebrate locomotor systems. *Handbook of Physiology, Comparative Physiology.* Ed. by Dantzler, W. American Physiological Society, 853–930.

Full, R. J. and Tu, M. S. (1991). Mechanics of a rapid running insect: two-, four-, and six-legged locomotion. *J. Exp. Biol.* 156, 215–231.

Gal, R. and Libersat, F. (2006). New vistas on the initiation and maintenance of insect motor behaviors revealed by specific lesions of the head ganglia. *J. Comp. Physiol. A* 192, 1003–1020.

Godlewska-Hammel, E., Büschges, A., and Gruhn, M. (2017). Fiber-type distribution in insect leg muscles parallels similarities and differences in the functional role of insect walking legs. *J. Comp. Physiol. A* 203, 773–790.

Goldammer, J., Büschges, A., and Schmidt, J. (2012). Motoneurons, DUM cells, and sensory neurons in an insect thoracic ganglion: a tracing study in the stick insect *Carausius morosus*. *J. Comp. Neurol.* 520, 230–257.

Graham, D. (1979). Effects of circum-oesophageal lesion on the behaviour of the stick insect *Carausius morosus*. I. Cyclic behaviour patterns. *Biol. Cybern.* 32, 139–145.

Graham, D. (1985). Pattern and control of walking in insects. *Adv. In Insect Phys.* 18, 32–140.

Graham, D. and Wendler, G. (1981). Motor output to the protractor and retractor coxae muscles in stick insects walking on a treadwheel. *Physiol. Entomol.* 6, 161–174.

Gregor, R. J., Smith, D. W., and Prilutsky, B. I. (2006). Mechanics of slope walking in the cat: quantification of muscle load, length change, and ankle extensor EMG patterns. *J. Neurophysiol.* 95, 1397–1409.

Grillner, S. (1975). Locomotion in vertebrates: central mechanisms and reflex interaction. *Physiol. Rev.* 55, 247–304.

Grillner, S. (1981). Control of locomotion in bipeds, tetrapods, and fish. *Handbook of Physiology, The Nervous System: Motor Control.* Ed. by Brookhart, J. M. and Mountcastle, V. B. American Physiological Society, 1179–1236.

Guertin, P. A. (2013). Central pattern generator for locomotion: anatomical, physiological, and pathophysiological considerations. *Front. Neurol.* 3, 1–15.

Guo, P. and Ritzmann, R. E. (2013). Neural activity in the central complex of the cockroach brain is linked to turning behaviors. *J. Exp. Biol.* 216, 992–1002.

Guschlbauer, C., Scharstein, H., and Büschges, A. (2007). The extensor tibiae muscle of the stick insect: biomechanical properties of an insect walking leg muscle. *J. Exp. Biol.* 210, 1092–1108.

Guthrie, D. M. (1967). Multipolar stretch receptors and the insect leg reflex. *J. Insect Physiol.* 13, 1637–1644.

Harris, J. and Ghiradella, H. (1980). The forces exerted on the substrate by walking and stationary crickets. *J. Exp. Biol.* 85, 263–279.

Hofmann, T. and Bässler, U. (1982). Anatomy and physiology of trochanteral campaniform sensilla in the stick insect, *Cuniculina impigra*. *Physiol. Entomol.* 7, 413–426.

Hofmann, T., Koch, U. T., and Bässler, U. (1985). Physiology of the femoral chordotonal organ in the stick insect, *Cuniculina impigra*. *J. Exp. Biol.* 114, 207–223.

Hooper, S. L. and Büschges, A., eds. (2017). *Neurobiology of Motor Control: Fundamental Concepts and New Directions*. Wiley.

Hooper, S. L. (2012). Body size and the neural control of movement. *Curr. Biol.* 22, R318–R322.

Hooper, S. L., Guschlbauer, C., Blümel, M., Rosenbaum, P., Gruhn, M., Akay, T., and Büschges, A. (2009). Neural control of unloaded leg posture and of leg swing in stick insect, cockroach, and mouse differs from that in larger animals. *J. Neurosci.* 29, 4109–4119.

Hooper, S. L. and Weaver, A. L. (2000). Motor neuron activity is often insufficient to predict motor response. *Curr. Opin. Neurobiol.* 10, 676–682.

Hoyle, G. and Burrows, M. (1973). Neural mechanisms underlying behavior in the locust *Schistocerca gregaria*. I. Physiology of identified motorneurons in the metathoracic ganglion. *J. Neurobiol.* 4, 3–41.

Hsu, C. T. and Bhandawat, V. (2016). Organization of descending neurons in *Drosophila melanogaster*. *Sci. Rep.* 6, 20259.

Hughes, G. M. (1952). The co-ordination of insect movements. I. The walking movements of insects. *J. Exp. Biol.* 29, 267–285.

Ijspeert, A. J. (2014). Biorobotics: using robots to emulate and investigate agile locomotion. *Science* 346, 196–203.

Isakov, A., Buchanan, S. M., Sullivan, B., Ramachandran, A., Chapman, J. K. S., Lu, E. S., Mahadevan, L., and Bivort, B. de (2016). Recovery of locomotion after injury in *Drosophila* depends on proprioception. *J. Exp. Biol.* 219, 1760–1771.

Jindrich, D. L. and Full, R. J. (2002). Dynamic stabilization of rapid hexapedal locomotion. *J. Exp. Biol.* 205, 2803–2823.

Kien, J. and Altman, J. S. (1984). Descending interneurones from the brain and suboesophageal ganglia and their role in the control of locust behaviour. *J. Insect Physiol.* 30, 59–72.

Kien, J., Fletcher, W. A., Altman, J. S., Ramirez, J.-M., and Roth, U. (1990). Organisation of intersegmental interneurons in the subesophageal ganglion of *Schistocerca gregaria* (Forksal) and *Locusta migratoria* migratorioides (Reiche and Fairmaire) (Acrididae, Orthroptera). *Int. J. Insect Morphol. Embryol.* 19, 35–60.

Kien, J. (1990). Neuronal activity during spontaneous walking - I. Starting and stopping. *Comp. Biochem. Physiol.* 95, 607–621.

Kittmann, R. and Schmitz, J. (1992). Functional specialization of the scoloparia of the femoral chordotonal organ in stick insects. *J. Exp. Biol.* 173, 91–108.

Kram, R., Wong, B., and Full, R. J. (1997). Three-dimensional kinematics and limb kinetic energy of running cockroaches. *J. Exp. Biol.* 200, 1919–1929.

Labonte, D. and Federle, W. (2013). Functionally different pads on the same foot allow control of attachment: stick insects have load-sensitive "heel" pads for friction and shear-sensitive "toe" pads for adhesion. *PLoS One* 8, e81943.

Lay, A. N., Hass, C. J., and Gregor, R. J. (2006). The effects of sloped surfaces on locomotion: a kinematic and kinetic analysis. *J. Biomech.* 39, 1621–1628.

Lay, A. N., Hass, C. J., Nichols, R. T., and Gregor, R. J. (2007). The effects of sloped surfaces on locomotion: an electromyographic analysis. *J. Biomech.* 40, 1276–1285.

Libersat, F., Clarac, F., and Zill, S. N. (1987). Force-sensitive mechanoreceptors of the dactyl of the crab: single-unit responses during walking and evaluation of function. *J. Neurophysiol.* 57, 1618–1637.

Macmillan, D. L. and Kien, J. (1983). Intra- and intersegmental pathways active during walking in the locust. *Proc. R. Soc. B* 218, 287–308.

Mamiya, A., Gurung, P., and Tuthill, J. (2018). Neural coding of leg proprioception in *Drosophila*. *bioRxiv*, https://doi.org/10.1101/274498.

Marchand, A. R., Leibrock, C. S., Auriac, M. C., Barnes, W. J. P., and Clarac, F. (1995). Morphology, physiology and in vivo activity of cuticular stress detector afferents in crayfish. *J. Comp. Physiol. A* 176, 409–424.

Marder, E. and Bucher, D. (2001). Central pattern generators and the control of rythmic movements. *Curr. Biol.* 11, R986–R996.

Markl, H. (1962). Borstenfelder an den Gelenken als Schweresinnesorgane bei Ameisen und anderen Hymenopteren. *Z. Vgl. Physiol.* 45, 475–569.

Marquardt, F. (1939). Beiträge zur Anatomie der Muskulatur und der peripheren Nerven von *Carausius (Dixippus) morosus*. *Zool. Jahrb. Abt. Anat. Ontog. Tiere* 66, 63–128.

Martin, J. P., Guo, P., Mu, L., Harley, C. M., and Ritzmann, R. E. (2015). Central-complex control of movement in the freely walking cockroach. *Curr. Biol.* 25, 2795–2803.

Matheson, T. (1992). Range fractionation in the locust metathoracic femoral chordotonal organ. *J. Comp. Physiol. A.* 170, 509–520.

Matheson, T. and Field, L. H. (1995). An elaborate tension receptor system highlights sensory complexity in the hind leg of the locust. *J. Exp. Biol.* 198, 1673–1689.

Mendes, C. S., Bartos, I., Akay, T., Márka, S., and Mann, R. S. (2013). Quantification of gait parameters in freely walking wild type and sensory deprived *Drosophila melanogaster*. *eLife* 2, e00231.

Mendes, C. S., Rajendren, S. V., Bartos, I., Márka, S., and Mann, R. S. (2014). Kinematic responses to changes in walking orientation and gravitational load in *Drosophila melanogaster*. *PLoS One* 9, e109204.

Mu, L. and Ritzmann, R. E. (2008). Interaction between descending input and thoracic reflexes for joint coordination in cockroach: I. Descending influence on thoracic sensory reflexes. *J. Comp. Physiol. A* 194, 283–298.

Newland, P. L. and Emptage, N. J. (1996). The central connections and actions during walking of tibial campaniform sensilla in the locust. *J. Comp. Physiol. A* 178, 749–762.

Nishikawa, K. et al. (2007). Neuromechanics: an integrative approach for understanding motor control. *Integr. Comp. Biol.* 47, 16–54.

Okada, R., Sakura, M., and Mizunami, M. (2003). Distribution of dendrites of descending neurons and its implications for the basic organization of the cockroach brain. *J. Comp. Neurol.* 458, 158–174.

Orlovsky, G. N., Deliagina, T. G., and Grillner, S. (1999). *Neuronal Control of Locomotion: From Mollusc to Man*. Oxford: Oxford University Press.

Page, K. L., Zakotnik, J., Dürr, V., and Matheson, T. (2008). Motor control of aimed limb movements in an insect. *J. Neurophysiol.* 99, 484–499.

Pearson, K. G. (1972). Central programming and reflex control of walking in the cockroach. *J. Exp. Biol.* 56, 173–193.

Pearson, K. G. (1995). Proprioceptive regulation of locomotion. *Curr. Opin. Neurobiol.* 5, 786–791.

Pearson, K. G. (2008). Role of sensory feedback in the control of stance duration in walking cats. *Brain Res. Rev.* 57, 222–227.

Pearson, K. G. and Fourtner, C. R. (1975). Nonspiking interneurons in walking system of the cockroach. *J. Neurophysiol.* 38, 33–52.

Pflüger, H.-J. (1980). The function of hair sensilla on the locust's leg: the role of tibial hairs. *J. Exp. Biol.* 87, 163–175.

Pflüger, H.-J., Bräunig, P., and Hustert, R. (1981). Distribution and specific central projections of mechanoreceptors in the thorax and proximal leg joints of locusts. II. The external mechanoreceptors: hair plates and tactile hairs. *Cell Tissue Res.* 216, 79–96.

Pflüger, H.-J. and Duch, C. (2011). Dynamic neural control of insect muscle metabolism related to motor behavior. *Physiology* 26, 293–303.

Pflüger, H.-J., Grillner, S., and Robertson, B. (2017). Motor pattern selection. *Neurobiology of Motor Control: Fundamental Concepts and New Directions*. Ed. by Hooper, S. L. and Büschges, A. Wiley, 177–223.

Pringle, J. W. S. (1938a). Proprioception in insects. I. A new type of mechanical receptor from the palps of the cockroach. *J. Exp. Biol.* 15, 101–113.

Pringle, J. W. S. (1938b). Proprioception in insects. II. The action of the campaniform sensilla on the legs. *J. Exp. Biol.* 15, 114–131.

Prochazka, A. (1996). Proprioceptive feedback and movement regulation. *Handbook of Physiology, Exercise: Regulation and Integration of Multiple Systems*. Ed. by Rowell, L. B. and Shepherd, J. T. American Physiological Society, 89–127.

Radnikow, G. and Bässler, U. (1991). Function of a muscle whose apodeme travels through a joint moved by other muscles: why the retractor unguis muscle in stick insects is tripartite and has no antagonist. *J. Exp. Biol.* 157, 87–99.

Reinhardt, L. and Blickhan, R. (2014). Level locomotion in wood ants: evidence for grounded running. *J. Exp. Biol.* 217, 2358–2370.

Ridgel, A. L. and Ritzmann, R. E. (2005). Effects of neck and circumoesophageal connective lesions on posture and locomotion in the cockroach. *J. Comp. Physiol. A* 191, 559–573.

Roeder, K. D. (1937). The control of tonus and locomotor activity in the praying mantis (*Mantis religiosa L.*) *J. Exp. Zool.* 76, 353–374.

Sane, S. P. and McHenry, M. J. (2009). The biomechanics of sensory organs. *Integr. Comp. Biol.* 49, i8–i23.

Schilling, M., Hoinville, T., Schmitz, J., and Cruse, H. (2013). Walknet, a bio-inspired controller for hexapod walking. *Biol. Cybern.* 107, 397–419.

Schmitz, J., Dean, J., and Kittmann, R. (1991). Central projections of leg sense organs in *Carausius morosus* (Insecta, Phasmida). *Zoomorphology* 111, 19–33.

Schmitz, J., Gruhn, M., and Büschges, A. (2015). The role of leg touchdown for the control of locomotor activity in the walking stick insect. *J. Neurophysiol.* 113, 2309–2320.

Schmitz, J. (1986a). Properties of the feedback system controlling the coxa-trochanter joint in the stick insect *Carausius morosus*. *Biol. Cybern.* 55, 35–42.

Schmitz, J. (1986b). The depressor trochanteris motoneurons and their role in the coxo-trochanteral feedback loop in the stick insect *Carausius morosus*. *Biol. Cybern.* 55, 25–34.

Schmitz, J. (1993). Load-compensating reactions in the proximal leg joints of stick insects during standing and walking. *J. Exp. Biol.* 33, 15–33.

Schmitz, J. and Stein, W. (2000). Convergence of load and movement information onto leg motoneurons in insects. *J. Neurobiol.* 42, 424–436.

Schöwerling, H. (1992). Untersuchungen zur Reflexaktivierung der Levator-Trochanteris Muskeln der Stabheuschrecke *Carausius mororsus*, Br. Thesis. Bielefeld University.

Spinola, S. M. and Chapman, K. M. (1975). Proprioceptive indentation of the campaniform sensilla of cockroach legs. *J. Comp. Physiol. A* 96, 257–272.

Sponberg, S. and Full, R. J. (2008). Neuromechanical response of musculo-skeletal structures in cockroaches during rapid running on rough terrain. *J. Exp. Biol.* 211, 433–446.

Staudacher, E. (1998). Distribution and morphology of descending brain neurons in the cricket *Gryllus bimaculatus*. *Cell Tissue Res.* 294, 187–202.

Stein, W. and Sauer, A. E. (1999). Physiology of vibration-sensitive afferents in the femoral chordotonal organ of the stick insect. *J. Comp. Physiol. A.* 184, 253–263.

Strauss, R. (2002). The central complex and the genetic dissection of locomotor behaviour. *Curr. Opin. Neurobiol.* 12, 633–638.

Tatar, G. (1976). Mechanische Sinnesorgane an den Beinen der Stabheuschrecke *Carausius morosus*. Thesis. University of Cologne.

Theophilidis, G. and Burns, M. D. (1979). A muscle tension receptor in the locust leg. *J. Comp. Physiol. A.* 131, 247–254.

Theunissen, L. M., Bekemeier, H. H., and Dürr, V. (2015). Comparative whole-body kinematics of closely related insect species with different body morphology. *J. Exp. Biol.* 218, 340–352.

Theunissen, L. M. and Dürr, V. (2013). Insects use two distinct classes of steps during unrestrained locomotion. *PLoS One* 8, e85321.

Theunissen, L. M., Vikram, S., and Dürr, V. (2014). Spatial co-ordination of foot contacts in unrestrained climbing insects. *J. Exp. Biol.* 217, 3242–3253.

Ting, L. H. and Chiel, H. J. (2017). Muscle, biomechanics, and implications for neural control. *Neurobiology of Motor Control: Fundamental Concepts and New Directions*. Ed. by Hooper, S. L. and Büschges, A. Wiley, 365–416.

Ting, L. H., Chiel, H. J., Trumbower, R. D., Allen, J. L., McKay, J. L., Hackney, M. E., and Kesar, T. M. (2015). Neuromechanical principles underlying movement modularity and their implications for rehabilitation. *Neuron* 86, 38–54.

Tsubouchi, A., Yano, T., Yokoyama, T. K., Murtin, C., Otsuna, H., and Ito, K. (2017). Topological and modality-specific representation of somatosensory information in the fly brain. *Science* 358, 615–623.

Tuthill, J. C. and Wilson, R. I. (2016). Mechanosensation and adaptive motor control in insects. *Curr. Biol.* 27, R1022–R1038.

Wahl, V., Pfeffer, S. E., and Wittlinger, M. (2015). Walking and running in the desert ant *Cataglyphis fortis*. *J. Comp. Physiol. A* 201, 645–656.

Watson, J. T. and Ritzmann, R. E. (1998). Leg kinematics and muscle activity during treadmill running in the cockroch, *Blaberus discoidalis*: I. Slow running. *J. Comp. Physiol. A* 182, 11–22.

Watson, J. T., Ritzmann, R. E., Zill, S. N., and Pollack, A. J. (2002). Control of climbing behavior in the cockroach, *Blaberus discoidalis*. I. Kinematics. *J. Comp. Physiol. A.* 188, 39–53.

Wendler, G. (1964). Laufen und Stehen der Stabheuschrecke *Carausius morosus*: Sinnesborstenfelder in den Beingelenken als Glieder von Regelkreisen. *Z. Vgl. Physiol.* 48, 198–250.

Whelan, P. J., Hiebert, G. W., and Pearson, K. G. (1995). Stimulation of the group I extensor afferents prolongs the stance phase in walking cats. *Exp. Brain Res.* 103, 20–30.

Williamson, R. and Burns, M. D. (1978). Multiterminal receptors in the locust leg. *J. Insect Physiol.* 24, 661–666.

Winter, D. A. (1990). *Biomechanics and Motor Control of Human Movement*. 2nd ed. New York: Wiley.

Winter, D. A. and Eng, P. (1995). Kinetics: our window into the goals and strategies of the central nervous system. *Behav. Brain Res.* 67, 111–120.

Wöhrl, T., Reinhardt, L., and Blickhan, R. (2017). Propulsion in hexapod locomotion: how do desert ants traverse slopes? *J. Exp. Biol.* 220, 1618–1625.

Wolf, H. (1990). Activity patterns of inhibitory motoneurones and their impact on leg movement in tethered walking locusts. *J. Exp. Biol.* 152, 281–304.

Wolf, H. (2014). Inhibitory motoneurons in arthropod motor control: organisation, function, evolution. *J. Comp. Physiol. A* 200, 693–710.

Wong, R. K. and Pearson, K. G. (1976). Properties of the trochanteral hair plate and its function in the control of walking in the cockroach. *J. Exp. Biol.* 64, 233–249.

Wosnitza, A., Bockemühl, T., Dübbert, M., Scholz, H., and Büschges, A. (2013). Inter-leg coordination in the control of walking speed in *Drosophila*. *J. Exp. Biol.* 216, 480–491.

Yox, D. P., DiCaprio, R. A., and Fourtner, C. R. (1982). Resting tension and posture in arthropods. *J. Exp. Biol.* 96, 421–425.

Zajac, F. E. (1993). Muscle coordination of movement: a perspective. *J. Biomech.* 26, 109–124.

Zakotnik, J., Matheson, T., and Dürr, V. (2006). Co-contraction and passive forces facilitate load compensation of aimed limb movements. *J. Neurosci.* 26, 4995–5007.

Zernicke, R. F. and Smith, J. L. (1996). Biomechanical insights into neural control of movement. *Handbook of Physiology, Exercise: Regulation and Integration of Multiple Systems*. Ed. by Rowell, L. B. and Shepherd, J. T. American Physiological Society, 293–330.

Zill, S. N. (1985). Plasticity and proprioception in insects. I. Responses and cellular properties of individual receptors of the locust metathoracic femoral chordotonal organ. *J. Exp. Biol.* 116, 435–461.

Zill, S. N., Büschges, A., and Schmitz, J. (2011). Encoding of force increases and decreases by tibial campaniform sensilla in the stick insect, *Carausius morosus*. *J. Comp. Physiol. A* 197, 851–867.

Zill, S. N., Chaudhry, S. S., Dallmann, C. J., Hoinville, T., Schmitz, J., and Büschges, A. (2017a). Generation and utilization of sensory signals encoding force decreases in insect legs. *Proceedings of the 47th Annual Meeting of the Society for Neuroscience*. Washington, D.C.

Zill, S. N., Chaudhry, S., Büschges, A., and Schmitz, J. (2013). Directional specificity and encoding of muscle forces and loads by stick insect tibial campaniform sensilla, including receptors with round cuticular caps. *Arthropod Struct. Dev.* 42, 455–467.

Zill, S. N., Chaudhry, S., Büschges, A., and Schmitz, J. (2015). Force feedback reinforces muscle synergies in insect legs. *Arthropod Struct. Dev.* 44, 541–553.

Zill, S. N., Chaudhry, S., Exter, A., Büschges, A., and Schmitz, J. (2014). Positive force feedback in development of substrate grip in the stick insect tarsus. *Arthropod Struct. Dev.* 43, 441–455.

Zill, S. N., Keller, B. R., and Duke, E. R. (2009). Sensory signals of unloading in one leg follow stance onset in another leg: transfer of load and emergent coordination in cockroach walking. *J. Neurophysiol.* 101, 2297–2304.

Zill, S. N. and Moran, D. T. (1981a). The exoskeleton and insect proprioception. I. Responses of tibial campaniform sensilla to external and muscle-generated forces in the American cockroach, *Periplaneta americana*. *J. Exp. Biol.* 91, 1–24.

Zill, S. N. and Moran, D. T. (1981b). The exoskeleton and insect proprioception. III. Activity of tibial campaniform sensilla during walking in the American cockroach, *Periplaneta americana*. *J. Exp. Biol.* 94, 57–75.

Zill, S. N., Neff, D., Chaudhry, S., Exter, A., Schmitz, J., and Büschges, A. (2017b). Effects of force detecting sense organs on muscle synergies are correlated with their response properties. *Arthropod Struct. Dev.* 46, 564–578.

Zill, S. N., Schmitz, J., and Büschges, A. (2004). Load sensing and control of posture and locomotion. *Arthropod Struct. Dev.* 33, 273–286.

Zill, S. N., Schmitz, J., Chaudhry, S., and Büschges, A. (2012). Force encoding in stick insect legs delineates a reference frame for motor control. *J. Neurophysiol.* 108, 1453–1472.

Zollikofer, C. P. E. (1994). Stepping patterns in ants. I. Influence of speed and curvature. *J. Exp. Biol.* 192, 95–106.

Chapter 2

Joint torques during level walking

This chapter was published with minor modifications as a research article in Proceedings of the Royal Society B: *Dallmann, C. J., Dürr, V. and Schmitz, J. (2016). Joint torques in a freely walking insect reveal distinct functions of leg joints in propulsion and posture control. Proc. R. Soc. B 283, 20151708*. C.J.D. and J.S. conceived the study; C.J.D. performed experiments and analyzed data; C.J.D., V.D. and J.S. interpreted results; C.J.D. prepared figures; C.J.D. drafted the manuscript; C.J.D., V.D. and J.S. revised the manuscript and gave final approval for publication. Supplementary videos and data are available online at rspb.royalsocietypublishing.org/content/283/1823/20151708 and www.nytimes.com/2016/02/15/science/stick-insect-helps-scientists-study-how-animals-move.html.

2.1 Abstract

Determining the mechanical output of limb joints is critical for understanding the control of complex motor behaviors such as walking. In the case of insect walking, the neural infrastructure for single-joint control is well described. However, a detailed description of the mechanical output in form of time-varying joint torques is lacking. Here, we determine joint torques in the stick insect to identify leg joint function in the control of body height and propulsion. Torques were determined by measuring whole-body kinematics and ground reaction forces in freely walking animals. We demonstrate that despite strong differences in morphology and posture, stick insects show a functional division of joints similar to other insect model systems. Propulsion was generated by strong depression torques about the coxa-trochanter joint, not by retraction or flexion/extension torques. Torques about the respective thorax-coxa and femur-tibia joints were often directed opposite to fore-aft forces and joint movements. This suggests a posture-dependent mechanism that counteracts collapse of the leg under body load and directs the resultant force vector such that strong depression torques can control both body height and propulsion. Our findings parallel propulsive mechanisms described in other walking, jumping and flying insects and challenge current control models of insect walking.

2.2 Introduction

Understanding the control of complex motor behaviors such as walking requires an understanding of the mechanical output during unrestrained locomotion. In the case of walking, the integrated actions of the nervous, muscular and skeletal systems are reflected in net torques about the leg joints. Joint torques are thus a critical measure in the study of motor control (Winter 1990).

Joint torques in walking are well described in humans (Winter 1990) and a number of other vertebrates (e.g., Andrada et al. 2010; Blob and Biewener 2001; Fowler et al. 1993; Sheffield and Blob 2011; Witte et al. 2002). However, similarly detailed descriptions of joint torques in invertebrates are lacking, in part because their relatively small legs complicate the measures required for inverse dynamics calculations. This is unfortunate, because detailed knowledge exists about the neural mechanisms of movement generation in invertebrates. In insects, much of the neural infrastructure driving the basic rhythmic motor activity of leg joints has been studied, including modulatory influences of sensory feedback (reviewed in Büschges and Gruhn 2007; Büschges 2012). Moreover, the control potential of muscles and skeletal structures has been demonstrated

(e.g., Ache and Matheson 2013; Ahn and Full 2002; Hooper et al. 2009; Sponberg et al. 2011). Although ground reaction forces have been measured in several insects species, including crickets (Harris and Ghiradella 1980), cockroaches (Full et al. 1991), ants (Reinhardt and Blickhan 2014) and stick insects (Cruse 1976), to date, no study could resolve both the magnitude and timing of joint torques in detail, let alone their variability during unrestrained locomotion. Therefore, our view of how the joints of an insect leg interact to control propulsion and body height in walking largely depend on kinematic findings. Kinematic analyses have provided much insight into spatial (Theunissen et al. 2014) and temporal (Dürr 2005) patterns of coordination in locomotion. However, they cannot reveal the functional contributions of single leg joints to a movement (Winter 1990). This is because in a mechanically coupled system, a given joint movement can be produced by multiple patterns of joint torques.

To unravel the relative contributions of single leg joints to the overall body dynamics, we choose to study the stick insect (*Carausius morosus*, Figure 2.1A). Next to the cockroach, the stick insect is a major model system for walking control in invertebrates (Ritzmann and Büschges 2007) and biomimetic hexapod robots (Dürr et al. 2004). The slow and adaptive joint movements of its unspecialized walking legs rely heavily upon sensory feedback, making them ideal candidates to study the sensory control of legged locomotion. Methodologically, the relatively long and sprawled legs facilitate ground reaction force measurements (Cruse 1976) and whole-body motion capture in locomotion (Theunissen and Dürr 2013). Here, we exploit these benefits to estimate the torques of all of its leg joints in unrestrained level walking. Our objectives are (i) to attribute functions to each leg joint in propulsion and body weight support, (ii) to test whether these functions reflect distinctly different leg postures in cockroaches and stick insects, and (iii) to identify potential commonalities of walking control and the control of other forms of locomotion, jumping in particular.

When judging on leg posture and kinematics alone, the function of individual leg joints appear to be very different among species and forms of locomotion. For example, the stick insect holds its legs out to the side of the body and moves its leg joints within an almost vertically oriented leg plane (Figure 2.1A), similar to sprawled-posture vertebrates (Blob and Biewener 2001; Sheffield and Blob 2011). This is different from the cockroach, where the hind legs move in a plane that is nearly horizontal (Kram et al. 1997), and different from the locust, where the specialized jumping legs are held upright, but parallel to the body (Burns 1973). In light of these differences, the leg joints of the stick insect are expected to control propulsion and body height quite differently. Here, we show that this is not the case, and that joint torques in stick insect legs suggest a functional division of joints for propulsion and posture control similar to that seen in

other animals and other forms of locomotion.

2.3 Methods

We tested 12 adult, female stick insects (*Carausius morosus*) reared in a laboratory colony (body mass: 0.8 $\pm$ 0.1 g, mean $\pm$ s.d; body length without antennae: approx. 75 mm; Figure 2.1A). Animals walked along a horizontal walkway (40 $\times$ 500 mm) and, during successful trials, stepped onto one of five integrated miniature force plates with their right hind, middle or front leg (Figure 2.1B). To determine joint torques, motion and force data were combined in a three-dimensional rigid link model of the leg (Figure 2.1C).

2.3.1 Motion capture

Body and leg motions were captured and reconstructed as described in Theunissen and Dürr (2013). In brief, we used a marker-based motion capture system, comprising eight infrared high-speed cameras (Vicon MX10 with T10 cameras, controlled by software Nexus 1.4.1; Vicon, Oxford, UK). The system automatically tracked the positions of lightweight retro-reflective markers (diameter: 1.5 mm; mass: 4 mg) at 200 Hz. Camera lenses had a focal length of 25 mm and were approximately 1.2 m away from the setup. The resulting spatial accuracy of three-dimensional marker trajectories was approximately 0.1 mm. One marker was attached to each femur (mass: approx. 9 mg) and tibia (mass: approx. 4 mg), three markers were attached to the metathorax, and one maker was attached to the mesothorax and prothorax (Figure 2.1A). Note that the additional mass of the leg markers did not affect torque calculations (supplementary information 2.6, Figure 2.6). The kinematic model was obtained by direct analytical calculations from segment dimensions and positions of all markers on the segments, which were measured from high-resolution photographs (approx. 0.02 mm per pixel). As the Vicon system recorded marker trajectories only, we used an additional digital video camera (Basler A602fc, Ahrensburg, Germany) to record a complementary, synchronized side view of the walkway at 50 Hz for visual validation of the kinematic analysis.

Marker coordinates were post-processed in Matlab (The MathWorks, Natick, MA, USA). Time courses were low-pass filtered using a zero-lag, fourth-order Butterworth filter with a cut-off frequency of 20 Hz. Kinematic calculations were based on a main kinematic chain for the thoracic segments and a kinematic side chain for each leg as described in Theunissen and Dürr (2013). We defined a body-fixed coordinate system [x, y, z] based on the three markers on the metathorax. It originated in the insect's center

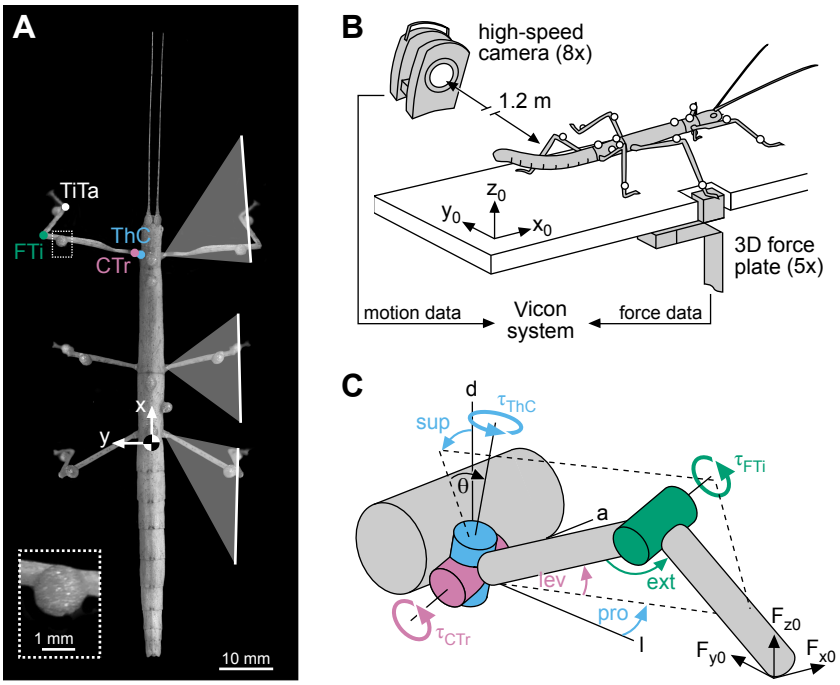

Figure 2.1: Torque calculations in stick insect legs
(**A**) The stick insect *Carausius morosus* with motion-capture markers. Motion of each leg is driven by three main joints: the thorax-coxa (ThC, blue) joint and the coxa-trochanter (CTr, purple) joint, which together act as the "hip," and the femur-tibia (FTi, green) joint, which acts as the "knee." White lines indicate average movement ranges of legs. (**B**) Whole-body motion capture was combined with ground reaction force measurements of single legs as animals walked freely along a horizontal walkway (one of eight Vicon cameras and one of five force plates are shown). (**C**) Rigid link model of a leg used for joint torque calculations. The ThC joint is slanted relative to the vertical body axis ($\theta = 30°$). Positive torques (τ) about this joint supinate (sup) and protract (pro) the leg. Positive torques about the CTr and FTi joint lift the femur (lev) and extend the tibia (ext) within the leg plane (dashed lines), respectively. a, anterior; l, lateral; d, dorsal.

of mass (COM) at the metathoracic-abdominal joint. The axes of the coordinate system were defined such that x points toward the head (fore-aft), y toward the left body side (medio-lateral) and z upward (dorso-ventral) (Figure 2.1A).

2.3.2 Force measurements

Single leg ground reaction forces were recorded at 1000 Hz with a resolution of approximately 0.05 mN using strain-gauge-based force plates (Lévy and Cruse 2008). Each force plate detected normal and horizontal forces along the three axes of the global coordinate system [x_0, y_0, z_0]. The axes of this coordinate system were defined relative to the walkway (Figure 2.1B). Forces along each axis were measured by two strain gauges, one attached to the front and one attached to the backside of a thin spring steel strip. To measure forces along all axes, three strips were connected perpendicularly to each other. The uppermost strip was oriented parallel to the ground. It carried a piece of balsa wood

(5 × 5 mm contact area), which served as a firm foothold for the tarsus during walking (Figure 2.1B). With a stiffness greater than 20 mN mm^{-1} in each direction, the force plates were considered hard ground. Signals from the strain gauges were amplified, A/D converted, fed into the Vicon system for synchronization, and post-processed in Matlab.

Time courses of forces were expressed in mN based on calibration data for each force plate. Calibration data were obtained prior to experimentation by applying known loads in the range of ±30 mN along x_0, y_0 and z_0. The relation between force and output voltage was linear in all directions. All time courses were low-pass filtered with a fourth-order, zero-lag Butterworth filter with cut-off frequencies of either 12.5 or 25 Hz, which were chosen based on fast Fourier transforms of the raw force signals. Signal drift within a single stance phase (approx. 700 ms) was negligible. Filtered data were corrected for a possible offset in each trial, based on a 200 ms time window prior to the touch-down of the leg. Due to the mechanical arrangement of the steel strips, there was a constant 50% cross-talk between forces measured along x_0 and z_0, which could be corrected by subtraction. Touch-down and lift-off events for each step were determined manually based on the normal force component. To combine motion and force data for torque calculations (below), data were normalized to the duration of the respective stance phase, using cubic spline interpolation. In the Results section, forces are expressed as action (not reaction) forces in body-fixed coordinates $[x, y, z]$.

2.3.3 Rigid link model for torque calculations

In stick insects, motion of each leg is driven by three joints (Figure 2.1A). The thorax-coxa (ThC) joint and the coxa-trochanter (CTr) joint together act as the "hip." The femur-tibia (FTi) joint acts as the "knee." Torques about these joints were determined from a three-dimensional rigid link model with three degrees of freedom (Figure 2.1C). The CTr and FTi joints were approximated as hinges with one degree of freedom each. They provide levation-depression and extension-flexion of the leg, respectively. Both joints move in the same plane, the leg plane (dashed line in Figure 2.1C). The ThC joint has actually three degrees of freedom, similar to a ball-and-socket joint. However, most of the movement around this joint is described by the coupled protraction-retraction and supination-pronation of the leg plane (Cruse and Bartling 1995). The ThC joint axis can thus be modeled as a single slanted axis (i.e., one degree of freedom). The tibia-tarsus (TiTa) joint was used as an estimate of the foot contacting the ground, because motion capture markers cannot be placed on the tarsus without restraining its movements. Owing to the short length of the coxa (approx. 1.5 mm) and associated difficulties in measuring its orientation accurately within the leg plane, we applied two further model simplifications. First, the ThC joint was considered slanted with respect to the vertical

body axis by $\theta = 30^\circ$ (see also Cruse and Bartling 1995). Second, the CTr joint was considered to be directly connected to the thorax, such that, with regard to leg depression, the torques about the ThC and CTr joints were lumped together. These model simplifications were justified and did not affect the conclusions reached in this study (supplementary information 2.6, Figures 2.6–2.9).

Torques about the leg joints ($\tau = [\tau_{ThC}, \tau_{CTr}, \tau_{FTi}]$) were calculated as external torques, assuming quasi-static dynamics. Torques due to gravity and inertia were negligible (supplementary information 2.6, Figure 2.6). We combined the orientations and positions of the joints (manipulator Jacobian J) with the three-dimensional force vector ($F = [F_{x0}, F_{y0}, F_{z0}]$) measured at the foot according to Spong et al. (2006)

$$\tau = J^T F \tag{2.1}$$

$$\text{with } J = [a_{ThC} \times (p_{TiTa} - p_{ThC}) a_{CTr} \times (p_{TiTa} - p_{CTr}) a_{FTi} \times (p_{TiTa} - p_{FTi})] \tag{2.2}$$

where a is the rotational *axis* of a joint and p its *position* in global coordinates. Note that $p_{CTr} = p_{ThC}$ in our model. Positive torques about the slanted ThC joint protract and supinate the leg; positive torques about the CTr and FTi joint lift the femur and extend the tibia, respectively (Figure 2.1C). To illustrate whether or not a joint rotated in the direction of the applied torque, we calculated each joint's mechanical power as the dot product of the joint's net torque and its angular velocity. To obtain a single angular velocity for the ThC joint (instead of two for the protraction and supination angle), we took the first derivative of the angle describing the rotation of the leg plane around the slanted ThC joint axis.

2.3.4 Statistical analysis

In the Results section, we first infer the contributions of individual leg joints to propulsion and body weight support from grand mean time courses (mean of animal means). Individual animals contributed at least 17 steps to an animal mean. Grand means of hind, middle and front legs were calculated from N = 9, N = 10 and N = 6 animal means, respectively.

To assess whether the shape of the grand mean was representative of the more variable single steps, we calculated the minimum accumulated cost (c) between single-step (s) and grand mean (m) time courses of torques. Unlike a simple point-by-point comparison, which results in large differences if two time series have the same shape but are shifted in time, the minimum accumulated cost allows for temporal variation by "synchronizing" the time series (Figure 2.5A, inset). Therefore, it represents a mean-

ingful measure of time course similarity. The accumulated cost was calculated using dynamic programming according to Rabiner and Juang (1993)

$$c(i,j) = d(s_i, m_j) + min[c(i-1, j-1), c(i-1, j), c(i, j-1)] \tag{2.3}$$

where d is the Euclidian *distance* between the value of s at time i (i = 1, 2,...,100% stance) and the value of m at time j (j = 1, 2,...,100% stance), and *min* is the *minimum* of cumulative distances of adjacent time points. To compare across joints and legs, the accumulated cost was normalized to the peak-to-peak amplitude of the respective grand mean, resulting in the variability index shown in Figure 2.5A. In calculating the accumulated cost, repeated measures of an animal were treated as independent observations and pooled across animals. Sample sizes for right hind, middle and front legs were n = 429, n = 270 and n = 142 steps, respectively. Statistical tests were performed using Matlab and R (R Core Team, www.R-project.com).

2.4 Results

To study the functions of insect leg joints during free walking, we determined joint torques in the legs of stick insects. Animals walked along a horizontal walkway (Figure 2.1B) at an intermediate forward velocity of 42 $\pm$ 10 mm/s (mean $\pm$ s.d.; n = 841 stance phases from N = 12 animals, pooled across legs). Typically, four legs were in ground contact at any time. Average stance and swing phase durations were 697 $\pm$ 190 ms and 254 $\pm$ 89 ms, respectively. The average stride frequency was 1.1 $\pm$ 0.2 strides/s.

We will focus on the two major motor tasks in this walking situation: body weight support and propulsion. The control of medio-lateral balance is discussed in supplementary information 2.6.

2.4.1 Body weight support

We hypothesized that torques about the CTr joint support the body weight, because this joint depresses the leg. We therefore expected the time courses of CTr torques to positively correlate with the time courses of the vertical leg forces.

The magnitude of vertical forces differed substantially between hind and middle legs, which moved close to the body's COM, and front legs (see also Cruse 1976). Peak forces in hind legs (-4.2 ± 0.6 mN, grand mean $\pm$ s.d. of animal means, N = 9) and middle legs (-4.8 ± 0.6 mN, N = 10) supported about 50% body weight each (Figures 2.2B and 2.3B). In contrast, peak forces in front legs (-1.6 ± 0.4 mN, N = 6) supported only about 20% body weight (Figure 2.4B). As expected, the time courses of

Table 2.1: Correlations between time courses of joint torques and leg forces (grand means).[a]

	hind leg		middle leg		front leg	
	r-value	p-value	r-value	p-value	r-value	p-value
τ_{ThC} versus F_x	0.19	$0.06^{(4/9)}$	−0.90	$<0.001^{(10/10)}$	−0.14	$0.17^{(1/6)}$
τ_{CTr} versus F_z	0.96	$<0.001^{(9/9)}$	1.00	$<0.001^{(10/10)}$	0.93	$<0.001^{(6/6)}$
τ_{FTi} versus F_x	0.28	$<0.01^{(6/9)}$	0.07	$0.47^{(2/10)}$	0.91	$<0.001^{(6/6)}$

[a]The superscripts following the p-values denote the number of individuals with the same correlation result (positive, negative or no correlation) as the grand means.

vertical forces and CTr torques correlated strongly for both grand means and per-animal means (Table 2.1; $p < 0.001$ each). CTr torques were directed toward leg depression throughout the stance phase ($\tau_{CTr} < 0$; Figures 2.2–2.4C). Peak torques in hind legs (-57.7 ± 6.6 μNm) and middle legs (-54.0 ± 8.8 μNm) were similarly high and much stronger than in front legs (-22.7 ± 6.0 μNm). These results corroborate the kinematic prediction that torques about the CTr joint are critical for body weight support.

2.4.2 Propulsion

We hypothesized that the proximal ThC joint and the distal FTi joint control propulsion, because all legs were substantially retracted and flexed/extended about these joints (Figures 2.2–2.4A). We therefore expected the time courses of ThC and FTi torques to positively correlate with the time courses of the fore-aft leg forces. Unexpectedly, correlations were generally weak (Table 2.1).

In hind legs, fore-aft forces were directed backward to propel the body until the end of the stance phase ($F_x < 0$; Figure 2.2B; see also Cruse 1976). Torques about the ThC joint, however, only initially pointed toward retraction ($\tau_{ThC} < 0$; Figure 2.2C). ThC torques peaked at approximately 30% of the stance phase (-16.3 ± 4.1 μNm), but were small or even switched toward protraction when propulsive forces were highest (Figure 2.2C, arrow). Accordingly, the mechanical power at the ThC joint peaked at approximately 30% of the stance phase and declined to zero thereafter (Figure 2.2D). Although the leg was extended throughout the stance phase (*ext* increased to 150°), torques about the FTi joint pointed toward flexion during the second half ($\tau_{FTi} < 0$; Figure 2.2C, arrow). Accordingly, the mechanical power was negative during this time. Torques about the ThC and FTi joints therefore correlated only weakly with the fore-aft forces of the leg. At the CTr joint, on the other hand, the mechanical power peaked at the time of maximum propulsive force (approx. 80% stance phase; Figure 2.2D). These

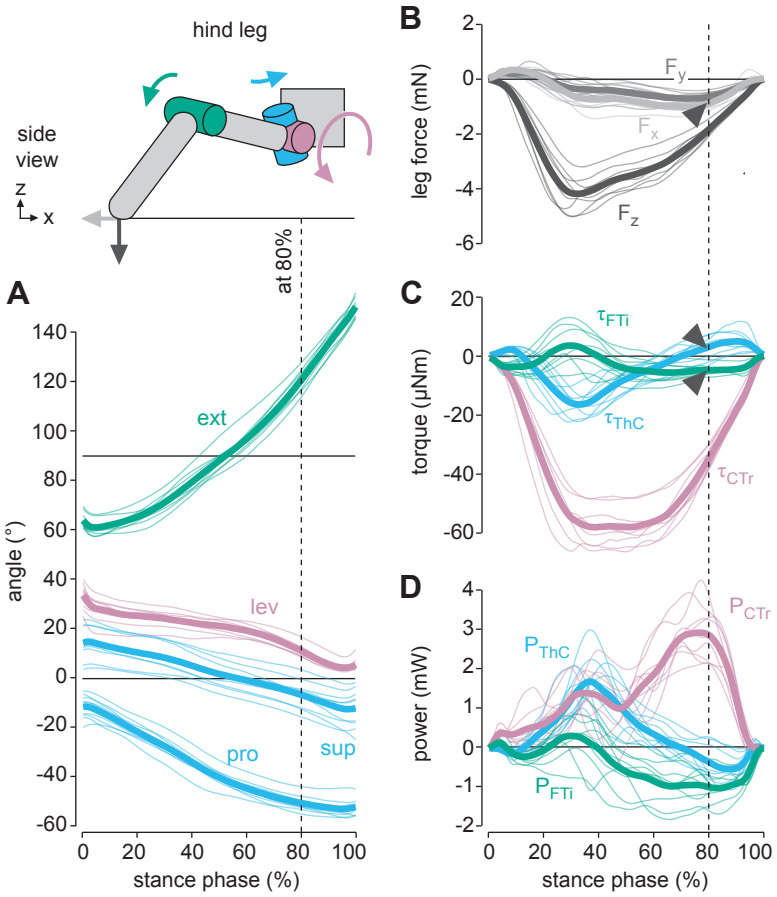

Figure 2.2: Kinematics and dynamics of hind legs
Angles (**A**), torques (**C**) and mechanical power (**D**) of the main leg joints together with ground action forces of the leg (**B**) during the stance phase. Thin lines show means of individual animals (N = 9). Bold lines show the grand mean. The schematic illustrates the kinematics and dynamics of the hind leg at 80% of the stance phase, when the propulsive force (F_x) was highest (arrow in **B**). Torques about the ThC and FTi joints counteracted the movement of the leg segments at this time (arrows in **C**). See online electronic supplementary material, Video S1, for an animation.

results suggest that propulsive fore-aft forces in hind legs resulted to a large extent from strong CTr torques pressing down the extended leg and, in turn, extending the tibia (see also electronic supplementary material, Video S1).

In middle legs, fore-aft forces were mainly directed forward ($F_x > 0$) to decelerate the body, and switched to backward directed propulsive forces ($F_x < 0$) only near the end of the stance phase (Figure 2.3B; see also Cruse 1976). Torques about the ThC joint, however, first pointed toward retraction, then toward protraction—opposite to the fore-aft forces measured on the ground (Figure 2.3C, arrow). Time courses of ThC torques were in fact strongly negatively correlated with the fore-aft forces for both grand means and per-animal means (Table 2.1; $p < 0.001$ each). The time point at which the ThC torque switched from net retraction to net protraction could be predicted by the time point at which the leg plane switched from supination to pronation (linear regression on

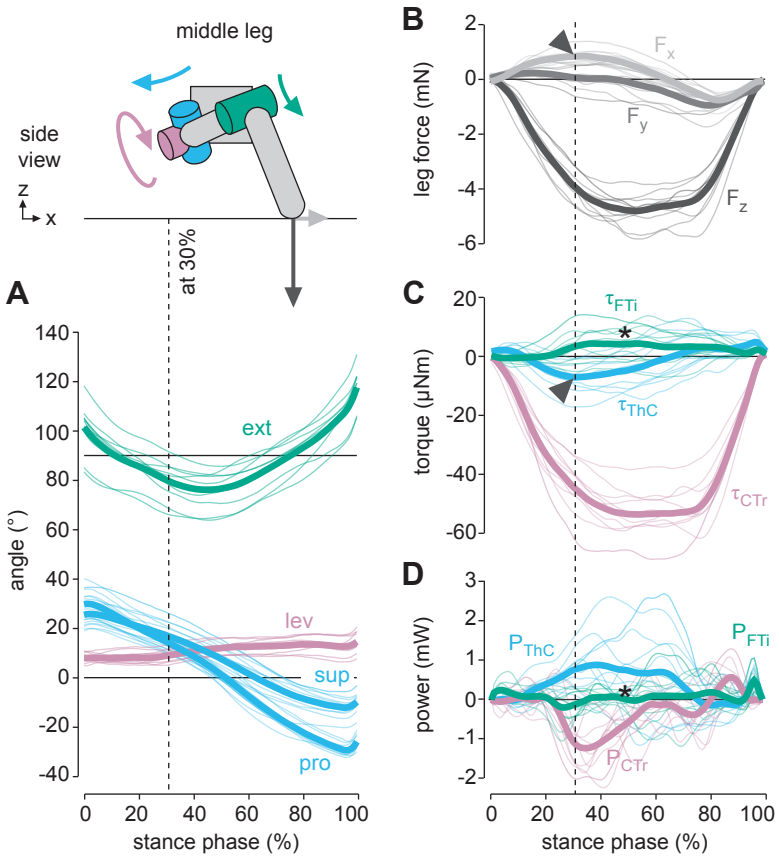

Figure 2.3: Kinematics and dynamics of middle legs
Angles (**A**), torques (**C**) and mechanical power (**D**) of the main leg joints together with ground action forces of the leg (**B**) during the stance phase. Thin lines show means of individual animals (N = 10). Bold lines show the grand mean. The schematic illustrates the kinematics and dynamics of the middle leg at 30% of the stance phase, when the braking force (F_x) was highest (arrow in **B**). Torques about the ThC joint counteracted the fore-aft force at this time (arrow in **C**). Asterisks in **C** and **D** mark the variability at the FTi joint, with time courses of opposing signs largely canceling each other out in the grand mean. See electronic supplementary material, Video S2, for an animation.

per-animal means; d.f. = 8, $p < 0.001$, $R^2 = 0.77$). Notably, torques about the FTi joint were highly variable (see below). The variability can be seen in Figure 2.3C (asterisk), where the grand mean shows only a small net extension torque because animal means of opposing signs largely cancelled each other out. Therefore, the correlation between time courses of FTi torques and fore-aft forces was weak (Table 2.1). Unexpectedly, fore-aft forces resulted again to a large extent from CTr torques. Strong depression torques reduced propulsion at the beginning of stance when the leg plane was supinated ($sup > 0$) and increased propulsion late in stance when the leg plane was pronated ($sup < 0$) (see also electronic supplementary material, Video S2). Accordingly, the time point at which the fore-aft force switched from pointing forward to pointing backward could be predicted by the time point at which the leg plane switched from supination to pronation (linear regression on per-animal means; d.f. = 8, $p < 0.01$, $R^2 = 0.65$).

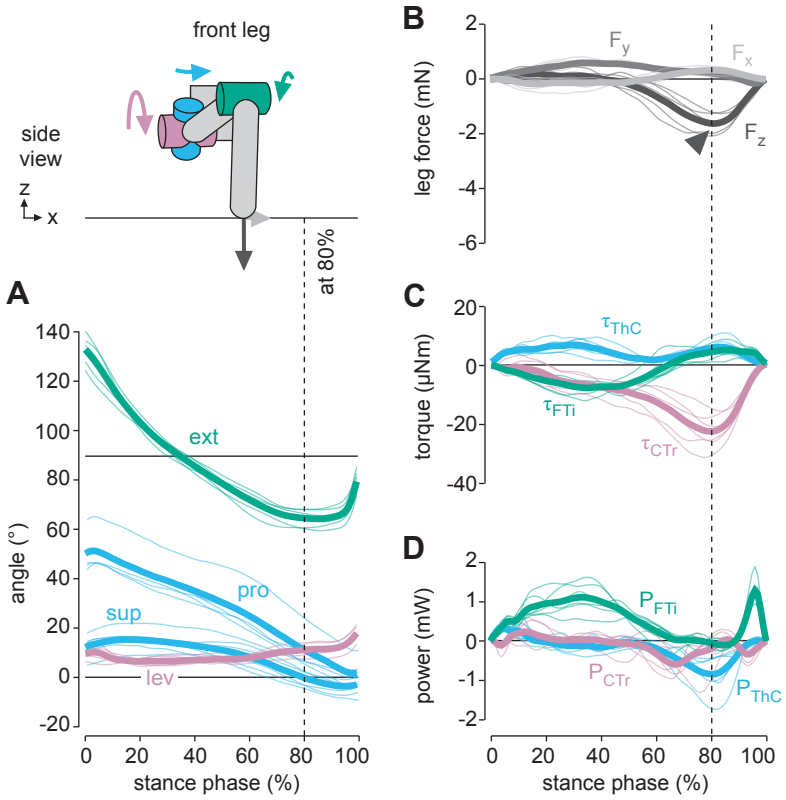

Figure 2.4: Kinematics and dynamics of front legs
Angles (**A**), torques (**C**) and mechanical power (**D**) of the main leg joints together with ground action forces of the leg (**B**) during the stance phase. Thin lines show means of individual animals (N = 6). Bold lines show the grand mean. The schematic illustrates the kinematics and dynamics of the front leg at 80% of the stance phase, when the vertical force (F_z) was highest. The arrow in **B** marks the relatively weak contribution to body weight support compared with hind and middle legs. Note that in some steps small positive vertical forces in the first half of stance resulted from the body being pulled forward. See electronic supplementary material, Video S3, for an animation.

These results suggest that depression torques about the CTr joint of hind and middle legs were critical for generating propulsion, in addition to supporting the body weight. Contrary to kinematic predictions, torques about the ThC and FTi joints contributed relatively little to propulsion in these legs and were often directed opposite to the movement of the leg segments. Only the relatively small propulsive forces of front legs were generated by torques about the FTi joint (Figure 2.4 and electronic supplementary material, Video S3). Torques toward flexion ($\tau_{FTi} < 0$) pulled the animal forward in the first half of the stance phase when the leg moved more in parallel to the long body axis. Correlations between time courses of FTi torques and fore-aft forces were significant in all animals (Table 2.1; $p < 0.001$).

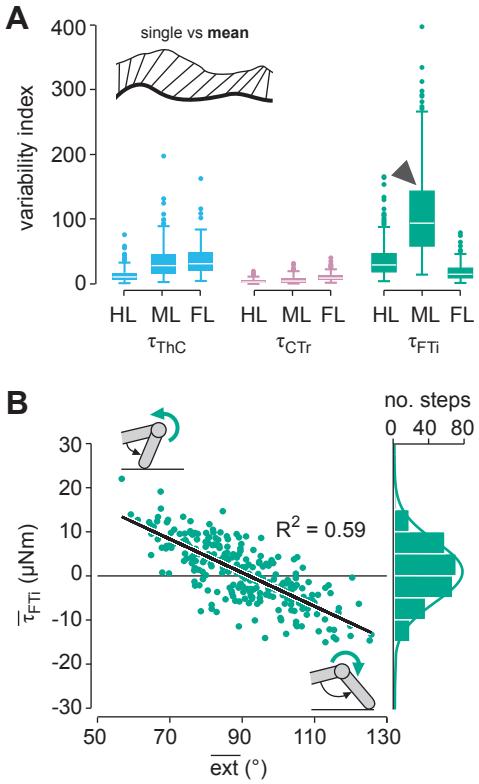

Figure 2.5: Joint torque variability during level walking
(**A**) Dissimilarity between single step and grand mean time courses of joint torques as a measure of step-to-step variability. Variability was particularly high at the middle leg's FTi joint (arrow). HL, hind leg (n = 429 steps from N = 9 animals); ML, middle leg (n = 270 steps from N = 10 animals); FL, front leg (n = 142 steps from N = 6 animals). (**B**) At the middle leg's FTi joint, torque magnitudes were negatively correlated with the net extension of the tibia so as to counteract deviations from the neutral posture at 90°.

2.4.3 Joint-specific variability

Torques about the middle leg's FTi joint appeared to be more variable than at any other joint. To analyze this observation statistically and compare across joints and legs, we assessed the variability of joint torques by comparing the shape of the grand mean time course to the time courses of single steps (see Methods). The resulting variability index differed significantly among joints (ANOVA for steps pooled across animals; $F_{8,2514} = 403.25$, $p < 0.001$) and was indeed highest for the middle leg's FTi joint (Figure 2.5A, arrow; Tukey's HSD tests at the 0.05 level of significance). Torques about this joint varied considerably from step to step, spanning a large continuum from net flexion to net extension (Figure 2.5B, histogram). Opposite time courses of torques were measured at the middle leg FTi joints of all animals, but did not occur at any of the other leg joints. A large part of the variability could be accounted for by step-to-step variations in the orientation of the tibia within the leg plane. For each step, we averaged the FTi torque and the extension angle across each stance phase to give the net torque magnitude and

the net tibia orientation. Torques tended to counteract a deviation from a tibial angle of 90° relative to the femur (*ext* = 90°), which is the neutral posture of the tibia (Figure 2.5B). That is, high torques toward flexion ($\tau_{\mathrm{FTi}} < 0$) tended to occur when the tibia was strongly extended (*ext* > 90°) and, vice versa, high torques toward extension ($\tau_{\mathrm{FTi}} > 0$) tended to occur when the tibia was strongly flexed (*ext* < 90°). A linear regression on steps pooled across animals was significant (d.f. = 268, $p < 0.001$, $R^2 = 0.59$; Figure 2.5B), as were the 10 per-animal regressions ($p < 0.01$ each).

In contrast to the FTi joint of the middle leg, the variability of torques about the other leg joints was related to smaller variations in timing and magnitude, such that the grand means captured the general shape of the time course. Linear correlations between torque magnitudes and any one postural parameter or walking speed were weak at these joints (data not shown). Smaller variations likely resulted from cumulative effects, which may include variable activation dynamics of insect muscle (Hooper et al. 2006), variable stance phase durations of the other legs, and other causes.

2.5 Discussion

We have determined complete time courses of joint torques in all legs of freely walking stick insects with a precision and resolution that was previously available only in vertebrate experiments. We found that the leg joints contributed differently to propulsion and body weight support (Figures 2.2–2.4), and that some joint torques were highly flexible (Figure 2.5).

2.5.1 Unexpected joint functions in walking stick insects

Unexpectedly, walking stick insects generated propulsive forces mainly by the same action that also supported the body weight against gravity: depression of their hind and middle leg femora. Owing to the pronation of the leg plane with regard to the vertical, hind legs could accelerate the body by CTr torques that depressed the femur and, in turn, extended the tibia (Figure 2.2). Similarly, middle legs decelerated or accelerated the body by CTr torques whenever the leg plane was supinated or pronated, respectively (Figure 2.3). These mechanisms were not directly predicted from kinematics, because all legs are retracted and flexed/extended around the ThC and FTi joints in the direction expected for propulsion. Instead, ThC and FTi torques were often directed opposite to the movement of the leg segments or the fore-aft forces measured on the ground. Albeit counterintuitive at first sight, these torque patterns can be explained by a posture-dependent mechanism that counteracts gravity-induced collapse of the leg under body

load. For example, further extension of a highly extended leg is counteracted by a flexion torque, as seen in hind and middle legs (Figures 2.2C and 2.5B). Similarly, further supination of an already supinated middle leg is counteracted by a retraction torque (Figure 2.3C). The requirement for torques counteracting the effects of gravity is similar in sprawled-posture vertebrates that lift their body above the ground (Blob and Biewener 2001; Sheffield and Blob 2011). Upright/sagittal postures like those of humans typically require extension torques to counteract gravity-induced flexion of the leg joints (Winter 1980).

2.5.2 Common principles in locomotion control: power and steering units

Although details of stick insect joint torques might reflect specializations to meet the animal's distinct morphology and posture, the mechanism of controlling propulsion by means of femoral depression likely reflects a more common principle in locomotion.

Cockroaches, for example, move their hind legs in a plane that is more horizontal than vertical (Kram et al. 1997), very different to stick insects. In this posture, depression of the femur results not only in a downward but also a rearward push, which generates thrust. Accordingly, activity patterns of the cockroach depressor trochanteris muscle were interpreted in control of both body weight support and propulsion (Noah et al. 2004; Watson and Ritzmann 1998). Our measurements predict a similar role for the depressor trochanteris muscle in the stick insect. Despite substantial differences in leg posture and kinematics, the two major model systems in insect walking appear to control propulsion more similarly than previously thought.

At a more conceptual level, the ThC and FTi joints serve the leg to maintain a particular pushing direction, thus "steering" the power provided by the CTr joint to control walking. An analogous functional division into "power" and "steering" joints has been found in the control of insect escape jumps (Sutton and Burrows 2008; Sutton and Burrows 2010). Locusts, for example, power their jumps with torques about the FTi joint and steer by controlling jump elevation with the ThC joint (Sutton and Burrows 2008). Froghoppers power their jumps with torques about the CTr joint and steer by controlling jump azimuth with the FTi joint (Sutton and Burrows 2010). In a similar vein, large indirect flight power muscles of most insects provide the mechanical energy required for flapping the wings, while smaller steering muscles determine its transformation into lift and drag by adjusting the stroke plane and the wing's angle of attack (Balint and Dickinson 2001; Walker et al. 2014). Our findings provide the prospect that such a control strategy is also common in walking insects with distinctly different leg posture and kinematics. Note that this does not necessarily imply a total functional separation into power and steering units. Insect flight power muscles, for example, can modulate

steering as well (Lehmann et al. 2013; Sponberg and Daniel 2012). And in the case of stick insect walking, the anatomically complex ThC joint could assist the CTr joint in body support and depression-driven propulsion if it was modeled with more than one degree of freedom (see supplementary information 2.6).

2.5.3 Implications of joint torques for models of walking control

Current models of sensory control of insect walking incorporate both behavior-derived mechanisms (Dürr et al. 2004) and physiological mechanisms inferred from reduced preparations (Büschges 2012). While these models replicate basic joint kinematics (Ekeberg et al. 2004), some control aspects may have to be revised to account for the joint torques in free walking.

One aspect concerns the timing of step phase transitions. Our data suggest that load signals from the CTr joint might be more suitable in this regard than proprioceptive signals from the other leg joints, from the FTi joint (Büschges and Gruhn 2007) in particular. This is because CTr joint torques were comparatively high and invariable (see low step-to-step variability in Figure 2.5A). High torques are a consequence of the horizontal posture of the trochantero-femur, being nearly orthogonal to the resultant ground reaction force vector. This situation is very similar to that in sprawled-posture vertebrates (Blob and Biewener 2001; Sheffield and Blob 2011). From a mechanical perspective, high CTr torques and associated high strains in the trochantero-femur may seem undesirable. Fast running cockroaches, for example, appear to minimize the total amount of torques produced by the leg joints (Full et al. 1991). From a control perspective, on the other hand, strong and reliable changes in CTr torques may facilitate the control of stance by means of local load sensors. Indeed, strain sensors in the form of campaniform sensilla are highly concentrated near the CTr joint and are known to provide reinforcing excitatory input to the motor neurons of the depressor muscle (Zill et al. 2012). A strong decrease in CTr torques could cause a sudden drop in this excitatory input and terminate the stance phase in a reliable manner.

Another aspect concerns the timing and magnitude of torque generation at the ThC and FTi joints. In current control models, joint torques are generated assuming distinct states of antagonistic neural activity (Büschges 2012; Ekeberg et al. 2004). These states of activity are thought to reflect joint kinematics, in that for example leg retraction and extension are generated by retraction and extension torques. Our data challenge this assumption, because the need to counteract gravity-induced collapse of a leg under load also requires torques counteracting a joint's movement (Figures 2.2, 2.3 and 2.5). Generating these flexible, posture-dependent torques might in turn require a more flexible activation of leg muscles than currently envisaged, possibly even co-activation.

In revising current models of walking control, it will thus be helpful to understand how torques are related to antagonistic muscle activity at the joints, and how torques are shaped by passive forces from muscles (Hooper et al. 2009) and skeletal structures (Ache and Matheson 2013). As joint torques represent the net effect of active and passive forces acting at the joint (Winter 1980), future studies will need to combine inverse dynamics with electromyographic recordings in freely walking insects to reveal the relationship between motor input and mechanical output at the leg joints.

2.6 Supplementary information

2.6.1 Model evaluation

We calculated net torques about individual leg joints using a rigid link model (Figure 2.1C). The use of rigid links was justified, because leg segments did not bend on a measurable scale during walking. The model neglects inertial and gravitational effects due to small segment masses and simplifies the orientation of the ThC joint axis, the position of the CTr joint, and the leg's center of pressure. We evaluated the effects of all assumptions on torque calculations by re-running our analysis for the entire data set including inertia and gravity and using alternative leg model configurations (see below). This evaluation confirmed that the simplifications made did not change the conclusions reached in this chapter.

Inertial and gravitational effects

Our analysis considered external joint torques only and did not include torques produced by segment inertia and gravity. In larger vertebrates, this simplification can introduce substantial errors in torque magnitudes, particularly at proximal joints (Wells 1981). In smaller animals, on the other hand, these errors are typically negligible due to relatively small segment masses (Biewener and Full 1992).

To confirm that inertial and gravitational effects were also negligible in our experiments, we calculated joint torques using the traditional recursive Newton-Euler algorithm. Calculations were performed in Matlab, using the *Spatial_v2* library (R. Featherstone, see also Featherstone 2008). The ThC joint was considered to be connected to a fixed base. The leg segments were modeled as homogeneous solid cylinders with the center of mass being located at the geometrical center of each cylinder. Corresponding inertia matrices were calculated from typical segment masses and segment dimensions of a stick insect leg (Table 2.2). Markers on the femur and tibia (Figure 2.6A) were modeled as homogeneous solid spheres (Table 2.2). Their positions on the leg segments

Table 2.2: Morphometric data of a stick insect hind leg and motion capture markers used for exemplary inverse dynamics calculations.

	mass (g)	radius (m)	length (m)
coxa-trochantero-femur	$11 \cdot 10^{-3}$	$6.0 \cdot 10^{-4}$	$14.4 \cdot 10^{-3}$
tibia	$4 \cdot 10^{-3}$	$2.5 \cdot 10^{-4}$	$13.9 \cdot 10^{-3}$
marker	$4 \cdot 10^{-3}$	$7.5 \cdot 10^{-4}$	

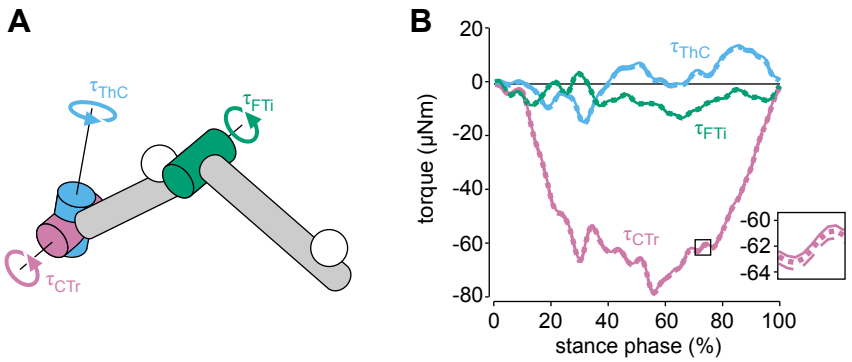

Figure 2.6: Effects of inertia and gravity on torque calculations
(**A**) Schematic of the leg model with motion capture markers (white spheres). Torques were calculated about the three main leg joints: the thorax-coxa (ThC, blue) joint, the coxa-trochanter (CTr, purple) joint, and the femur-tibia (FTi, green) joint. (**B**) Torque time courses for an exemplary hind leg step, neglecting all inertial and gravitational effects (solid lines, as above), including inertial and gravitational effects of the leg segments (dotted lines), and including inertial and gravitational effects of both the leg segments and the motion capture markers (dashed lines).

were measured from high-resolution photographs prior to experimentation. The compound moment of inertia (leg segment plus marker) was determined using the parallel axis theorem. The compound center of mass was determined from the weighted mean of the segment and marker mass.

The example calculations for a hind leg step demonstrate that including inertial and gravitational effects of the leg segments and motion capture markers has no significant effect on the timing and magnitude of joint torques (Figure 2.6B). These results confirm that torques produced by segment inertia and gravity during the stance phase are small in relation to those exerted by the ground reaction force and can indeed be neglected in our experiments.

Orientation of the thorax-coxa joint axis

The second simplification concerned the most proximal leg joint, the ThC or subcoxal joint. As in many other insect species, it is more complex than the CTr and FTi joints, which act as hinges in *C. morosus*. The dorsal side of the coxa forms a ball-and-socket-like articulation with a rounded prominence of the thorax (pleural condyle). The ventral side is attached to the thorax by the elastically articulated trochantin (Cruse 1976). As a consequence, the position of the ThC joint axis is not necessarily fixed. In principle, the joint can provide a wide range of leg movements, including levation/depression of the leg. During the stance phase of walking, however, most of the movement around this joint is described by the retraction and supination angles, which define the leg plane (Cruse and Bartling 1995; Theunissen et al. 2015). Both angles vary almost in direct proportion during the stance phase (Figures 2.2–2.4A), indicating that the ThC joint can be modeled as a single axis that is slanted to the side of the body within the leg

plane. To estimate the angle by which the ThC joint axis (a_{ThC}) is slanted outward, we reconstructed its orientation by intersecting leg planes at successive points in time. That is, we approximated the time course of a_{ThC} by taking the cross product of the leg plane's normal vectors (n) at successive time points (t) during the stance phase according to

$$a_{ThC}(t+1) \approx n(t) \times n(t-1) \tag{2.4}$$

We used angle θ to describe the resulting orientation of a_{ThC} relative to the vertical thorax axis a_{Th} (Figure 2.7A). Figure 2.7B shows representative time courses of θ for a hind, middle and front leg step. During the portion of the stance phase in which the leg was continuously retracted (white area in Figure 2.7B), θ oscillated around 30°. Note that calculation artifacts occurred when the leg moved slowly—mainly directly after the touch-down or before the lift-off of the leg (gray areas in Figure 2.7B). The corresponding θ-values were not considered for evaluation.

Given that θ varied relatively little for much of the stance phase, we simplified the kinematic calculations in our analysis and approximated the rotational axis of the ThC joint by rotating a_{Th} in the leg plane by $\theta = 30°$ in each step. To compare the resulting orientation of the joint axis with previously reported estimates (Cruse 1976; Cruse and Bartling 1995), we projected the joint axis into a spherical body-fixed coordinate system. In this coordinate system, the azimuth angle ϕ describes the projection of the joint axis on the horizontal body plane. This plane is spanned by the fore-aft (x) and medio-lateral (y) body axis, with $\phi = 0°$ pointing toward the head and $\phi = 90°$ pointing toward the right body side. The elevation angle ψ gives the orientation of the joint axis relative to the vertical (z) body axis, with $\psi = 0°$ indicating a vertical joint axis. For the steps shown in Figure 2.7B, rotating a_{Th} in the leg plane by $\theta = 30°$ resulted in little movement of the joint axis (solid lines in Figure 2.7C). The range of axis movement described by angles ϕ and ψ corresponded well to earlier reported estimates for freely walking stick insects (Cruse 1976; Cruse and Bartling 1995).

To estimate the effect of our choice of θ on torque calculations at the ThC joint, we re-ran our analysis setting $\theta = 0°$. For the latter, the ThC axis moved considerably (dotted lines in Figure 2.7C). However, the shape of the joint torque time courses remained essentially unchanged, and effects on torque magnitudes were small. Effects were small both at the level of single steps (Figure 2.7D) and grand means (Figure 2.7E), giving us good assurance that our choice of θ did not influence any conclusions drawn from torques at the ThC joint.

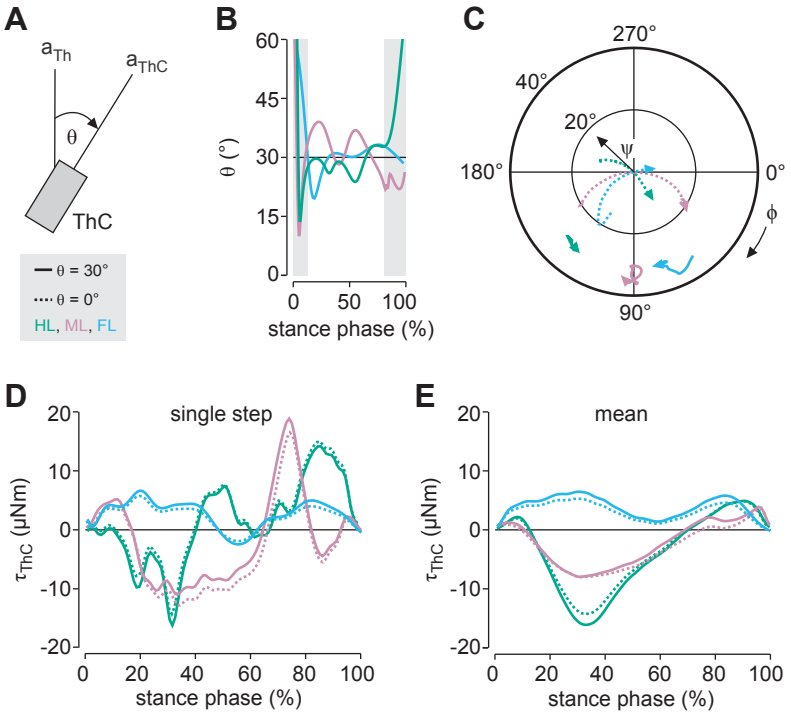

Figure 2.7: Effects of the ThC joint orientation on torque calculations
(**A**) The orientation of the ThC joint axis (a_{ThC}) with respect to the dorsal thorax axis (a_{Th}) within the leg plane can be described by angle θ. (**B**) Reconstructing θ in individual steps reveals oscillations around 30°. Gray areas mark the beginning and end of the stance phase when calculation artifacts occurred. (**C**) Setting $\theta = 30°$ (solid lines) in our analysis results in little movement of the ThC joint axis in the body-fixed coordinate system compared with $\theta = 0°$ (dotted lines). In this spherical coordinate system, $\phi = 0°$ points toward the head and $\psi = 0°$ points vertically upward. Lines show the end point of the unit vector describing the orientation of the ThC joint axis. (**D**–**E**) Using $\theta = 30°$ or $\theta = 0°$ has only minor effects on joint torque calculations for both single steps (**D**) and grand means (**E**). For comparison, **B**–**D** show the same three hind leg (HL, green), middle leg (ML, purple) and front leg (FL, blue) steps.

As mentioned above, our leg model neglects a possible second degree of freedom at the ThC joint that could produce torques in the direction of leg depression, similar to the CTr joint. While this assumption is common in the stick insect literature (e.g., Büschges 2012; Dürr et al. 2004), the actual contribution of the ThC joint to leg depression remains unknown. If another degree of freedom was introduced in our model, the ThC joint could assist the CTr joint in producing depression torques and thereby play a role in body support and depression-driven propulsion as well. The assumption of a single degree of freedom for the ThC joint should therefore be re-examined in future studies. This, however, will not affect the main conclusion that propulsion is controlled by leg depression rather than leg retraction.

Position of the coxa-trochanter joint

The third simplification concerned the CTr joint, a hinge joint that connects the coxa with the trochantero-femur segment (trochanter and femur are fused in stick insects).

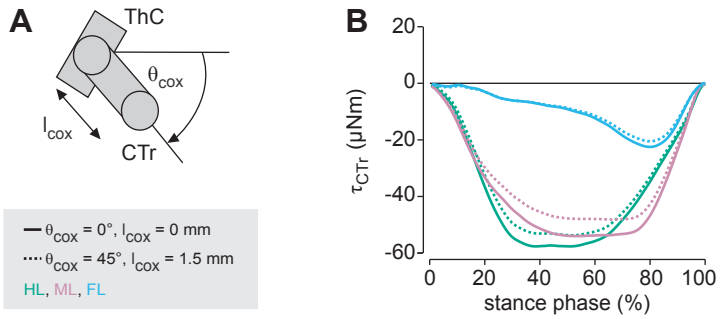

Figure 2.8: Effects of the CTr joint position on torque calculations
(**A**) The position of the CTr joint relative to the ThC joint can be described by two parameters within the leg plane: the length of the coxa, l_{cox}, and the angle between the coxa and the horizontal body plane, θ_{cox}. (**B**) Joint torque calculations for $l_{cox} = 0$ mm and $\theta_{cox} = 0°$ (solid lines, as above) and $l_{cox} = 1.5$ mm and $\theta_{cox} = 45°$ (dotted lines). Varying the position of the CTr joint has only small effects on the grand mean time courses of torques at the CTr joint in hind leg (HL, green), middle leg (ML, purple) and front leg (FL, blue) steps.

Rotations about the CTr joint levate or depress the leg. Above, we show that torques about this joint are critical for controlling body weight support and propulsion. Unfortunately, determining the exact position of the CTr joint relative to the thorax is difficult in freely walking animals. The short length of the coxa (approx. 1.5 mm) did not permit the use of a motion capture marker (1.5 mm in diameter), because joint movements needed to be unrestrained. In principle, the joint position can be inferred from triangulation based on known segment lengths of the coxa and femur and the relative position of the motion capture marker on the femur. However, this calculation was highly sensitive to small inaccuracies in initial length measurements and did not result in sufficiently accurate joint positions in all steps. Therefore, we assumed that the CTr joint was connected directly to the thorax. This had two implications for torque calculations. First, neglecting the coxa as a moving segment effectively lumped the levation/depression of the coxa and the levation/depression of the trochantero-femur into a single joint angle estimate. While recent motion analysis of the trochantero-femur indeed suggests that most leg levation/depression is caused by rotation about the CTr joint (Theunissen et al. 2015), the ThC joint could assist the CTr joint in leg depression if it was modeled with an additional degree of freedom (see above). This possibility should be re-examined in future studies. Second, re-locating the CTr joint overestimated the lever arm (distance from joint to ground reaction force acting at the foot) by approximately the length of the coxa.

To estimate the effect of the change in lever arm on torque calculations, we re-ran our analysis with a "rigid coxa," i.e., we set the CTr joint in constant distance to the ThC joint (Figure 2.8A). We set the distance to $l_{cox} = 1.5$ mm, which corresponds to an average coxa length. The rotation angle of the coxa segment relative to the lateral body

axis was set to $\theta_{cox} = 45°$. As expected, the slightly shortened lever arm resulted in slightly smaller torque magnitudes, but effects on grand mean time courses were small in all legs (Figure 2.8B). Most importantly, the shape of the time courses remained essentially unchanged. As we consider the temporal torque profile to be more relevant for interpretation of joint function than exact magnitudes, the simplified position of the CTr joint was sufficiently accurate for our purposes.

Tibia-tarsus joint as center of pressure

The last simplification concerned the leg's center of pressure (COP), the point where the ground reaction force vector acts on the leg. In our leg model, we used the TiTa joint as an estimate. The tarsus was not tracked directly because attaching a motion capture marker to the highly flexible and multi-segmented structure would have restrained its movements. Based on our digital videos and previous reports on standing stick insects (Labonte and Federle 2013), the actual center of pressure was likely the proximal part of the second tarsal segment. Changing the COP accordingly would increase the lever arms for all joints and, in turn, affect the magnitudes of all joint torques.

To estimate the effect of the change in lever arm on torque calculations, we re-ran our analysis assuming that the COP lies within the leg plane in constant distance to the TiTa joint (Figure 2.9A). We set the distance to $l_{cop} = 2$ mm, which corresponds to the average length of a first tarsal segment. Further, we assumed a constant angle of attack relative to the ground of $\theta_{cop} = 45°$, which corresponds to an estimated average angle based on our digital videos (Figure 2.9A, inset). Effects on grand mean torques about the ThC and CTr joints were small (Figure 2.9B,C). Effects were more pronounced at the FTi joint, particularly in middle legs (Figure 2.9D). However, the conclusions reached above remain unaffected. Above, we demonstrate that torques about the middle leg's FTi joint were most variable and highly sensitive to the current leg posture. This result holds even when assuming a different COP (Figure 2.9E). To confirm that variability at the middle leg's FTi joint did not result from assuming a fixed COP position, we re-ran our analysis assuming randomly varying COP positions. We varied the COP either from step to step or from frame to frame within steps, using random combinations of $l_{cop} = \{1,2,3,4\}$ mm and $\theta_{cop} = \{30,45,60\}°$. The effects on joint torque time courses and the correlation at the middle leg's FTi joint were similar to assuming a systematic variation of the COP (Figure 2.9).

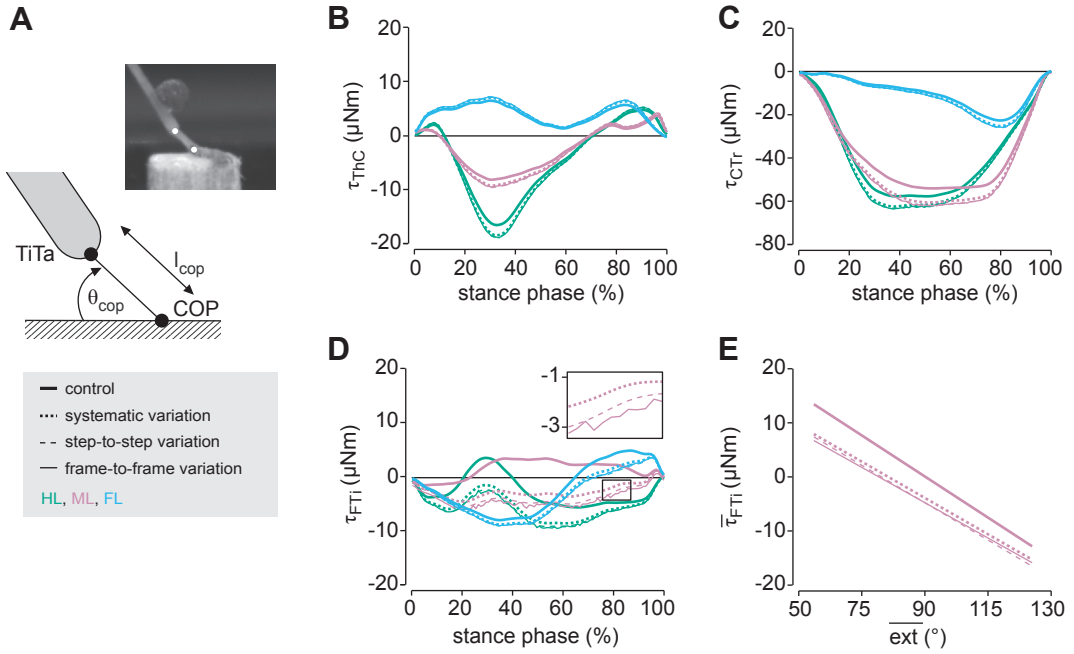

Figure 2.9: Effects of the COP position on torque calculations
(**A**) The position of the COP relative to the TiTa joint can be described by two parameters within the leg plane: distance l_{cop} and angle θ_{cop}. The inset shows a close-up of a stick insect leg during stance. White dots mark the TiTa joint and approximate COP. (**B–D**) Joint torque calculations assuming either the TiTa joint as COP ($l_{cop} = 0$ mm and $\theta_{cop} = 0°$, bold solid lines, as above), a fixed COP relative to the TiTa joint ($l_{cop} = 2$ mm and $\theta_{cop} = 45°$, thin dotted lines), or a randomly changing COP from step to step or frame to frame (combinations of $l_{cop} = \{1,2,3,4\}$ mm and $\theta_{cop} = \{30,45,60\}°$, thin dashed and thin solid lines, respectively). Effects of the artificial COP are small on grand mean times courses of torques at the ThC joint (**B**) and the CTr joint (**C**). Effects are strongest at the middle leg's FTi joint (**D**). (**E**) At the middle leg's FTi joint, torque magnitudes are negatively correlated with the net extension of the tibia (see also Figure 2.5), irrespective of the position of the COP.

2.6.2 Supplementary results and discussion

Correlations between joint torques and leg forces

Table 2.3: Correlations between time courses of joint torques and leg forces (grand means).[a]

	hind leg		middle leg		front leg	
	r-value	p-value	r-value	p-value	r-value	p-value
τ_{ThC} versus F_x	**0.19**	**$0.06^{(4/9)}$**	**−0.90**	**$<0.001^{(10/10)}$**	**−0.14**	**$0.17^{(1/6)}$**
τ_{ThC} versus F_y	0.04	$0.71^{(4/9)}$	−0.63	$<0.001^{(8/10)}$	0.39	$<0.001^{(2/6)}$
τ_{ThC} versus F_z	0.85	$<0.001^{(9/9)}$	0.52	$<0.001^{(7/10)}$	0.08	$0.46^{(1/6)}$
τ_{CTr} versus F_x	0.76	$<0.001^{(9/9)}$	−0.21	$0.04^{(4/10)}$	−0.83	$<0.001^{(6/6)}$
τ_{CTr} versus F_y	0.66	$<0.001^{(9/9)}$	0.25	$0.01^{(5/10)}$	0.04	$0.70^{(5/6)}$
τ_{CTr} versus F_z	**0.96**	**$<0.001^{(9/9)}$**	**1.00**	**$<0.001^{(10/10)}$**	**0.93**	**$<0.001^{(6/6)}$**
τ_{FTi} versus F_x	**0.28**	**$<0.01^{(6/9)}$**	**0.07**	**$0.47^{(2/10)}$**	**0.91**	**$<0.001^{(6/6)}$**
τ_{FTi} versus F_y	0.37	$<0.001^{(4/9)}$	−0.37	$<0.001^{(7/10)}$	−0.85	$<0.001^{(6/6)}$
τ_{FTi} versus F_z	−0.34	$<0.001^{(5/9)}$	−0.87	$<0.001^{(7/10)}$	−0.82	$<0.001^{(6/6)}$

[a]The superscripts following the p-values denote the number of individuals with the same correlation result (positive, negative or no correlation) as the grand means. Correlations set in bold are reported in Table 2.1 above.

Medio-lateral balance

In addition to body weight support and propulsion, the control of medio-lateral balance is a third important motor task during walking. It is particularly important if a narrow base of support and a center of mass high above the ground increase the risk of falling sideways, like in humans (Winter and Eng 1995).

In the stick insect, all legs contributed to the control of medio-lateral balance with lateral forces during straight walking (Figures 2.2–2.4). Peak forces were similarly high in all legs, but differed in direction (-0.7 ± 0.2 mN in the hind leg, -0.9 ± 0.4 mN in the middle leg, and 0.6 ± 0.1 mN in the front leg; grand mean $\pm$ s.d. of animal means). Hind legs mainly pushed outward ($F_y < 0$; Figure 2.2B), front legs mainly pulled inward ($F_y > 0$; Figure 2.4B), and middle legs first pulled inward, then pushed outward (Figure 2.3B). These patterns confirm previous findings in the stick insect (Cruse 1976), but are quite different from those observed in sprawled-posture animals moving at faster speeds. Cockroaches and geckos, for example, push all legs outward during level running (Chen et al. 2006; Full et al. 1991), possibly to achieve dynamic self-stabilization (Kubow 1999). Notably, however, both animals change the direction of the lateral force to inward pulling during climbing (Autumn et al. 2006; Goldman et al. 2006). Pulling forces of the stick insect during walking might thus be

related to their climbing behavior in nature, where these forces likely aid attachment mechanisms (Zill et al. 2014; Zill et al. 2015).

Because stick insects moved their legs considerably backward during the stance phase, lateral forces were not attributable to the action of any one leg joint alone (Table 2.3). Direct positive correlations between time courses of joint torques and lateral forces were weak even for torques at the FTi joints. In fact, correlations were strongest with torques at the CTr joint of the hind leg (Table 2.3). At this joint, large torques toward depression resulted in backward and outward directed forces, while flexion torques at the FTi joint counteracted a further extension of the leg so that forces could be transmitted to the ground (see also Figure 2.2C).

2.7 References

Ache, J. M. and Matheson, T. (2013). Passive joint forces are tuned to limb use in insects and drive movements without motor activity. *Curr. Biol.* 23, 1418–1426.

Ahn, A. N. and Full, R. J. (2002). A motor and a brake: two leg extensor muscles acting at the same joint manage energy differently in a running insect. *J. Exp. Biol.* 205, 379–389.

Andrada, E., Mämpel, J., Schmidt, A., Fischer, M. S., Karguth, A., and Witte, H. (2010). Biomechanical analyses of rat locomotion during walking and climbing as a base for the design and construction of climbing robots. *Design & Nature V*. Ed. by Brebbia, C. and Carpi, A. WIT Press, 165–177.

Autumn, K., Hsieh, S. T., Dudek, D. M., Chen, J., Chitaphan, C., and Full, R. J. (2006). Dynamics of geckos running vertically. *J. Exp. Biol.* 209, 260–272.

Balint, C. N. and Dickinson, M. H. (2001). The correlation between wing kinematics and steering muscle activity in the blowfly *Calliphora vicina*. *J. Exp. Biol.* 204, 4213–4226.

Biewener, A. a. and Full, R. J. (1992). Force platform and kinematic analysis. *Biomechanics: Structures and Systems. A Practical Approach*. Oxford University Press, 45–73.

Blob, R. W. and Biewener, A. A. (2001). Mechanics of limb bone loading during terrestrial locomotion in the green iguana (*Iguana iguana*) and American alligator (*Alligator mississippiensis*). *J. Exp. Biol.* 204, 1099–1122.

Burns, M. D. (1973). The control of walking in Orthoptera. I. Leg movements in normal walking. *J. Exp. Biol.* 58, 45–58.

Büschges, A. (2012). Lessons for circuit function from large insects: towards understanding the neural basis of motor flexibility. *Curr. Opin. Neurobiol.* 22, 602–608.

Büschges, A. and Gruhn, M. (2007). Mechanosensory feedback in walking: from joint control to locomotor patterns. *Adv. In Insect Phys.* 34, 193–230.

Chen, J. J., Peattie, A. M., Autumn, K., and Full, R. J. (2006). Differential leg function in a sprawled-posture quadrupedal trotter. *J. Exp. Biol.* 209, 249–259.

Cruse, H. (1976). The function of the legs in the free walking stick insect, *Carausius morosus*. *J. Comp. Physiol. A* 112, 235–262.

Cruse, H. and Bartling, C. (1995). Movement of joint angles in the legs of a walking insect, *Carausius morosus*. *J. Insect Physiol.* 41, 761–771.

Dürr, V. (2005). Context-dependent changes in strength and efficacy of leg coordination mechanisms. *J. Exp. Biol.* 208, 2253–2267.

Dürr, V., Schmitz, J., and Cruse, H. (2004). Behaviour-based modelling of hexapod locomotion: linking biology and technical application. *Arthropod Struct. Dev.* 33, 237–250.

Ekeberg, Ö., Blümel, M., and Büschges, A. (2004). Dynamic simulation of insect walking. *Arthropod Struct. Dev.* 33, 287–300.

Featherstone, R. (2008). *Rigid Body Dynamics Algorithms*. New York: Springer.

Fowler, E., Gregor, R., Hodgson, J., and Roy, R. (1993). Relationship between ankle muscle and joint kinetics during the stance phase of locomotion in the cat. *J. Biomech.* 26, 465–483.

Full, R. J., Blickhan, R., and Ting, L. H. (1991). Leg design in hexapedal runners. *J. Exp. Biol.* 158, 369–390.

Goldman, D. I., Chen, T. S., Dudek, D. M., and Full, R. J. (2006). Dynamics of rapid vertical climbing in cockroaches reveals a template. *J. Exp. Biol.* 209, 2990–3000.

Harris, J. and Ghiradella, H. (1980). The forces exerted on the substrate by walking and stationary crickets. *J. Exp. Biol.* 85, 263–279.

Hooper, S. L., Guschlbauer, C., Blümel, M., Rosenbaum, P., Gruhn, M., Akay, T., and Büschges, A. (2009). Neural control of unloaded leg posture and of leg swing in stick insect, cockroach, and mouse differs from that in larger animals. *J. Neurosci.* 29, 4109–4119.

Hooper, S. L., Guschlbauer, C., Uckermann, G. von, and Büschges, A. (2006). Natural neural output that produces highly variable locomotory movements. *J. Neurophysiol.* 96, 2072–88.

Kram, R., Wong, B., and Full, R. J. (1997). Three-dimensional kinematics and limb kinetic energy of running cockroaches. *J. Exp. Biol.* 200, 1919–1929.

Kubow, T. M. (1999). The role of the mechanical system in control: a hypothesis of self-stabilization in hexapedal runners. *Phil. Trans. R. Soc. B* 354, 849–861.

Labonte, D. and Federle, W. (2013). Functionally different pads on the same foot allow control of attachment: stick insects have load-sensitive "heel" pads for friction and shear-sensitive "toe" pads for adhesion. *PLoS One* 8, e81943.

Lehmann, F. O., Skandalis, D. A., and Berthe, R. (2013). Calcium signalling indicates bilateral power balancing in the *Drosophila* flight muscle during manoeuvring flight. *J. R. Soc. Interface* 10, 20121050.

Lévy, J. and Cruse, H. (2008). Controlling a system with redundant degrees of freedom. I. Torque distribution in still standing stick insects. *J. Comp. Physiol. A* 194, 719–733.

Noah, J. A., Quimby, L., Frazier, S. F., and Zill, S. N. (2004). Sensing the effect of body load in legs: responses of tibial campaniform sensilla to forces applied to the thorax in freely standing cockroaches. *J. Comp. Physiol. A* 190, 201–215.

Rabiner, L. and Juang, B.-H. (1993). *Fundamentals of Speech Recognition*. 1st ed. Upper Saddle River: Prentice Hall.

Reinhardt, L. and Blickhan, R. (2014). Level locomotion in wood ants: evidence for grounded running. *J. Exp. Biol.* 217, 2358–2370.

Ritzmann, R. E. and Büschges, A. (2007). Adaptive motor behavior in insects. *Curr. Opin. Neurobiol.* 17, 629–636.

Sheffield, K. M. and Blob, R. W. (2011). Loading mechanics of the femur in tiger salamanders (*Ambystoma tigrinum*) during terrestrial locomotion. *J. Exp. Biol.* 214, 2603–2615.

Sponberg, S. and Daniel, T. L. (2012). Abdicating power for control: a precision timing strategy to modulate function of flight power muscles. *Proc. R. Soc. B* 279, 3958–3966.

Sponberg, S., Spence, A. J., Mullens, C. H., and Full, R. J. (2011). A single muscle's multifunctional control potential of body dynamics for postural control and running. *Phil. Trans. R. Soc. B* 366, 1592–1605.

Spong, M., Hutchinson, S., and Vidyasagar, M. (2006). *Robot Modeling and Control*. London: Wiley.

Sutton, G. P. and Burrows, M. (2008). The mechanics of elevation control in locust jumping. *J. Comp. Physiol. A* 194, 557–563.

Sutton, G. P. and Burrows, M. (2010). The mechanics of azimuth control in jumping by froghopper insects. *J. Exp. Biol.* 213, 1406–1416.

Theunissen, L. M., Bekemeier, H. H., and Dürr, V. (2015). Comparative whole-body kinematics of closely related insect species with different body morphology. *J. Exp. Biol.* 218, 340–352.

Theunissen, L. M. and Dürr, V. (2013). Insects use two distinct classes of steps during unrestrained locomotion. *PLoS One* 8, e85321.

Theunissen, L. M., Vikram, S., and Dürr, V. (2014). Spatial co-ordination of foot contacts in unrestrained climbing insects. *J. Exp. Biol.* 217, 3242–3253.

Walker, S., Schwyn, D. A., Mokso, R., Wicklein, M., Müller, T., Doube, M., Stampanoni, M., Krapp, H. G., and Taylor, G. K. (2014). In vivo time-resolved microtomography reveals the mechanics of the blowfly flight motor. *PLoS Biol.* 12, e1001823.

Watson, J. T. and Ritzmann, R. E. (1998). Leg kinematics and muscle activity during treadmill running in the cockroch, *Blaberus discoidalis*: I. Slow running. *J. Comp. Physiol. A* 182, 11–22.

Wells, R. P. (1981). The projection of the ground reaction force as a predictor of internal joint moments. *Bull. Prosthet. Res.* 18, 15–19.

Winter, D. A. (1980). Overall principle of lower limb support during stance phase of gait. *J. Biomech.* 13, 923–927.

Winter, D. A. (1990). *Biomechanics and Motor Control of Human Movement*. 2nd ed. New York: Wiley.

Winter, D. A. and Eng, P. (1995). Kinetics: our window into the goals and strategies of the central nervous system. *Behav. Brain Res.* 67, 111–120.

Witte, H., Biltzinger, J., Hackert, R., Schilling, N., Schmidt, M., Reich, C., and Fischer, M. S. (2002). Torque patterns of the limbs of small therian mammals during locomotion on flat ground. *J. Exp. Biol.* 205, 1339–1353.

Zill, S. N., Chaudhry, S., Büschges, A., and Schmitz, J. (2015). Force feedback reinforces muscle synergies in insect legs. *Arthropod Struct. Dev.* 44, 541–553.

Zill, S. N., Chaudhry, S., Exter, A., Büschges, A., and Schmitz, J. (2014). Positive force feedback in development of substrate grip in the stick insect tarsus. *Arthropod Struct. Dev.* 43, 441–455.

Zill, S. N., Schmitz, J., Chaudhry, S., and Büschges, A. (2012). Force encoding in stick insect legs delineates a reference frame for motor control. *J. Neurophysiol.* 108, 1453–1472.

Chapter 3

Inter-leg coordination based on local load feedback

This chapter was published with minor modifications as a research article in Proceedings of the Royal Society B: *Dallmann, C. J., Hoinville, T., Dürr, V. and Schmitz, J. (2017). A load-based mechanism for inter-leg coordination in insects. Proc. R. Soc. B 284, 20171755*. C.J.D., T.H., V.D. and J.S. conceived the study; C.J.D. performed experiments; T.H. contributed simulation data; C.J.D. analyzed experimental data; C.J.D. and T.H. analyzed simulation data; C.J.D., T.H., V.D. and J.S. interpreted results; C.J.D. prepared figures; C.J.D. drafted the manuscript; C.J.D., T.H., V.D. and J.S. revised the manuscript and gave final approval for publication. Supplementary videos and data are available online at rspb.royalsocietypublishing.org/content/284/1868/20171755.

3.1 Abstract

Animals rely on an adaptive coordination of legs during walking. However, which specific mechanisms underlie coordination during natural locomotion remains largely unknown. One hypothesis is that legs can be coordinated mechanically based on a transfer of body load from one leg to another. To test this hypothesis, we simultaneously recorded leg kinematics, ground reaction forces and muscle activity in freely walking stick insects (*Carausius morosus*). Based on torque calculations, we show that load sensors (campaniform sensilla) at the proximal leg joints are well suited to encode the unloading of the leg in individual steps. The unloading coincides with a switch from stance to swing muscle activity, consistent with a load reflex promoting the stance-to-swing transition. Moreover, a mechanical simulation reveals that the unloading can be ascribed to the loading of a specific neighboring leg, making it exploitable for inter-leg coordination. We propose that mechanically mediated load-based coordination is used across insects analogously to mammals.

3.2 Introduction

Adaptive coordination of multiple legs is key for walking animals and robots. It ensures stability and propulsion of the body despite changes in locomotion speed or the environment. Inter-leg coordination is generally thought to arise from interconnected neural circuits in the spinal cord or ventral nerve cord, which are regulated by descending inputs from the brain and afferent inputs from the legs (Borgmann and Büschges 2015; Frigon 2017; Kiehn 2016). However, the specific mechanisms at work during natural locomotion—when the body mechanically interacts with the environment—remain largely unknown.

One hypothesis is that mechanical interactions directly contribute to adaptive coordination (Duysens et al. 2000). In the case of walking, for example, body load is transferred among legs that are mechanically coupled through the ground. In theory, a leg in stance could start its stance-to-swing transition once its load sensors detect an unloading induced by the touch-down and subsequent loading of a neighboring leg. That is, an intra-leg load reflex could couple the leg's step cycle to that of the neighboring leg, simply by exploiting the load transfer between legs. Such a decentralized, load-based coordination mechanism would be a fast, computationally inexpensive and inherently adaptive complement to neural coordination signals between legs.

Recent experiments on a minimalistic four-legged robot suggest that the mechanical coupling of legs can indeed be exploited for inter-leg coordination (Owaki et al.

2013; Owaki and Ishiguro 2017). In these experiments, local load feedback from the legs was sufficient to couple otherwise uncoupled leg oscillators and generate different stepping patterns. As mechanical coupling of legs is a hallmark of walking, this could also be a common control strategy in animals. In mammals, an intra-leg load reflex could be mediated in part by load-sensitive Golgi tendon organs (GTOs) (Pearson 1995; Pearson 2008). While a leg is under load, feedback from GTOs is thought to sustain the stance phase by exciting extensor (stance) and inhibiting flexor (swing) motor neurons. Once the leg is being unloaded, feedback from GTOs decreases (GTOs do not encode load decreases). Simulation studies suggest that this can facilitate the stance-to-swing transition and might suffice to coordinate two contralateral legs (Aoi et al. 2012; Ekeberg and Pearson 2005). In insects, an intra-leg load reflex could be mediated by load-sensitive campaniform sensilla. These mechanoreceptors detect load as strain in the cuticle (Pringle 1938; Zill et al. 2004). Analogously to GTOs, campaniform sensilla have been implicated in facilitating the stance-to-swing transition once the leg is being unloaded (Bässler 1977; Newland and Emptage 1996; Zill et al. 2009). Moreover, activity of campaniform sensilla on the tibia were found to coincide with the touch-down of a neighboring leg, suggesting they signal load transfer between legs (Zill et al. 2009).

However, it has been difficult to show that the mechanical coupling of legs can be decoded and exploited for inter-leg coordination in natural locomotion. One reason is that recordings of load sensors in freely moving animals have been limited to a few accessible subgroups (for example, campaniform sensilla on the insect tibia; Noah et al. 2001; Zill and Moran 1981; Zill et al. 2009). Another reason is that changes in leg motor activity could not be measured simultaneously with changes in leg load; this, however, would be required to study intra-leg load reflexes during walking. Finally, the mechanical coupling of legs has not been quantified. This is critical, because load must be transferred effectively between specific legs to be exploitable for coordination. Such specific load transfer might be obvious in a biped, but cannot be intuitively inferred if more than two legs are mechanically coupled.

Here, we address these issues in freely walking stick insects (*Carausius morosus*, Figure 3.1A), using a combination of 3D motion capture, ground reaction force measurements, electromyography and modeling. Stick insects are important invertebrate model systems for mechanosensation and motor control (Borgmann and Büschges 2015; Dürr et al. 2004; Ritzmann and Büschges 2007; Tuthill and Wilson 2016). Like other insects, stick insects move their legs in a back-to-front sequence during walking (Figure 3.1B). Importantly, their primary load sensors, campaniform sensilla, are comparatively well described, from physiology to motor effects (Akay et al. 2007; Zill et al. 2011; Zill et al. 2012; Zill et al. 2015; Zill et al. 2017). Moreover, the large size

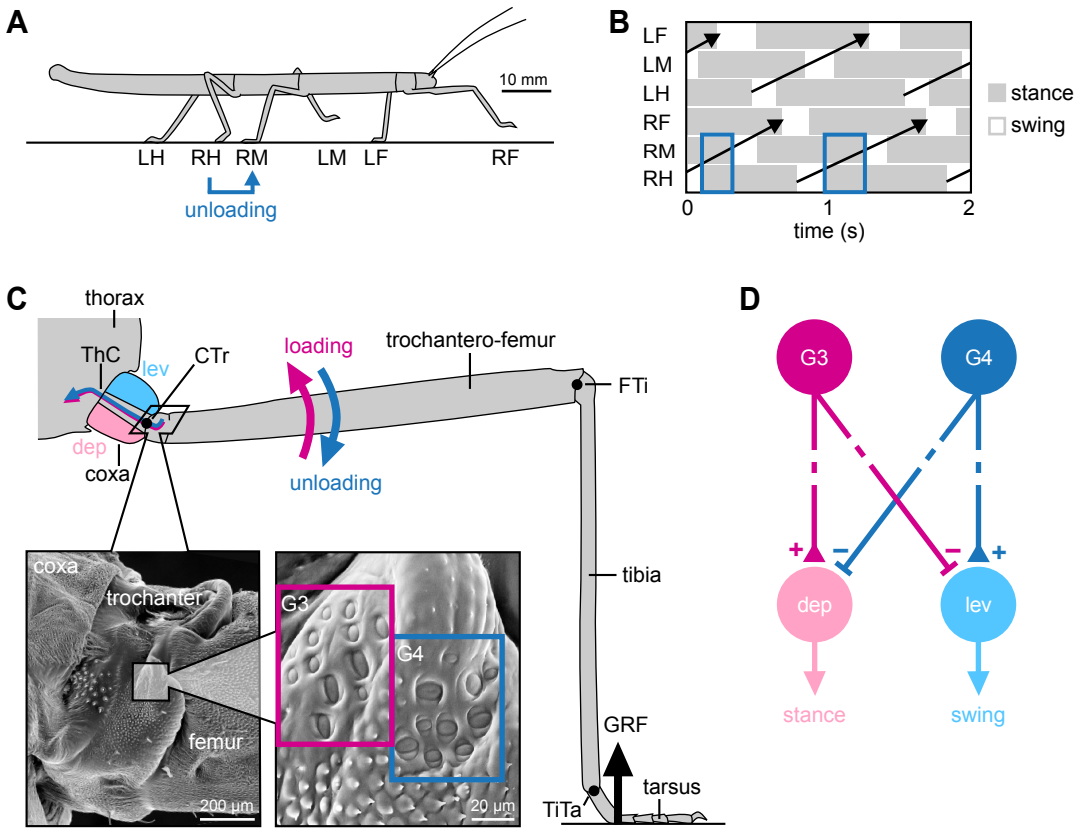

Figure 3.1: Load-based inter-leg coordination in an insect
(**A**) Schematic side view of a stick insect during walking. Each leg is labeled as being a right (R) or left (L) and a front (F), middle (M) or hind (H) leg. If a leg touches down on the ground (e.g., RH), it may unload the leg in front (e.g., RM). (**B**) Example coordination pattern of stance (gray) and swing (white) phases for each leg. Legs are coordinated in a back-to-front sequence (black arrows). Stance phases of ipsilateral neighboring legs overlap, providing potential time for load transfer (e.g., RM and RH, blue boxes). (**C**) Schematic front view of a stick insect leg during stance. The ground reaction force (GRF) induces high bending torques at the proximal coxa-trochanter (CTr) joint. Campaniform sensilla groups G3 and G4 on the dorsal trochanter are highly sensitive to the associated strain in the trochantero-femur. G3 is activated when dorsal bending torques increase (loading of leg), G4 when they decrease (unloading of leg). (**D**) Schematic of G3/G4 reflex pathways onto coxal muscles in active animals. Broken lines indicate functional motor effects. G3 afferent activity excites (+) the depressor (stance) muscle and inhibits (−) the levator (swing) muscle (Zill et al. 2012). G4 afferent activity is assumed to have the opposite effect. Unloading induced by a neighboring leg may reverse afferent activity from G3 to G4, thereby promoting the leg's stance-to-swing transition.

and sprawled posture of stick insect legs permits measuring joint torques and thus loading/unloading of individual leg segments during unrestrained walking (Dallmann et al. 2016). Here, we use this unique advantage to relate the known encoding properties of campaniform sensilla directly to behavior.

We find that campaniform sensilla at the proximal leg joints are well suited to encode the unloading of the leg during stance. The onset of unloading is strongly correlated with a change from stance to swing muscle activity, in agreement with an intra-leg

load reflex promoting the stance-to-swing transition. Moreover, a mechanical simulation reveals that the unloading of a leg can be specifically ascribed to the loading of the ipsilateral posterior leg. This indicates that the mechanical coupling of legs during walking can directly contribute to establish adaptive inter-leg coordination.

3.3 Methods

We tested 20 adult, female stick insects (*Carausius morosus*) reared in a laboratory colony (body mass: 0.9 ± 0.1 g, mean $\pm$ s.d.). Animals walked along a horizontal walkway (40×500 mm). A subset of 12 animals was used to record leg kinematics and dynamics (supplementary Video S1). These are the same animals elaborated on in Dallmann et al. (2016). A subset of eight animals was used to additionally record muscle activities (supplementary Video S2).

3.3.1 Leg kinematics and dynamics

Kinematics and dynamics were determined as described previously (Dallmann et al. 2016). In brief, kinematics were calculated from light-weight (4 mg) motion capture markers attached to the insect's body and leg segments. We used either 17 markers to capture movements of all legs, or eight markers to capture movements of a subset of legs. Markers were tracked with a Vicon system at 200 Hz (Vicon MX10 with eight T10 cameras, controlled by software Nexus 1.8.5; Vicon, Oxford, UK). For visual validation, we used an additional digital video camera (Basler A602fc, Ahrensburg, Germany) recording a synchronized side view (Figure 3.3A). Ground reaction forces (GRF) were recorded from individual right legs at 1 kHz using three-dimensional, strain-gauge-based force plates integrated in the walkway (Figure 3.3A). Kinematic and GRF data were low-pass filtered with a zero-lag, fourth-order Butterworth filter using cut-off frequencies of 20 Hz and 10 Hz, respectively. Torques at the leg joints were derived from inverse dynamics calculations in Matlab (The MathWorks, Natick, MA, USA), which combined the single leg kinematic and GRF data in a rigid body model of the leg. The coxa-trochanter (CTr) joint was modeled as a hinge with one degree of freedom. As described previously (Dallmann et al. 2016), we considered it to be directly connected to the thorax. We thereby overestimated the lever arm of the joint by approximately the length of the coxa (approx. 1.5 mm). This resulted in slightly larger torque magnitudes (Dallmann et al. 2016), but did not affect the conclusions reached in this study. Note that we calculated net torques, which represent the combined action of all forces acting

in the plane of joint movement and can thus be directly related to campaniform sensilla activation.

3.3.2 Muscle recordings

We recorded electromyograms (EMGs) from the coxal parts of the levator and depressor trochanteris muscles of right middle legs simultaneously with joint kinematics and GRFs. EMGs of each muscle were recorded with a pair of copper wires (35 µm diameter, insulated except for the tips). Wires were implanted through small holes in the cuticle made with an insect pin and held in place with dental glue. Correct electrode implantation was verified using standard criteria including resistance reflex responses to imposed movements of the CTr joint. We designed a lightweight EMG backpack (50 mg aluminium hook, Figure 3.3A) to direct the electrodes to the amplifiers without risking entanglement with the legs during walking. The backpack was fixated with bees wax close to the center of mass (COM) just behind the hind leg coxae so as to affect overall body dynamics only minimally. The backpack was connected to a string fixed midway above the walkway. String and electrodes were twisted to form a loose tether, allowing for unrestrained walking. Backpack attachment and electrode implantation did not affect joint kinematics (supplementary Figure 3.8A).

EMG signals were amplified 5000-fold and filtered with a 50 Hz notch, 250 Hz high-pass, and 7.5 kHz low-pass filter using a custom-built amplifier (MA102, Electronics Workshop, Zoological Institute, Cologne, Germany). Filtered signals were A/D converted (Power 1401 mk II) and recorded with Spike2 with a sampling rate of 25 kHz (both Cambridge Electronic Design, Cambridge, UK). EMG recordings were synchronized with motion and GRF recordings of the Vicon system via a custom-built external trigger box. Muscle spikes were detected in Matlab based on amplitude thresholds. The levator EMG contained activity of slow and fast motor neurons (Figure 3.3B and supplementary Figure 3.8B, 9-11 excitatory motor neurons innervate the muscle, Goldammer et al. 2012). The depressor EMG contained activity of the fast depressor trochanteris motor neuron (Goldammer et al. 2012; Schmitz 1993).

3.3.3 Mechanical simulation

To determine the mechanical load transfer among legs in stance, we simulated the animal as a rigid body in static equilibrium (Open Dynamics Engine v. 0.11.1). The body was idealized as a point mass. Each leg in stance was modeled as a frictionless, spherical (three degrees-of-freedom) joint attaching the body to the ground. For a given point in time, the simulation converged quickly to a stable GRF distribution among the legs

in stance based on their positions relative to the COM and the animal's weight. The simulation was run for all stance phases of a reference leg (right middle leg in Figure 3.5B, right front and hind leg in supplementary Figure 3.7). The CTr torque of the reference leg was obtained by combining its simulated vertical GRF with its measured joint kinematics. Given the frame-by-frame simulation in static equilibrium, the torque time course of the reference leg showed step-like changes that were directly related to the touch-down and lift-off events of the other legs (Figure 3.5B).

3.4 Results

3.4.1 Proximal campaniform sensilla can encode the unloading of the leg during walking

To study load-based inter-leg coordination, we first asked which load sensors would be suited to reliably encode the unloading of the leg during the stance phase. We recently showed that load changes in the legs of walking stick insects are most pronounced and least variable at the proximal coxa-trochanter (CTr) joint (Dallmann et al. 2016) (Figure 3.1C). This joint is primarily responsible for moving the leg up and down. During the stance phase, the main muscles controlling the joint (levator and depressor trochanteris) hold the fused trochantero-femur segment almost horizontally. As a consequence, GRFs induce particularly high bending torques at the CTr joint (Dallmann et al. 2016), and compressive strain on the dorsal trochantero-femur. Two groups of campaniform sensilla on the trochanter, G3 and G4 (Figure 3.1C, SEM images), are highly sensitive to the magnitude and rate of dorsal bending (Zill et al. 2012). The elliptic sensilla are preferentially excited by compression along their short axes. Owing to the mutually perpendicular orientations of G3 and G4 sensilla, an increase in dorsal bending activates G3 afferents without activating G4 afferents. Conversely, the release from dorsal bending activates G4 afferents without activating G3 afferents. In active animals, G3 afferents are known to excite the depressor (stance) muscle and inhibit the levator (swing) muscle of the leg (Zill et al. 2012) (Figure 3.1D). The motor effects of G4 afferents have not been tested specifically in active animals. However, we assume that G4 afferents have antagonistic motor effects, much like it is known for mutually perpendicular groups of campaniform sensilla at other leg joints (Akay et al. 2007; Schmitz 1993; Zill and Moran 1981; Zill et al. 2011). G3/G4 have been characterized in stick insect middle legs (Zill et al. 2012). Therefore, our study focuses on middle legs, too (but see supplementary Figures 3.6 and 3.7 for other legs).

To test whether G3/G4 are suited to encode the unloading of the leg during walking, we analyzed the time courses of torques and torque rates at the middle leg CTr

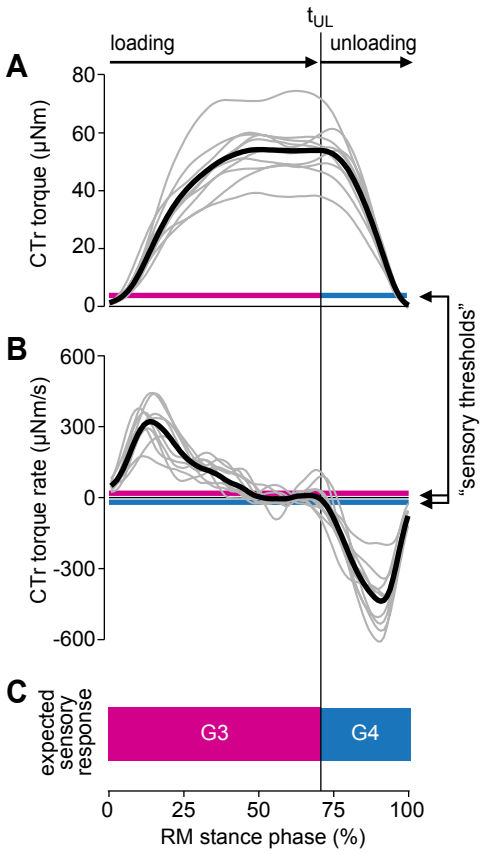

Figure 3.2: Joint torques indicate that campaniform sensilla on the trochanter encode the unloading of the leg during walking
(**A**,**B**) Torque and torque rate at the CTr joint of the right middle (RM) leg during stance. Bold black lines show the grand mean of all steps (n = 244 steps from N = 10 animals). Gray lines show means per animal. Magenta and blue lines indicate torques and torque rates above which G3/G4 afferent activity was confirmed in reduced leg preparations ("sensory thresholds," calculated based on data in Zill et al. 2012). The vertical black line marks the mean onset of unloading, t_{UL}. (**C**) Schematic of the expected sensory response of campaniform sensilla groups G3 and G4 based on the mean torque and torque rate time courses. Leg unloading is expected to terminate G3 afferent activity and initiate G4 afferent activity.

joint. Torques were determined via inverse dynamics calculations based on simultaneous recordings of leg kinematics and single leg GRFs (see Methods and supplementary Video S1). Upon leg touch-down, the CTr torque increased rapidly to a plateau of 54 $\pm$ 9 µNm (mean $\pm$ s.d.; n = 244 steps from N = 10 animals, Figure 3.2A, loading phase). After about 70% of the stance phase, the torque decreased rapidly before the leg lifted off (unloading phase). The onset of unloading, t_{UL}, was marked by a sudden change in torque rate peaking at -440 ± 192 µNm/s (Figure 3.2B). A direct, un-masked recording of G3/G4 afferent responses to the unloading of the leg is not feasible in freely walking animals, as the afferents of both groups run in the main leg nerve (nervus cruris) together with multiple other afferent and efferent axons (Goldammer et al. 2012). Therefore, we estimated the joint torques applied in previous physiological experiments on leg preparations that were effectively denervated except for G3/G4 (Zill et al. 2012). We did so

by multiplying the reported bending forces with the lever between force application and CTr joint (an average trochanter-femur length, 11.7 mm in our experiments). The lowest torque and torque rate at which G3/G4 afferent activity was confirmed were 3.4 μNm and 10.5 μNm/s, respectively (Figure 3.2A,B, magenta and blue lines). These sensory thresholds lie well below the sensitivities required for reliably signaling t_{UL} as measured during walking. This was also the case in front and hind legs (supplementary Figure 3.6). Given the directional sensitivities of G3/G4, we can thus predict that t_{UL} is encoded by a change from G3 to G4 afferent activity (Figure 3.2C).

3.4.2 The onset of unloading coincides with a change from stance to swing muscle activity

Assuming the motor effects illustrated in Figure 3.1D, a change from G3 to G4 afferent activity should promote the leg's stance-to-swing transition. Until t_{UL}, the depressor muscle should be excited and the levator muscle should be inhibited. After t_{UL}, the depressor muscle should be inhibited and the levator muscle should be excited.

To test whether t_{UL} is in fact reliably followed by a change in muscle activity, we recorded EMGs from the levator and depressor muscles of right middle legs simultaneously with leg kinematics and GRFs (see Methods and supplementary Video S2). Animals carried a lightweight EMG backpack (Figure 3A), from which electrodes were implanted in the coxa of the middle leg. To correlate muscle activity with t_{UL}, we first determined t_{UL} in each stance phase. This was possible because the variability of torque time courses is particularly low at the CTr joint (Dallmann et al. 2016). Specifically, we used the time point at which the CTr torque rate reached 25% of the maximum unloading rate during the stance phase. This relative, non-zero threshold allowed us to reliably detect the rapid decrease in torque toward the end of stance in individual steps with negligible delay, while ignoring small fluctuations around the plateau earlier in stance (see example in Figure 3.3B).

Figure 3.3B shows that levator activity started only after t_{UL} and before the leg was lifted off the ground. Conversely, depressor activity was high during the loading phase and terminated with t_{UL}. A similar pattern of motor activity was present in all steps recorded, independent of walking speed (n = 73 steps from N = 8 animals, Figure 3.3C, top, see also supplementary Figure 3.8B). To quantify the change in muscle activity, we determined the likelihood of muscle activation relative to t_{UL} by checking for the presence of a motor spike in every 50-ms time bin before and after the event. In agreement with the predicted motor effects of G3/G4 afferents, the likelihood of depressor activity declined abruptly after t_{UL}, whereas the likelihood of levator activity strongly increased (Figure 3.3C, bottom).

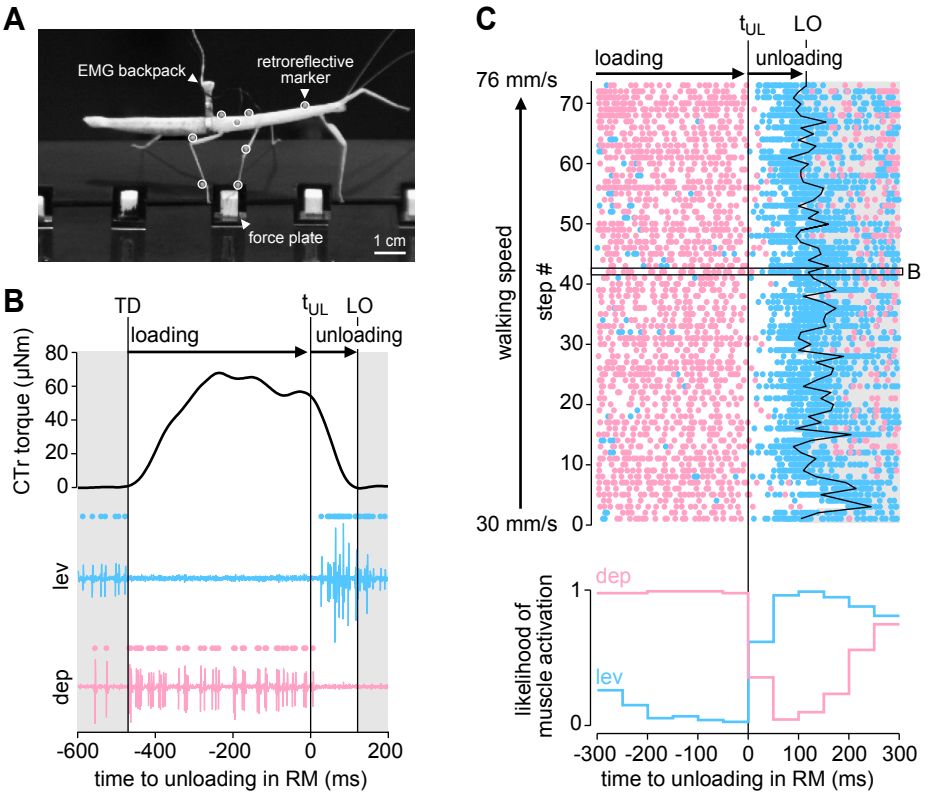

Figure 3.3: Leg unloading coincides with a switch from stance to swing muscle activity
(**A**) Side view of an animal carrying a lightweight EMG backpack and motion capture markers (white circles) while stepping onto a force plate. (**B**) CTr torque of the right middle (RM) leg and simultaneously recorded activity of the levator muscle (light blue) and depressor muscle (light red) of an example step. Dots above EMG traces indicate muscle spikes detected based on amplitude. TD, touch-down, LO, lift-off. (**C**) Raster plot of detected muscle spikes (top) and likelihood of muscle activation (bottom) relative to t_{UL} of the right middle leg (n = 73 steps from N = 8 animals). Walking speed corresponds to the mean speed of the COM during stance. The black box marks the step shown in **B**.

Note that depressor activity was much stronger than in tethered animals walking with body load supported (Cruse et al. 1993; Rosenbaum et al. 2010). This would be expected if depressor activity were driven in part by excitatory feedback from G3, and suggests that the depressor muscle contributes to body support and propulsion in free walking (Dallmann et al. 2016; Pearson 1972; Quimby et al. 2006)—a somewhat neglected aspect in current control models (Toth et al. 2012; Schilling et al. 2013). Levator activity after t_{UL} could result from decreased inhibitory feedback from G3. Note here that levator activity and, consequently, the lift-off of the leg were variable with respect to t_{UL} (Figure 3.3C, top). Part of this variability can be explained by step-to-step variations in unloading rate: the higher the unloading rate, the earlier the peak levator activity (Figure 3.4A, $r = -0.67$, $p < 0.001$). This would be expected if levator activity were driven in part by excitatory feedback from G4, because G4 afferent activity increases with increasing unloading rate (Zill et al. 2012) (Figure 3.4A, dark blue line).

In principle, levator activity could also be initiated by position and movement sig-

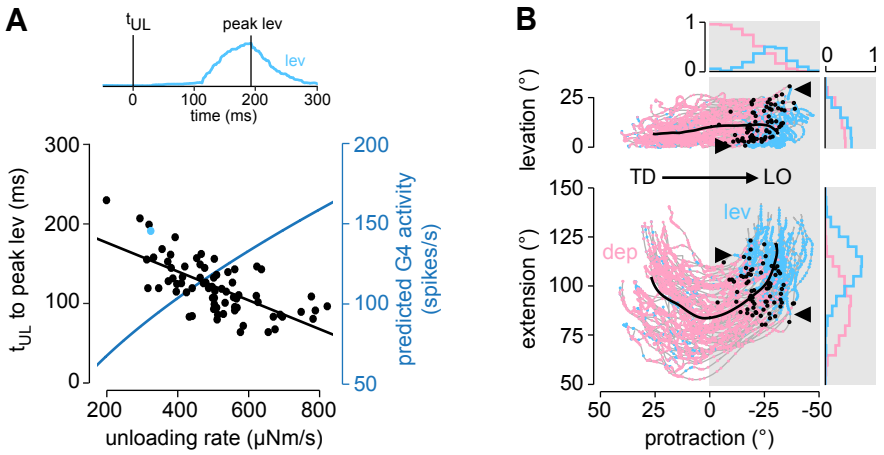

Figure 3.4: Levator activity is correlated with leg load, not leg movement
(**A**) Time from the onset of unloading (t_{UL}) to peak levator (lev) activity as a function of unloading rate ($r = -0.67$, $p < 0.001$, $n = 73$ steps from $N = 8$ animals). Peak levator activity was determined from rectified and smoothed EMG signals (moving average filter with 80 ms window). The inset on top shows the rectified and smoothed EMG signal for an example step (step is highlighted in light blue in the scatter plot and corresponds to step 28 in Figure 3.3C). The unloading rate corresponds to the mean CTr torque rate from t_{UL} to the lift-off of the leg in each step. The dark blue line shows the corresponding predicted G4 afferent activity (calculated based on data in Zill et al. 2012). (**B**) Leg movements during the stance phases in Figure 3.3C plotted in joint angle space. Colored dots indicate detected muscle spikes. Movement direction is from left to right (positive to negative protraction). Bold black lines show the mean movement trajectory. Black dots mark t_{UL} in individual stance phases. Histograms indicate the likelihood of muscle activation per 5° joint angle bins in the second half of stance (gray shaded area). Arrowheads mark the variable onset of levator muscle activity in two exemplary stance phases. At zero degree protraction and levation, the leg is perpendicular to the long body axis in the horizontal plane; at zero degree extension, the tibia is completely flexed.

nals from the leg. For example, flexion/extension of the tibia is signaled by the femoral chordotonal organ (Bucher et al. 2003; Hess and Büschges 1999), and leg levation is signaled by a hair plate on the trochanter (Schmitz 1986) and strand receptors in the coxa (Schöwerling 1992). However, the onset of levator activity did not correlate strongly with any specific joint angle or a change in movement direction, such as from flexion to extension (Figure 3.4B). Rather, the levator started firing at various leg angles from step to step (Figure 3.4B, arrowheads). Accordingly, the likelihood of muscle activation did not change abruptly with any one postural parameter (Figure 3.4B, histograms), contrary to the observed change with t_{UL}. The latter did not correlate strongly with any specific joint angle either (Figure 3.4B, black dots).

Taken together, these results indicate that load feedback from G3/G4 afferents can reliably promote the leg's stance-to-swing transition on a step-by-step basis.

3.4.3 Unloading of a leg can be specifically ascribed to loading of the ipsilateral posterior leg

The patterns of coxal muscle activity indicate that t_{UL} is not induced by the leg itself. Levator activity started only after t_{UL}, and given the slow temporal filter properties of insect muscle (Hooper et al. 2007), relaxation of the depressor must be expected to occur only after t_{UL} as well. Therefore, we tested whether t_{UL} and the ensuing change in muscle activity could be ascribed to mechanical load transfer within a specific pair of legs. This would be required for proper inter-leg coordination to emerge. If so, one would predict that t_{UL} is closely preceded by the touch-down of another leg, and that this leg can significantly unload the middle leg on a step-by-step basis.

To test for temporal correlation, we determined t_{UL} in individual steps of the right middle leg as above. In addition, we automatically detected the stance phases of all other legs relative to it based on the velocity of their tibia-tarsus joints (supplementary Figure 3.9A). Detected stance phases corresponded well with manually identified stance phases based on GRFs and digital video data (average difference $<$20 ms, supplementary Figure 3.9B). Figure 3.5A shows that t_{UL} was indeed closely preceded by the touch-down of a leg over the entire range of walking speeds. The temporal correlation was strongest with the right hind leg. It touched down most frequently 25-50 ms before t_{UL} (Figure 3.5A, arrowhead), or 35 $\pm$ 33 ms on average (n = 244 steps from N = 10 animals). In contrast, the relative touch-down times of the other legs were more scattered and did not coincide with middle leg unloading.

Assessing the magnitude of unloading in one leg due to loading of another is difficult in the experimentally measured torque profiles. Therefore, we used a mechanical simulation of the animal in static equilibrium (see Methods). The example time course depicted in Figure 3.5B shows the typical step-like increases and decreases in simulated torque induced by touch-downs and lift-offs of the other legs, with the right hind leg having the largest effect (arrowheads). The step-like decreases in torque provide a direct measure of the maximum unloading achievable through pure mechanical coupling, which we define as "unloading efficacy." Comparing the unloading efficacy across legs revealed that the right hind leg had the largest effect in all steps (Figure 3.5C, arrowhead). On average, it unloaded the middle leg by 23 $\pm$ 5 μNm (n = 244 steps from N = 10 animals). This corresponds to almost 50% of the CTr torque magnitude measured during walking (see Figure 2A)—the theoretical maximum load transfer between two neighboring legs in static equilibrium. In contrast, the unloading effects of the other legs were significantly weaker (ANOVA; $F_{4,876}$ = 2069.15, $p < 0.001$; Tukey's HSD post-hoc test at the 0.05 level of significance). The effects were consistent across animals.

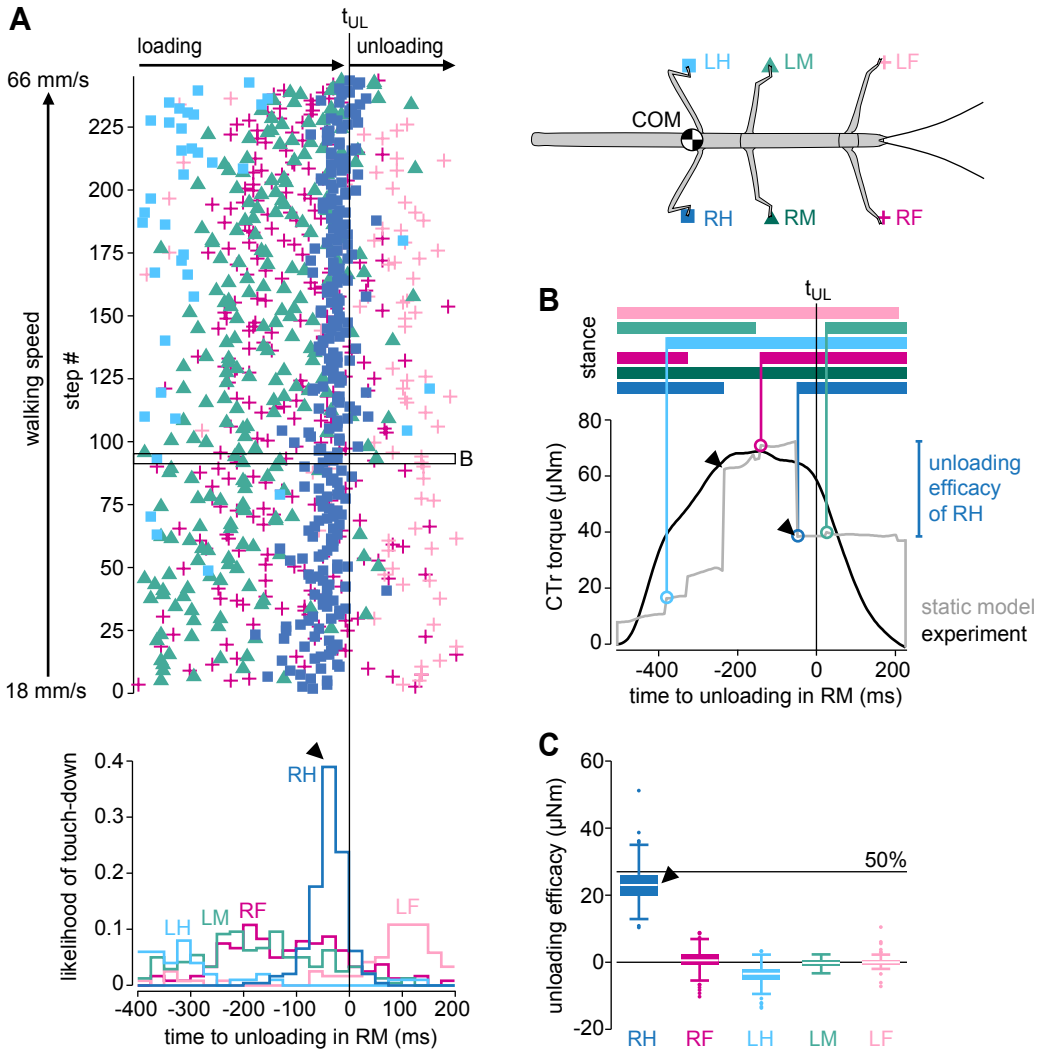

Figure 3.5: Leg unloading is linked to loading of posterior neighboring leg
(**A**) Touch-down events of all legs (top) and likelihood of touch-down per leg (bottom) relative to the onset of unloading, t_{UL}, in the right middle (RM) leg (n = 244 steps from N = 10 animals). Touch-downs of the right hind (RH) leg reliably precede t_{UL} in the middle leg with short latency (arrowhead). The black box marks the step shown in **B**. (**B**) Exemplary stance phase showing the CTr torque of the right middle leg from the experiment (black) and the static model (gray). Horizontal bars on top indicate the stance phases of the legs. Vertical lines mark the times of leg touch-downs. Touch-down induced changes in simulated torque provide a measure of a leg's unloading efficacy. The biggest changes in simulated torque are linked to the lift-off and touch-down of the right hind leg (arrowheads). (**C**) Simulated efficacy of legs in unloading the right middle leg, pooled across all steps. The hind leg has the highest unloading efficacy in all steps (arrowhead). The 50%-line corresponds to 50% of the mean torque measured during walking (see Figure 3.2A).

Taken together, the timing and magnitude of load transfer suggest that the unloading of the middle leg can be caused purely mechanically by the touch-down of the ipsilateral hind leg. Load transfer was similarly effective between ipsilateral front and middle legs (supplementary Figure 3.7).

3.5 Discussion

In this study, we tested whether animals can exploit the mechanical coupling of their legs during walking to establish adaptive inter-leg coordination. To this end, we provided the first simultaneous recordings of leg kinematics, ground reaction forces and muscle activity in a freely walking insect and a mechanical simulation of load transfer among legs. Our results suggest that the touch-down of a leg effectively unloads the neighboring leg in front, which can reliably detect the unloading and elicit motor effects promoting its stance-to-swing transition. This indicates that neighboring legs can be coordinated in a back-to-front sequence during walking based on their mechanical coupling through the ground.

Our results provide new insights into the flexible leg coordination found in insects (Bender et al. 2011; Dürr 2005; Pearson and Franklin 1984; Wosnitza et al. 2013). Intriguingly, much of this flexibility can be accounted for when assuming a simple set of coordination rules acting between direct neighboring legs ("Cruse rules"; Cruse 1990; Dürr et al. 2004; Schilling et al. 2013). Two core rules state that a leg's stance-to-swing transition is suppressed while the posterior neighboring leg is in swing (rule 1), but promoted as soon as the latter has touched down (rule 2). The load-based coordination mechanism described here could readily be a corresponding neuromechanical implementation. For example, while the hind leg is in swing, load of the middle leg is high. Local load feedback can then reinforce ongoing stance muscle activity in the middle leg and suppress the leg's stance-to-swing transition (rule 1). When the hind leg touches down, load of the middle leg effectively decreases due to mechanical coupling. The altered local load feedback can then promote the stance-to-swing transition of the middle leg (rule 2).

The hypothesis that campaniform sensilla on the trochanter mediate this feedback is supported by previous observations. For example, one study in stick insects described that continuous pressure on the trochanter can suppress the leg's stance-to-swing transition (Bässler 1977). Other studies in the stick insect, locust and cockroach, in which distal parts of a leg were denervated or replaced by a prosthesis, suggested that load feedback from proximal campaniform sensilla might be sufficient for coordination (Macmillan and Kien 1983; Noah et al. 2004; Wendler 1965). By linking biomechanics to mechanosensation in freely walking insects, our study builds upon these previous results in several ways. First, joint torque calculations allowed us to predict that G3/G4 are suited to reliably encode the unloading of the leg on a step-by-step basis. Second, relating leg motor activity directly to changes in leg load allowed us to investigate the corresponding intra-leg load reflex. Third, simulating the load transfer among legs

revealed that, through mechanical coupling, the load reflex can contribute to inter-leg coordination.

In natural locomotion, coordination likely results from integration of load feedback with other somatosensory feedback from the same and neighboring legs, as well as input from the brain (Borgmann and Büschges 2015). For example, G3/G4 feedback could be integrated with feedback from tibial and femoral campaniform sensilla local to the leg. These sensilla too respond to load changes in the plane of leg levation/depression (Zill et al. 2011; Zill et al. 2017). Indeed, activity of tibial campaniform sensilla has been suggested to reflect the unloading of the leg in cockroaches and locusts (Newland and Emptage 1996; Zill et al. 2009). In addition, G3/G4 feedback could be integrated with feedback from position and movement sensors of the leg (Schmitz and Stein 2000). For example, levator and depressor muscle activity could be modulated by input from the femoral chordotonal organ, which signals the position and movement of the tibia (Bucher et al. 2003; Hess and Büschges 1999). We found no strong correlation between the change in muscle activity and any one postural parameter (Figure 3.4B). However, it remains a possibility that a combination of changes in position and movement could contribute to timing the stance-to-swing transition (Cruse 1985). Finally, G3/G4 feedback could be integrated with proprioceptive signals from other legs (Borgmann et al. 2009; Brunn and Dean 1994; Dean 1989; Laurent and Burrows 1989). For example, campaniform sensilla on the hind leg could signal ground contact to the middle leg via polysynaptic pathways. This might explain why basic coordination patterns can be generated across legs even in the absence of mechanical coupling (Epstein and Graham 1983; Graham and Wendler 1981; Gruhn et al. 2006; Rosenbaum et al. 2010). Nevertheless, our results strongly suggest that mechanical coupling is exploited in natural locomotion to complement neural coordination signals between legs. To further understand this interplay, future studies might benefit from combining detailed biomechanical analyses like ours with genetic techniques (Tuthill and Wilson 2016) to selectively manipulate load feedback during unrestrained behavior.

It is plausible to assume that load-based coordination is used across insect species. Groups of campaniform sensilla similar to G3/G4 in stick insects (mutually perpendicular orientations in the plane of leg movement) are present on proximal leg segments of other insect species, including cockroaches (Zill et al. 1999), locusts (Hustert et al. 1981), blowflies and fruit flies (Gnatzy et al. 1987; Merritt and Murphey 1992). Although the load experienced by individual leg segments will depend on leg morphology, posture and body weight, cuticular strains can be expected particularly high on proximal leg segments. Therefore, these campaniform sensilla might well be similarly suited to reliably encode the mechanical interactions of legs during locomotion. Importantly,

a mechanical stimulus applied to the tarsus can propagate to campaniform sensilla on the trochanter almost instantly (less than 1 ms in a locust leg, Höltje and Hustert 2003). This might enable rapid local reflexes (Höltje and Hustert 2003) that mediate inter-leg coordination even at relatively high walking speeds.

The main features of the load-based coordination mechanism in stick insects also parallel findings in mammals. Studies in cats indicate that load feedback from GTOs reinforces extensor (stance) and inhibits flexor (swing) muscle activity while the leg is under load (Pearson 1995; Pearson 2008), analogously to load feedback from campaniform sensilla G3. Interestingly, simulation studies in cats and humans predict that this load feedback, rather than position feedback from the hip, leads to stable coordination between contralateral legs (Aoi et al. 2012; Ekeberg and Pearson 2005). Recent experiments in freely moving mice, in which proprioceptive feedback could be eliminated genetically, confirm a dominant role of local load feedback in coordination (Akay et al. 2014).

Together, these results indicate the possibility that mechanically mediated load-based coordination is a widespread control strategy. Implemented in multi-legged robots, the mechanism described here could provide a computationally inexpensive, robust and inherently adaptive alternative to control strategies based on explicit kinematic models.

3.6 Supplementary information

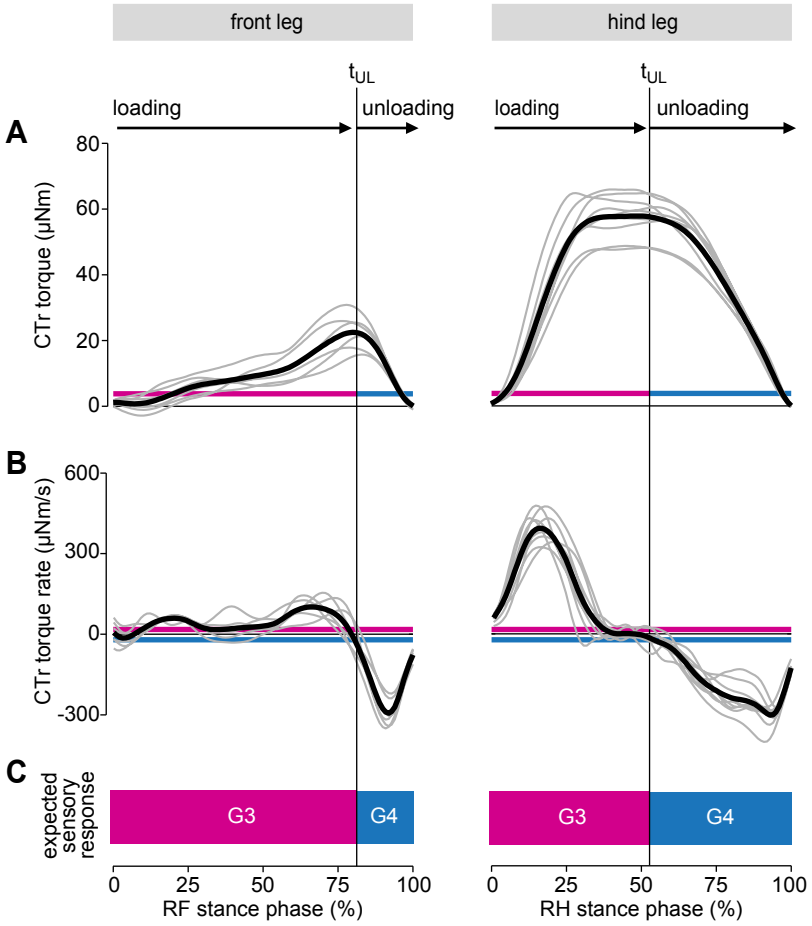

Figure 3.6: Joint torques of front and hind legs indicate that campaniform sensilla on the trochanter encode the unloading of the legs during walking
(**A**,**B**) Torque and torque rate at the CTr joint of the right front (RF) and right hind (RH) leg during stance. Bold black lines show the grand mean of all steps (RF, n = 140 steps from N = 6 animals; RH, n = 427 steps from N = 9 animals). Gray lines show means per animal. Magenta and blue lines indicate torques and torque rates above which G3/G4 afferent activity was confirmed in reduced middle leg preparations (calculated based on data in Zill et al. 2012). The vertical black line marks the onset of unloading, t_{UL}. (**C**) Schematic of the expected sensory response of campaniform sensilla groups G3 and G4 in front and hind legs based on the mean torque and torque rate time courses. Like in middle legs, leg unloading is expected to terminate G3 afferent activity and initiate G4 afferent activity.

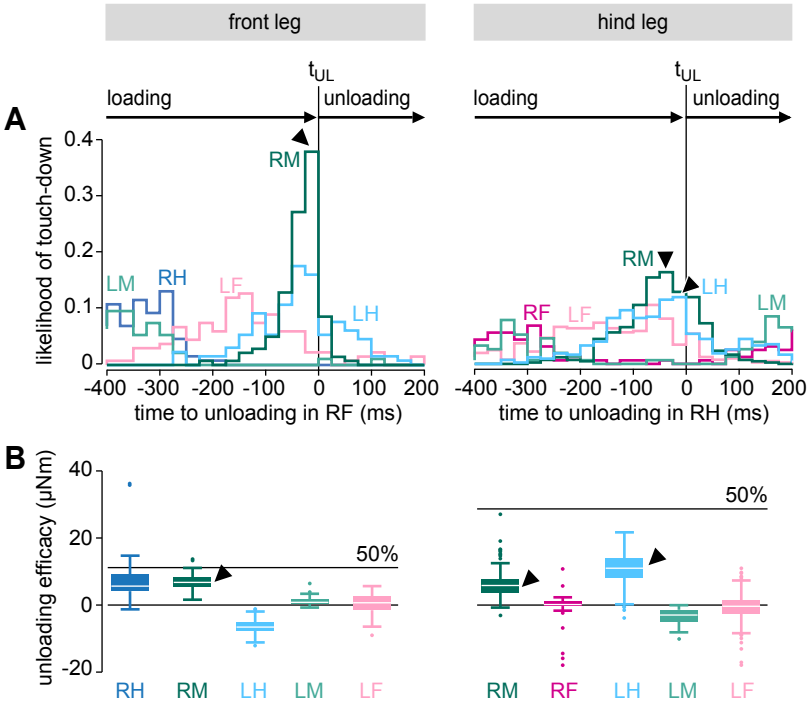

Figure 3.7: Unloading effects in front and hind legs due to mechanical coupling
(**A**) Likelihood of touch-down per leg relative to the onset of unloading, t_{UL}, in the right front (RF) and right hind (RH) leg (RF, n = 140 steps from N = 6 animals; RH, n = 427 steps from N = 9 animals). Unloading of the right front leg is closely preceded by the touch-down of the right middle (RM) leg (arrowhead left). Unloading of the right hind leg is preceded by touch-downs of both the right middle and the left hind (LH) leg (arrowheads right), but not any one leg alone. (**B**) Efficacy of legs in unloading the front and hind legs, pooled across steps. The 50%-lines corresponds to 50% of the mean CTr torques measured during walking (see supplementary Figure 3.6A). The right front leg can be unloaded by both ipsilateral legs. However, only the touch-downs of the middle leg (arrowhead left) coincide with front leg unloading (see **A**). The right hind leg can be unloaded by both the right middle and the left hind leg (arrowheads right). Their touch-downs also coincide with hind leg unloading (see **A**). Note though that the unloading effect is considerably smaller compared with the unloading effects of the hind on the middle leg (see Figure 3.5C) and the middle on the front leg (see **B**). Thus, the load-based mechanism depicted in Figure 3.1 might be particularly effective in coordinating ipsilateral legs in a back-to-front sequence. That is, the stance-to-swing transition in the middle leg is linked to the touch-down of the hind leg, and the stance-to-swing transition in the front leg is linked to the touch-down of the middle leg.

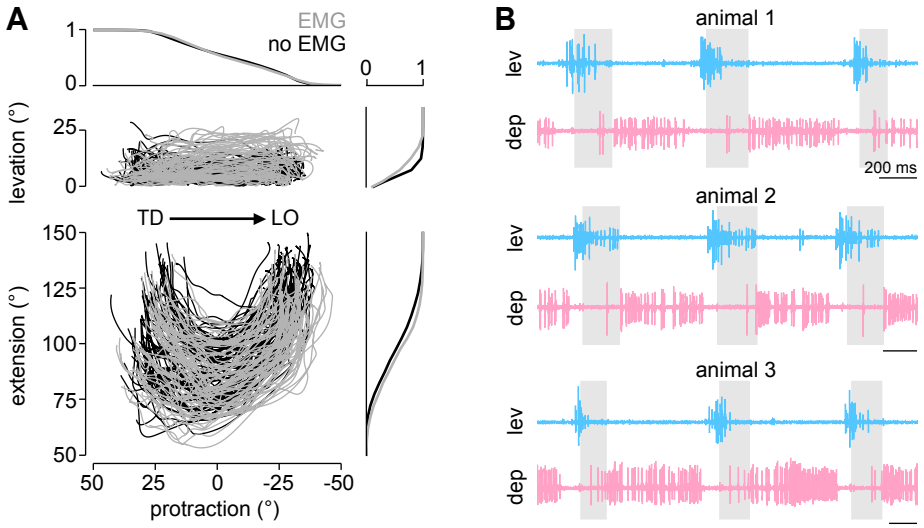

Figure 3.8: Effects of the EMG backpack on leg kinematics, and activity of the levator and depressor muscles during walking

(**A**) Electrode implantation and backpack attachment do not affect intra-leg coordination. Levation and extension angles versus protraction angles and their cumulative probabilities in right middle legs. Gray lines show data with EMG backpack attached and electrodes implanted (n = 73 steps from N = 8 animals, see Figure 3.3). Black lines show data recorded from the same animals prior to backpack attachment and electrode implantation (n = 80 steps from N = 8 animals). Movement direction is from left to right (positive to negative protraction). TD, touch-down, LO, lift-off. (**B**) Example EMG recordings of the coxal levator (swing) muscle and the coxal depressor (stance) muscle of right middle legs during unrestrained walking. Examples are from three different animals walking at slightly different speeds (note different lengths of scale bars, approx. 45 mm/s on average). Gray boxes indicate swing phases. Activity of the two muscles is largely reciprocal. Depressor activity starts during swing and is highest during stance. Main levator activity starts toward the end of stance after termination of depressor activity and continues into swing. Note that muscle activity during stance is stronger and less variable than in tethered animals walking with body load supported (Cruse et al. 1993; Rosenbaum et al. 2010). This difference could readily result from load feedback from campaniform sensilla G3/G4 (Figure 3.1D). Note also that levator EMGs are multiunit recordings containing activities of slow and fast motor neurons.

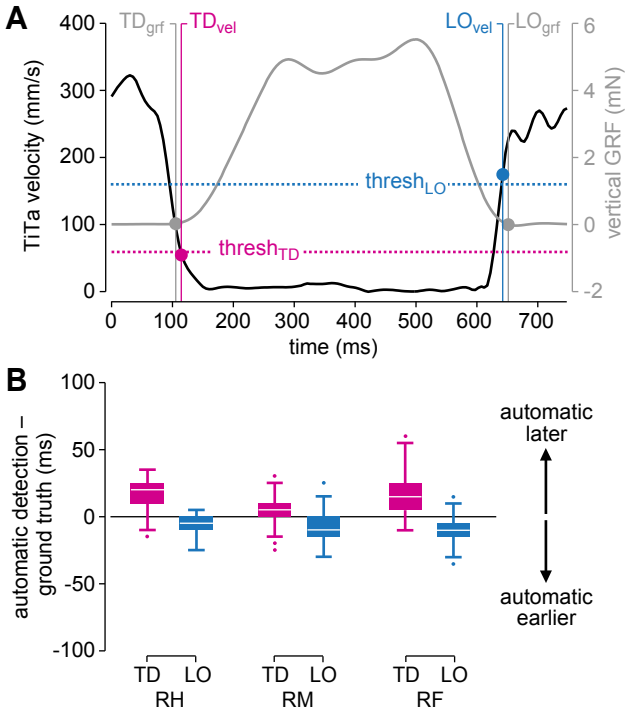

Figure 3.9: Automatic detection of stance phases
(**A**) Single step example of a right middle leg, illustrating the similarity of results from automatic and manual detection of leg touch-down (TD) and leg lift-off (LO). The automatic detection was based on the velocity magnitude of the tibia-tarsus joint (black) using threshold crossing (dotted lines, thresh_{TD} = 60 mm/s, thresh_{LO} = 160 mm/s). The manual detection was based on the vertical ground reaction force (GRF) of the leg (gray). The delay between automatically and manually detected events is small (10 ms, equivalent to two motion capture sampling points). (**B**) Delays between automatically detected and manually detected (ground truth) stance phases for all reference steps. The automatic detection worked reliably with small delays only. The sample numbers are: right hind (RH) leg, n = 427 steps from N = 9 animals; right middle (RM) leg, n = 244 steps from N = 10 animals; right front (RF) leg, n = 140 steps from N = 6 animals.

3.7 References

Akay, T., Ludwar, B. C., Göritz, M. L., Schmitz, J., and Büschges, A. (2007). Segment specificity of load signal processing depends on walking direction in the stick insect leg muscle control system. *J. Neurosci.* 27, 3285–3294.

Akay, T., Tourtellotte, W. G., Arber, S., and Jessell, T. M. (2014). Degradation of mouse locomotor pattern in the absence of proprioceptive sensory feedback. *Proc. Natl. Acad. Sci. U.S.A.* 111, 16877–16882.

Aoi, S., Ogihara, N., Funato, T., and Tsuchiya, K. (2012). Sensory regulation of stance-to-swing transition in generation of adaptive human walking: a simulation study. *Rob. Auton. Syst.* 60, 685–691.

Bässler, U. (1977). Sensory control of leg movement in the stick insect *Carausius morosus*. *Biol. Cybern.* 25, 61–72.

Bender, J. A., Simpson, E. M., Tietz, B. R., Daltorio, K. A., Quinn, R. D., and Ritzmann, R. E. (2011). Kinematic and behavioral evidence for a distinction between trotting and ambling gaits in the cockroach *Blaberus discoidalis*. *J. Exp. Biol.* 214, 2057–2064.

Borgmann, A., Hooper, S. L., and Büschges, A. (2009). Sensory feedback induced by front-leg stepping entrains the activity of central pattern generators in caudal segments of the stick insect walking system. *J. Neurosci.* 29, 2972–2983.

Borgmann, A. and Büschges, A. (2015). Insect motor control: methodological advances, descending control and inter-leg coordination on the move. *Curr. Opin. Neurobiol.* 33, 8–15.

Brunn, D. E. and Dean, J. (1994). Intersegmental and local interneurons in the metathorax of the stick insect *Carausius morosus* that monitor middle leg position. *J. Neurophysiol.* 72, 1208–1219.

Bucher, D., Akay, T., DiCaprio, R. A., and Büschges, A. (2003). Interjoint coordination in the stick insect leg-control system: the role of positional signaling. *J. Neurophysiol.* 89, 1245–1255.

Cruse, H. (1985). Which parameters control the leg movement of a walking insect? II. The start of the swing phase. *J. Exp. Biol.* 116, 357–362.

Cruse, H. (1990). What mechanisms coordinate leg movement in walking arthropods? *Trends Neurosci.* 13, 15–21.

Cruse, H., Schmitz, J., Braun, U., and Schweins, A. (1993). Control of body height in a stick insect walking on a treadwheel. *J. Exp. Biol.* 181, 141–155.

Dallmann, C. J., Dürr, V., and Schmitz, J. (2016). Joint torques in a freely walking insect reveal distinct functions of leg joints in propulsion and posture control. *Proc. R. Soc. B* 283, 20151708.

Dean, J. (1989). Leg coordination in the stick insect *Carausius morosus*: effects of cutting throacic connectives. *J. Exp. Biol.* 145, 103–131.

Dürr, V. (2005). Context-dependent changes in strength and efficacy of leg coordination mechanisms. *J. Exp. Biol.* 208, 2253–2267.

Dürr, V., Schmitz, J., and Cruse, H. (2004). Behaviour-based modelling of hexapod locomotion: linking biology and technical application. *Arthropod Struct. Dev.* 33, 237–250.

Duysens, J., Clarac, F., and Cruse, H. (2000). Load-regulating mechanisms in gait and posture: comparative aspects. *Physiol. Rev.* 80, 83–133.

Ekeberg, Ö. and Pearson, K. G. (2005). Computer simulation of stepping in the hind legs of the cat: an examination of mechanisms regulating the stance-to-swing transition. *J. Neurophysiol.* 94, 4256–4268.

Epstein, S. and Graham, D. (1983). Behaviour and motor output of stick insects walking on a slippery surface. I. Forward walking. *J. Exp. Biol.* 105, 215–229.

Frigon, A. (2017). The neural control of interlimb coordination during mammalian locomotion. *J. Neurophysiol.* 117, 2224–2241.

Gnatzy, W., Grünert, U., and Bender, M. (1987). Campaniform sensilla of *Calliphora vicina* (Insecta, Diptera). I. Topography. *Zoomorphology* 106, 312–319.

Goldammer, J., Büschges, A., and Schmidt, J. (2012). Motoneurons, DUM cells, and sensory neurons in an insect thoracic ganglion: a tracing study in the stick insect *Carausius morosus*. *J. Comp. Neurol.* 520, 230–257.

Graham, D. and Wendler, G. (1981). Motor output to the protractor and retractor coxae muscles in stick insects walking on a treadwheel. *Physiol. Entomol.* 6, 161–174.

Gruhn, M., Hoffmann, O., Dübbert, M., Scharstein, H., and Büschges, A. (2006). Tethered stick insect walking: a modified slippery surface setup with optomotor stimulation and electrical monitoring of tarsal contact. *J. Neurosci. Methods* 158, 195–206.

Hess, D. and Büschges, A. (1999). Role of proprioceptive signals from an insect femur-tibia joint in patterning motoneuronal activity of an adjacent leg joint. *J. Neurophysiol.* 81, 1856–1865.

Höltje, M. and Hustert, R. (2003). Rapid mechano-sensory pathways code leg impact and elicit very rapid reflexes in insects. *J. Exp. Biol.* 206, 2715–2724.

Hooper, S. L., Guschlbauer, C., Uckermann, G. von, and Büschges, A. (2007). Slow temporal filtering may largely explain the transformation of stick insect (*Carausius morosus*) extensor motor neuron activity into muscle movement. *J. Neurophysiol.* 98, 1718–1732.

Hustert, R., Pflüger, H. J., and Bräunig, P. (1981). Distribution and specific central projections of mechanoreceptors in the thorax and proximal leg joints of locusts. III. The external mechanoreceptors: the campaniform sensilla. *Cell Tissue Res.* 216, 97–111.

Kiehn, O. (2016). Decoding the organization of spinal circuits that control locomotion. *Nat. Rev. Neurosci.* 17, 224–238.

Laurent, G. and Burrows, M. (1989). Intersegmental interneurons can control the gain of reflexes in adjacent segments of the locust by their action on nonspiking local interneurons. *J. Neurosci.* 9, 3030–3039.

Macmillan, D. L. and Kien, J. (1983). Intra- and intersegmental pathways active during walking in the locust. *Proc. R. Soc. B* 218, 287–308.

Merritt, D. J. and Murphey, R. K. (1992). Projections of leg proprioceptors within the CNS of the fly *Phormia* in relation to the generalized insect ganglion. *J. Comp. Neurol.* 322, 16–34.

Newland, P. L. and Emptage, N. J. (1996). The central connections and actions during walking of tibial campaniform sensilla in the locust. *J. Comp. Physiol. A* 178, 749–762.

Noah, A. J., Quimby, L., Frazier, F. S., and Zill, S. N. (2001). Force detection in cockroach walking reconsidered: discharges of proximal tibial campaniform sensilla when body load is altered. *J. Comp. Physiol. A* 187, 769–784.

Noah, J. A., Quimby, L., Frazier, S. F., and Zill, S. N. (2004). Sensing the effect of body load in legs: responses of tibial campaniform sensilla to forces applied to the thorax in freely standing cockroaches. *J. Comp. Physiol. A* 190, 201–215.

Owaki, D., Kano, T., Nagasawa, K., Tero, A., and Ishiguro, A. (2013). Simple robot suggests physical interlimb communication is essential for quadruped walking. *J. R. Soc. Interface* 10, 20120669.

Owaki, D. and Ishiguro, A. (2017). A quadruped robot exhibiting spontaneous gait transitions from walking to trotting to galloping. *Sci. Rep.* 7, 277.

Pearson, K. G. (1972). Central programming and reflex control of walking in the cockroach. *J. Exp. Biol.* 56, 173–193.

Pearson, K. G. (1995). Proprioceptive regulation of locomotion. *Curr. Opin. Neurobiol.* 5, 786–791.

Pearson, K. G. (2008). Role of sensory feedback in the control of stance duration in walking cats. *Brain Res. Rev.* 57, 222–227.

Pearson, K. G. and Franklin, R. (1984). Characteristics of leg movements and patterns of coordination in locusts walking on rough terrain. *Int. J. Rob. Res.* 3, 101–112.

Pringle, J. W. S. (1938). Proprioception in insects. II. The action of the campaniform sensilla on the legs. *J. Exp. Biol.* 15, 114–131.

Quimby, L. A., Amer, A. S., and Zill, S. N. (2006). Common motor mechanisms support body load in serially homologous legs of cockroaches in posture and walking. *J. Comp. Physiol. A* 192, 247–266.

Ritzmann, R. E. and Büschges, A. (2007). Adaptive motor behavior in insects. *Curr. Opin. Neurobiol.* 17, 629–636.

Rosenbaum, P., Wosnitza, A., Büschges, A., and Gruhn, M. (2010). Activity patterns and timing of muscle activity in the forward walking and backward walking stick insect *Carausius morosus*. *J. Neurophysiol.* 104, 1681–1695.

Schilling, M., Hoinville, T., Schmitz, J., and Cruse, H. (2013). Walknet, a bio-inspired controller for hexapod walking. *Biol. Cybern.* 107, 397–419.

Schmitz, J. (1986). The depressor trochanteris motoneurons and their role in the coxo-trochanteral feedback loop in the stick insect *Carausius morosus*. *Biol. Cybern.* 55, 25–34.

Schmitz, J. (1993). Load-compensating reactions in the proximal leg joints of stick insects during standing and walking. *J. Exp. Biol.* 33, 15–33.

Schmitz, J. and Stein, W. (2000). Convergence of load and movement information onto leg motoneurons in insects. *J. Neurobiol.* 42, 424–436.

Schöwerling, H. (1992). Untersuchungen zur Reflexaktivierung der Levator-Trochanteris Muskeln der Stabheuschrecke *Carausius mororsus*, Br. Thesis. Bielefeld University.

Toth, T. I., Knops, S., and Daun-Gruhn, S. (2012). A neuromechanical model explaining forward and backward stepping in the stick insect. *J. Neurophysiol.* 107, 3267–3280.

Tuthill, J. C. and Wilson, R. I. (2016). Mechanosensation and adaptive motor control in insects. *Curr. Biol.* 27, R1022–R1038.

Wendler, G. (1965). The co-ordination of walking movements in arthropods. *Symp. Soc. Exp. Biol.* 20, 229–249.

Wosnitza, A., Bockemühl, T., Dübbert, M., Scholz, H., and Büschges, A. (2013). Inter-leg coordination in the control of walking speed in *Drosophila*. *J. Exp. Biol.* 216, 480–491.

Zill, S. N., Büschges, A., and Schmitz, J. (2011). Encoding of force increases and decreases by tibial campaniform sensilla in the stick insect, *Carausius morosus*. *J. Comp. Physiol. A* 197, 851–867.

Zill, S. N., Chaudhry, S., Büschges, A., and Schmitz, J. (2015). Force feedback reinforces muscle synergies in insect legs. *Arthropod Struct. Dev.* 44, 541–553.

Zill, S. N., Keller, B. R., and Duke, E. R. (2009). Sensory signals of unloading in one leg follow stance onset in another leg: transfer of load and emergent coordination in cockroach walking. *J. Neurophysiol.* 101, 2297–2304.

Zill, S. N. and Moran, D. T. (1981). The exoskeleton and insect proprioception. III. Activity of tibial campaniform sensilla during walking in the American cockroach, *Periplaneta americana*. *J. Exp. Biol.* 94, 57–75.

Zill, S. N., Neff, D., Chaudhry, S., Exter, A., Schmitz, J., and Büschges, A. (2017). Effects of force detecting sense organs on muscle synergies are correlated with their response properties. *Arthropod Struct. Dev.* 46, 564–578.

Zill, S. N., Ridgel, A. L., DiCaprio, R. A., and Frazier, S. F. (1999). Load signalling by cockroach trochanteral campaniform sensilla. *Brain Res.* 822, 271–275.

Zill, S. N., Schmitz, J., and Büschges, A. (2004). Load sensing and control of posture and locomotion. *Arthropod Struct. Dev.* 33, 273–286.

Zill, S. N., Schmitz, J., Chaudhry, S., and Büschges, A. (2012). Force encoding in stick insect legs delineates a reference frame for motor control. *J. Neurophysiol.* 108, 1453–1472.

Chapter 4

Mechanics and muscle activity during incline walking

This chapter is an unpublished manuscript. It was co-authored by Volker Dürr and Josef Schmitz. C.J.D. and J.S. conceived the study; C.J.D. performed experiments and analyzed data; C.J.D., V.D. and J.S. interpreted results; C.J.D. prepared figures; C.J.D. drafted the manuscript; C.J.D., V.D. and J.S. revised the manuscript.

4.1 Abstract

Walking is a complex control task that requires continuous adjustments in leg muscle activity to changes in the environment, such as the inclination of the ground. In the case of insect walking, understanding the underlying control has been limited in part because little is known about how leg muscle activity changes with leg kinematics (movements) and leg dynamics (forces, torques) in different walking situations. Here we approach this issue by combining electromyography with motion capture and ground reaction force measurements in hind legs of stick insects (*Carausius morosus*) walking freely on level ground and up and down inclines ($\pm 45^\circ$). We found that kinematics including leg joint angles and body height varied little across inclines, although dynamics revealed substantial changes in mechanical demand. During downhill walking, for example, horizontal leg forces and torques at the thorax-coxa and femur-tibia joints reversed in sign. At the thorax-coxa joint, the altered mechanical demand was met by adjustments in timing and magnitude of antagonistic muscle activity. Adjustments occurred primarily in the first half of stance after the touch-down of the leg. When insects transitioned from level to incline walking, the characteristic adjustments in muscle activity occurred with the first step of the leg on the incline, but not in anticipation. Together, these findings indicate that stick insects adjust leg muscle activity on a step-by-step basis so as to maintain the same kinematic pattern under different mechanical demands. The underlying control might rely primarily on local feedback from leg proprioceptors signaling leg position and movement.

4.2 Introduction

The ability to adjust leg muscle activity to changes in the mechanical demand acting on the body is critical for stable walking. During walking, the mechanical demand can vary considerably from one situation to the next. For example, while the gravitational force pulls the body toward the surface during level walking, it pulls the body backward during uphill walking and forward during downhill walking. How is leg muscle activity adjusted to adequately propel and stabilize (balance) the body in these situations?

From insects to mammals, leg muscle activity is thought to be controlled via neural circuits in the central nervous system that integrate descending inputs from the brain and afferent inputs from the leg (Hooper and Büschges 2017; Orlovsky et al. 1999; Pearson 1995; Prochazka 1996). Thus, one possibility is that descending inputs mediate distinct motor programs for inclines, for example by modifying muscle synergies (Smith et al. 1998). Another possibility is that afferent inputs from leg proprioceptors adjust leg muscle activity reflexively on a step-by-step basis. For example, if leg extensors

are loaded more during uphill walking and less during downhill walking, load feedback could reflexively activate leg extensors more or less strongly and thereby automatically account for changes in the inclination of the ground (Donelan et al. 2009; Gregor et al. 2006).

To understand the potential contribution of descending and afferent inputs to control, it is important to determine leg muscle activity together with leg kinematics (movements) and leg dynamics (forces, torques) during level and incline walking. These parameters may indicate whether a distinct motor program is used on inclines (Lay et al. 2006; Lay et al. 2007), or to what extent movement- and load-related afferent inputs from the leg can account for adjustments in muscle activity (Donelan et al. 2009; Gregor et al. 2006). Here, we study these parameters in a freely walking insect.

Due to their accessible nervous and musculoskeletal systems, insects have served as important model systems for studying the adaptive control of walking (Büschges and Gruhn 2007; Tuthill and Wilson 2016; Zill et al. 2004). Previous studies on insects walking on inclines examined inclination-dependent changes in leg muscle activity (cockroach: Larsen et al. 1995; locust: Duch and Pflüger 1995), leg kinematics (fruit fly: Mendes et al. 2014; ant: Seidl and Wehner 2008; cockroach: Spirito and Mushrush 1979), or leg forces (ant: Wöhrl et al. 2017; cockroach: Goldman et al. 2006; stick insect: Cruse 1976b). However, no study has combined all measurements in a single animal. As a consequence, changes in parameters such as joint torques, which are closely related to load feedback (Dallmann et al. 2017), remain unknown. In addition, the different species, walking speeds and inclinations investigated make it difficult to compare measurements and draw conclusions about control.

Here, we approach this issue by combining electromyography (EMG) with 3D motion capture and ground reaction force measurements in stick insects walking freely on level ground and up and down inclines ($\pm 45°$). Stick insects move slowly and are thought to rely heavily upon sensory feedback during walking (Bässler 1983; Büschges and Gruhn 2007; Dürr et al. 2018; Graham 1985). Importantly, their comparatively long and unspecialized legs permit analyses of leg kinematics (Theunissen and Dürr 2013), dynamics (Dallmann et al. 2016), and muscle activity (Dallmann et al. 2017) during unrestrained locomotion. The present study focuses on hind legs, which are critical to propel the body and stabilize it above ground during level walking (Dallmann et al. 2016). To better understand how insects control walking on inclines, we ask (1) whether stick insects use distinct kinematic patterns on inclines, (2) how walking on inclines affects the mechanical demand on the leg and on individual leg joints, and (3) how antagonistic muscle activity is adjusted to meet this mechanical demand. Our results suggest that stick insects adjust leg muscle activity on a step-by-step basis using

local position and movement signals from the legs so as to maintain the same kinematic pattern under different mechanical demands.

4.3 Methods

We tested seven adult, female stick insects (*Carausius morosus*) reared in a laboratory colony (body mass: 0.9 $\pm$ 0.1 g, mean $\pm$ s.d.; body length without antennae: approx. 75 mm). Animals walked freely along a walkway (40 $\times$ 500 mm) with five integrated force plates (Figure 4.1A). The walkway was either horizontal or inclined at +45° (uphill) or -45° (downhill). Five animals were equipped with motion capture markers and an EMG backpack for kinematic and electromyographic analyses (Figures 4.2, 4.4 and 4.5). To maintain the same EMG signal quality within animals, all trials of a given animal were recorded on a single day. To increase the number of force plate measurements, two additional animals without an EMG backpack were tested on multiple days. Data from all animals were used for dynamic analyses (Figure 4.3).

4.3.1 Motion capture and force measurements

Leg movements and single leg ground reaction forces (GRFs) were measured and analyzed similarly to our previous studies (Dallmann et al. 2016; Theunissen and Dürr 2013). Although the present study focuses on hind legs, we recorded movements of the whole body by attaching 18 small (1.5 mm diameter), lightweight (4 mg) motion capture markers to the insect's body and leg segments. Three markers were glued to the metathorax, one to the mesothorax, one to the prothorax, one to the head, and one to each femur and tibia (Figure 4.1A). Markers were tracked in 3D at 200 Hz using an eight-camera motion capture system (Vicon MX10 with T10 cameras, controlled by software Nexus 1.8.5; Vicon, Oxford, UK). GRFs of the right hind leg were measured with one of five strain-gauge-based force plates (5 $\times$ 5 mm contact area; Figure 4.1A). GRFs were measured in 3D at 6000 Hz. Kinematic and GRF data were low-pass filtered with a zero-lag, fourth-order Butterworth filter using cut-off frequencies of 20 Hz and 10 Hz, respectively. Joint kinematics and joint torques were calculated in Matlab (The MathWorks, Natick, MA, USA) using a 3D rigid link model of the leg as described previously (Dallmann et al. 2016). The three main leg joints—the thorax-coxa (ThC) joint, the coxa-trochanter (CTr) joint, and the femur-tibia (FTi) joint—were modeled as hinges with one degree of freedom each (Figure 4.1B). Touch-down and lift-off events of the hind leg were determined manually based on a synchronized side view of the walkway, which was recorded with an additional digital video camera at 100 Hz (Basler A602fc, Ahrensburg, Germany).

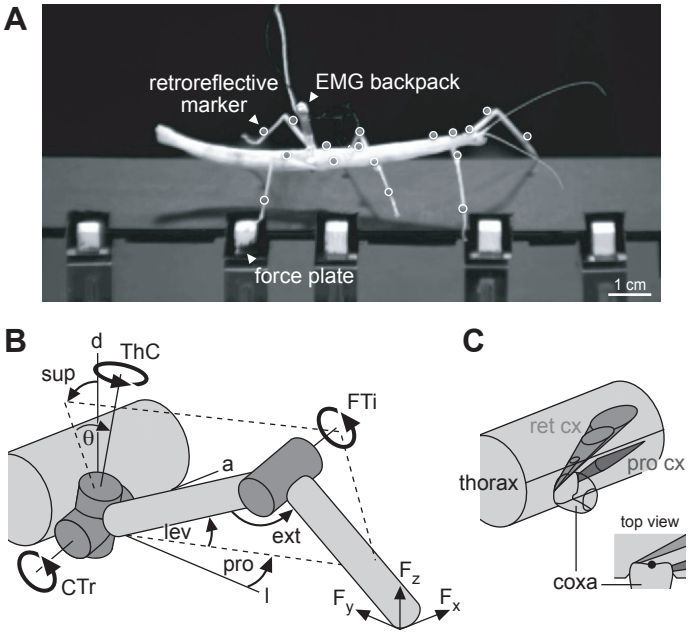

Figure 4.1: Combining motion capture, ground reaction force measurements and electromyography in freely walking stick insects
(**A**) Side view of a stick insect carrying a lightweight EMG backpack and motion capture markers (white circles) while stepping onto a force plate with its right hind leg. The walkway was either level (as shown here) or inclined at $\pm 45°$. (**B**) Rigid link model of a right leg used for calculations of joint kinematics and torques (Dallmann et al. 2016). The thorax-coxa (ThC), coxa-trochanter (CTr) and femur-tibia (FTi) joints were modeled as hinges (dark gray). The ThC joint is slanted relative to the vertical body axis ($\theta = 30°$). The CTr joint is considered to be directly connected to the thorax. Therefore, leg segments indicate the tibia and an artificial segment comprising the coxa and the trochantero-femur (trochanter and femur are fused in stick insects). Positive torques about the ThC joint supinate (sup) and protract (pro) the leg. Positive torques about the CTr and FTi joint lift the coxa-trochantero-femur (lev) and extend the tibia (ext) within the leg plane (dashed lines), respectively. Leg forces (F) are shown in body-centered coordinates. a, anterior; l, lateral; d, dorsal. (**C**) EMGs were recorded from the protractor coxae (pro cx) and retractor coxae (ret cx) muscles of the hind leg in the metathorax. The protractor inserts at the anterior rim of the coxa and can move the leg forward; the retractor inserts at the posterior rim of the coxa and can move the leg backward. Schematic based on two-dimensional drawings in Graham (1985).

4.3.2 Muscle recordings

We recorded EMGs from the protractor and retractor coxae muscles of right hind legs (Figure 4.1C). EMGs of each muscle were recorded with a pair of steel wires (50 µm diameter, insulated except for the tips). Wires were implanted through small holes in the metathorax and held in place with dental glue. Correct electrode placement was verified using standard criteria including resistance reflex responses to imposed forward-backward movements of the leg around the ThC joint. Animals carried a lightweight (50 mg) EMG backpack to direct the EMG electrodes to the amplifiers without impairing leg movements (Figure 4.1A; see Dallmann et al. 2017). To affect overall body dynamics only minimally, the backpack was attached close to the body's center of mass (COM), which is located just behind the hind leg coxae (rear end of the fused metatho-

racic and first abdominal segment). Backpack attachment and electrode implantation did not affect joint kinematics (supplementary Figure 4.6). EMG signals were amplified and filtered with a 50 Hz notch, 250 Hz high-pass, and 7.5 kHz low-pass filter using a custom-built amplifier (MA102, Electronics Workshop, Zoological Institute, Cologne, Germany). Filtered signals were A/D converted and recorded in parallel with Vicon Nexus and Spike2 (Cambridge Electronic Design, Cambridge, UK) with sampling rates of 6 kHz and 25 kHz, respectively. Vicon and Spike2 recordings were synchronized via a custom-built external trigger box.

The protractor and retractor EMGs were multiunit recordings, containing activity of slow and fast motor neurons (Figure 4.4A). The protractor muscle is innervated by 6-9 excitatory motor neurons; the retractor muscles are innervated by up to 17 excitatory motor neurons (Goldammer et al. 2012). With the exception of large amplitude protractor units (Figure 4.4A, asterisks), single units generally could not be discriminated. Therefore, muscle activity for level walking was compared to incline walking based on rectified and low-pass filtered EMG recordings. We used a first-order low-pass filter with a short time constant of 5 ms to accurately reflect the onset and offset of muscle activity. First, recordings were divided into single step cycles (swing phase plus subsequent stance phase) based on the manually determined touch-down and lift-off events of the leg (see above). Swing and stance phases were normalized to 1000 data points each. Next, the minimum activity per step cycle of each muscle was set to zero. Typically, protractor activity was minimal at some time point during stance, whereas retractor activity was minimal during swing (Figure 4.4A). Finally, for each animal, we calculated the average EMG time courses over the step cycle for level, uphill and downhill walking and then normalized the amplitude of these time courses to the mean amplitude of the average EMG time course for level walking. The resulting measure indicated changes in the magnitude of muscle activity relative to level walking (Figure 4.4B). In addition, we thresholded the amplitude of the rectified and smoothed EMG signals to better resolve the timing of muscle activation (Figure 4.4A). Pooled across trials, the times of muscle activation allowed us to calculate a likelihood of muscle activation relative to a given event, such as the touch-down of the leg (Figure 4.4C). Careful inspection revealed that the retractor recording was occasionally contaminated by cross-talk from large amplitude protractor spikes during swing. This cross-talk was edited out manually for likelihood calculations.

4.3.3 Statistical analysis

Some kinematic parameters varied with walking speed (Figure 4.2). To test for the effect of inclination on these parameters while accounting for the effect of speed, we used a

linear mixed model approach. The analysis was performed in R (R Core Team, www.R-project.com) using the lme4 package (Bates et al. 2015). The inclination of the walkway (0°, +45°, -45°) and walking speed (average speed of the COM over the step cycle) were specified as categorial and continuous fixed effects, respectively, without an interaction term. Individual animals were set as a random effect with random intercept and random slope. Visual inspection of residual plots did not reveal any obvious deviations from normality or homoscedasticity (homogeneity of variance). To test whether inclination had a significant effect on a given parameter, we used the likelihood ratio test to compare the model with inclination as a fixed effect to a model without it.

Other parameters like leg forces and joint torques (Figure 4.3) and likelihoods of muscle activation (Figure 4.4C) varied only little with walking speed. For these parameters, repeated measures of an animal were treated as independent observations and pooled across animals.

4.4 Results

4.4.1 Kinematics change little on inclines

To test whether stick insects use distinct kinematic patterns on inclines, we compared hind leg kinematics during level (0°) walking with those during uphill (+45°) and downhill (-45°) walking. Animals walked readily up and down the inclines. Like in level walking, the hind leg closely followed the middle leg on the same side of the body, which in turn followed the front leg (Figure 4.2A; see also Cruse 1979; Dean and Wendler 1983; Theunissen et al. 2014). Walking speeds ranged from 23-85 mm/s (approx. 0.3-1.1 body lengths/s; defined as the average speed of the COM over the step cycle). In all walking conditions, stance durations of the hind leg decreased with increasing walking speed, whereas swing durations varied little (Figure 4.2B). The dependence of stance duration on walking speed was approximately hyperbolic as suggested previously (Figure 4.2B; Wendler 1964). Stance durations tended to be longer on inclines (Figure 4.2B, boxplots side). However, the longer stance durations were correlated with slower walking speeds (Figure 4.2B, boxplots top). After accounting for the effect of speed, inclination had no significant effect on stance or swing durations (stance durations: $\chi^2(2) = 0.31$, $p = 0.85$; swing durations: $\chi^2(2) = 2.02$, $p = 0.36$). Accordingly, the hyperbolic fits of stance duration over walking speed were practically identical in all conditions (Figure 4.2B, see caption for details).

Other kinematic parameters also varied little on inclines, although small systematic trends were discernable for most of them (Table 4.1, arrows). The average height of the COM above the walking surface was approximately 11 mm during level walking

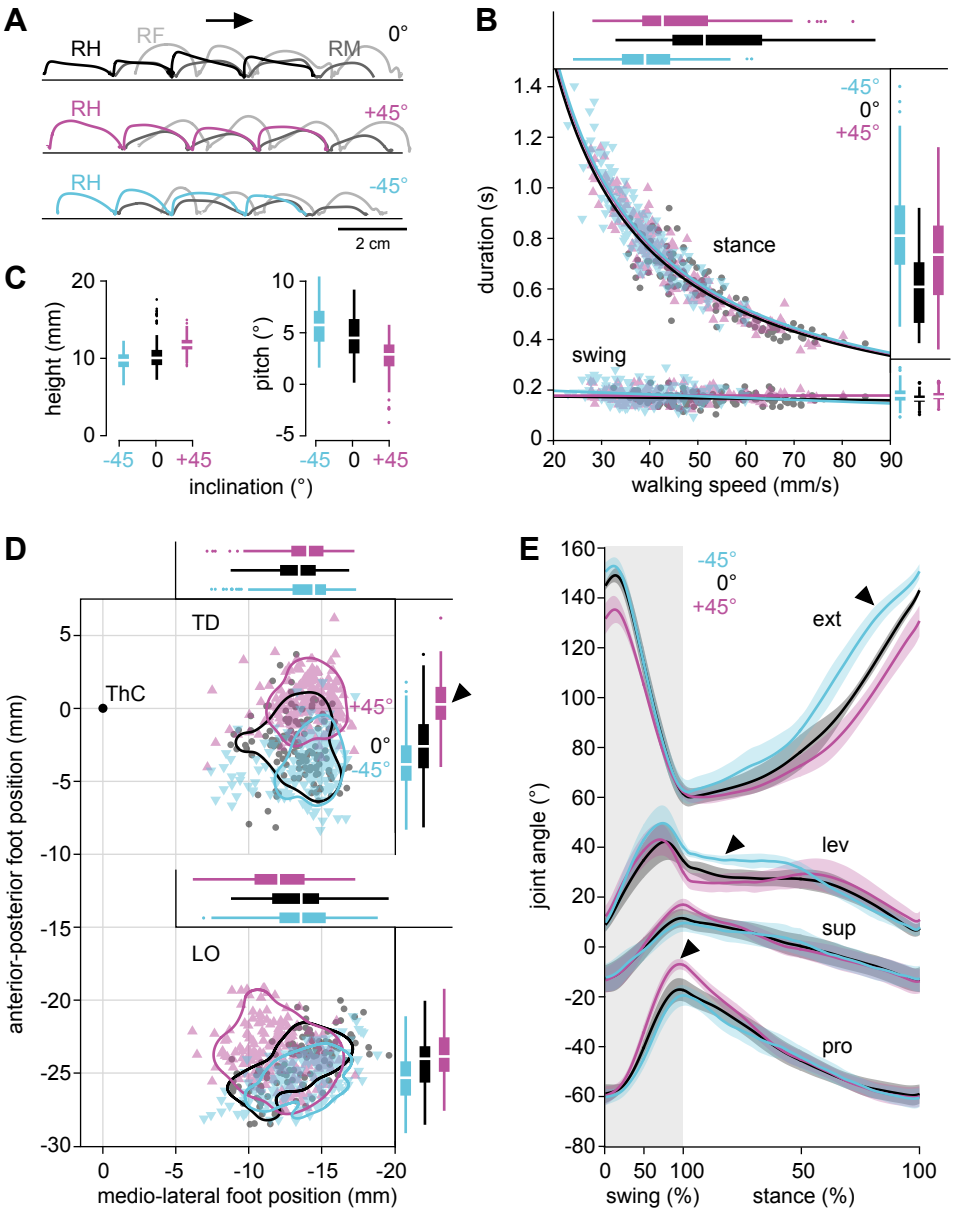

Figure 4.2: Hind leg kinematics during level and incline walking
(**A**) Example side-view trajectories of the tibia-tarsus joint of a right hind (RH) leg during level walking (black), uphill walking (magenta) and downhill walking (blue). Dark gray and light gray lines show trajectories of the right middle (RM) and right front (RF) leg, respectively. Walking direction is from left to right. (**B**) Stance and swing durations of the hind leg as a function of speed for level walking (black), uphill walking (magenta) and downhill walking (blue). Lines indicate hyperbolic fits of stance duration over speed (a/speed; 0°: a = 30.27, R^2 = 0.78; +45°: a = 31.06, R^2 = 0.89; -45°: a = 31.31, R^2 = 0.83). Sample numbers are n = 126 steps for 0°, n = 199 steps for +45°, n = 174 steps for -45°, pooled across N = 5 animals. (**C**) Body height and body pitch averaged over the step cycle as a function of inclination, pooled across the steps shown in **B**. (**D**) Touch-down (TD) and lift-off (LO) locations of the hind leg in body-centered coordinates. (0,0) marks the ThC joint. Contours indicate the 75th percentile ranges based on 2D kernel density estimates (Botev et al. 2010) of pooled steps. Boxplots are also based on pooled steps. The arrowhead marks the maximal deviation in foot placement from level walking. Sample numbers as in **B**. (**E**) Joint angles of the hind leg normalized to swing and stance duration (see Figure 4.1B for angle conventions). Lines show means of animal means, error bands show 95% confidence intervals of animal means (N = 5). Arrows mark the maximal angle deviations from level walking.

and differed by less than 1.2 mm on inclines (Figure 4.2C and Table 4.1). The average body pitch angle (angle between metathorax and walking surface) was approximately 5° during level walking and differed by less than 2° on inclines (Figure 4.2C and Table 4.1). That is, the body was kept at a similar height and almost in parallel to the walking surface in all walking conditions. Touch-down and lift-off locations of the hind leg were slightly shifted anteriorly with increasing inclination (Figure 4.2D, boxplots side; touch-down position: $\chi^2(2) = 15.243$, $p < 0.001$; lift-off position: $\chi^2(2) = 10.696$, $p < 0.01$). The change was largest for the touch-down position during uphill walking (3 mm on average, Table 4.1; Figure 4.2D, arrowhead). Accordingly, inclination had a small but significant effect on step length (defined as the Euclidean distance between touch-down and lift-off positions in body-centered coordinates; $\chi^2(2) = 15.792$, $p < 0.001$). On average, however, step length differed by less than 12% on inclines (Table 4.1).

Time courses of joint angles were also similar on inclines (Figure 4.2E). In all conditions, the leg was protracted, supinated, levated and flexed during swing and retracted, pronated, depressed and extended during stance. During uphill walking, the hind leg was slightly more protracted at the end of swing (10° difference on average, Table 4.1; Figure 4.2E, arrowhead). This was consistent with its more anterior touch-down position. During downhill walking, the hind leg was slightly more levated at the beginning of stance and more extended at the end of stance (7° and 17° difference on average, Table 4.1; Figure 4.2E, arrowheads). The latter was consistent with its more posterior lift-off position. The effect of inclination at these time points was significant (protraction: $\chi^2(2) = 12.518$, $p < 0.01$; levation: $\chi^2(2) = 14.125$, $p < 0.001$; extension: $\chi^2(2) = 12.989$, $p < 0.01$).

Taken together, stick insects tended to walk slower on inclines but with little change in kinematics, indicating that the same kinematic pattern was used across walking conditions.

4.4.2 Leg forces and joint torques reveal substantial changes in mechanical demands on inclines

Because animals kept their body almost in parallel to the walking surface, the orientation of the body with respect to gravity differed substantially across walking conditions. To study the consequent changes in the mechanical demand on the legs, we analyzed hind leg forces and joint torques during level and incline walking (Figure 4.3 and Table 4.2). Forces and torques during level walking corresponded well with our previous measurements on level ground (Dallmann et al. 2016). On inclines, they differed substantially. The hind leg pushed backward to accelerate (propel) the body during level and more strongly during uphill walking, but it pushed forward to decelerate (brake) the body

Table 4.1: Kinematic parameters for level (0°) and incline (±45°) walking.[a]

kinematic parameter	-45°	0°	+45°	positive trend
body height (mm)	9.84 ± 1.14	10.69 ± 2.15	11.84 ± 1.04	→
body pitch (°)	5.80 ± 2.04	4.68 ± 2.01	2.74 ± 1.61	←
step length (mm)	21.76 ± 2.22	21.86 ± 2.62	24.26 ± 2.20	→
TD a-p (mm)	-3.78 ± 1.77	-2.65 ± 2.15	0.33 ± 1.59	→
TD m-l (mm)	-13.83 ± 2.05	-13.28 ± 1.72	-13.88 ± 1.74	
LO a-p (mm)	-25.37 ± 1.59	-24.32 ± 1.85	-23.71 ± 1.82	→
LO m-l (mm)	-13.54 ± 2.32	-13.35 ± 2.32	-12.07 ± 2.15	→
pro at 100% swing (°)	-18.78 ± 6.49	-16.30 ± 6.87	-6.73 ± 5.02	→
lev at 20% stance (°)	35.28 ± 4.84	28.42 ± 5.13	26.72 ± 5.18	←
ext at 80% stance (°)	129.43 ± 13.29	112.35 ± 13.32	101.20 ± 13.06	←

[a]Values are mean ± s.d. (n = 126 steps for 0°, n = 174 steps for -45°, n = 199 steps for +45°, pooled across animals). Body height and body pitch are net values averaged over each step cycle. TD, touch-down; LO, lift-off; a, anterior; p, posterior; m, medial; l, lateral; pro, protraction angle; lev, levation angle; ext, extension angle. See Figure 4.1B for angle conventions. Arrows indicate systematic (albeit small), positive trends of parameter means with increasing (rightward) or decreasing (leftward) inclination.

during downhill walking (Figure 4.3B, F_x, arrowhead). This sign reversal was evident in all steps recorded. It was accompanied by a change in the medio-lateral direction, in which the hind leg reversed from pushing outward during level and uphill walking to pulling inward during downhill walking (Figure 4.3B, F_y, arrowhead). Vertical forces were similar for level and uphill walking, but reduced in magnitude for downhill walking (Figure 4.3B, F_z). The latter is to be expected considering the location of the body's COM just behind the hind leg coxae. On the -45° incline, much of the body load should be carried by the middle rather than the hind legs.

The changes in the anterior-posterior and the medio-lateral force were primarily reflected in changes in torques at the ThC and FTi joints (Figure 4.3C and Table 4.2). Torques at the ThC joint were directed toward retraction during level and uphill walking but toward protraction during downhill walking (Figure 4.3C, arrowhead left). Similarly, torques at the FTi joint were directed toward extension during uphill walking but toward flexion during downhill walking (Figure 4.3C, arrowhead right). That is, torques at both joints were directed opposite to the joint movement during downhill walking, suggesting a stabilizing function (Figure 4.3C, gray shaded regions; compare with Figure 4.2E). In contrast, torques at the CTr joint differed less across conditions (Figure 4.3C, middle). Torques at the CTr joint were generally correlated with vertical forces, although the smaller vertical force during downhill walking was not directly reflected in a smaller CTr torque.

Taken together, the changes in hind leg forces and joint torques reveal substantial

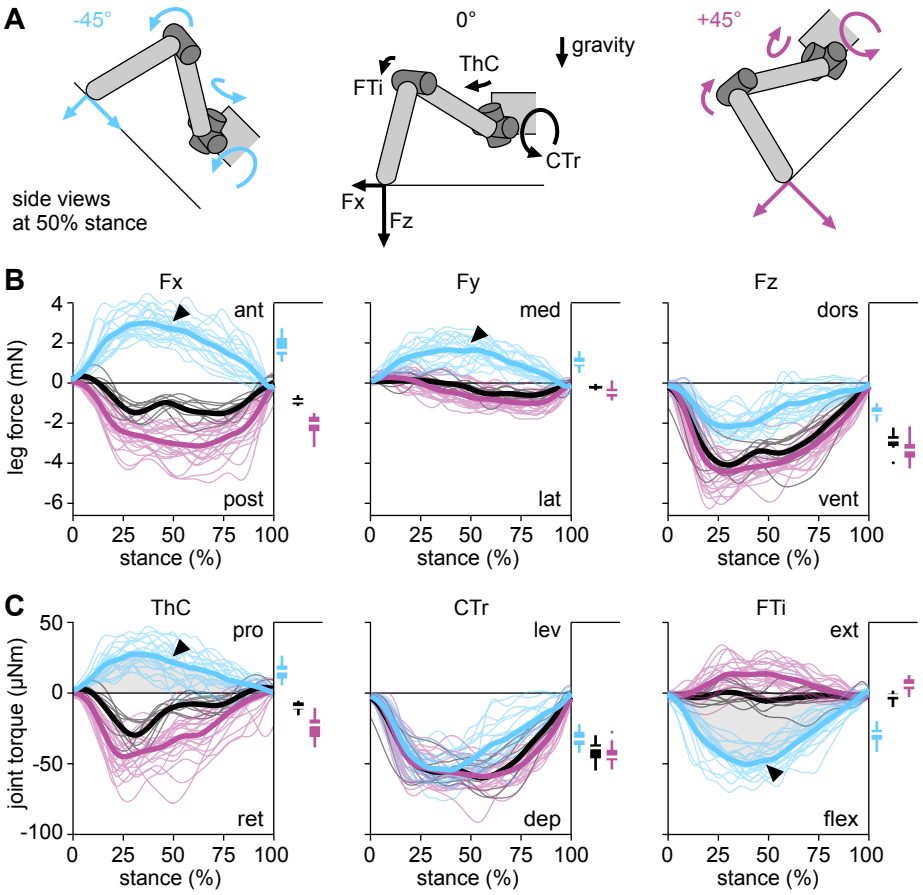

Figure 4.3: Hind leg forces and joint torques during level and incline walking
(**A**) Side-view schematic of the rigid link model, illustrating the average posture, forces and torques of the hind leg at 50% of the stance phase during level walking (black), uphill walking (magenta) and downhill walking (blue). Walking direction is from left to right. The COM of the body is located just behind the ThC joint. Note that the direction of forces and torques indicates the action of the leg, which is opposite to the direction of the ground reaction force. (**B**,**C**) Hind leg forces and joint torques during the stance phase of level walking (black), uphill walking (magenta) and downhill walking (blue). Thin lines show single steps. Bold lines show means of all steps. Boxplots show net forces and torques averaged over each stance phase, pooled across steps. Gray areas in **C** highlight stabilizing phases, in which the net joint torque is directed opposite to the movement of the joint (see Figure 4.2E). Arrowheads mark sign reversals for downhill walking. Note again that the direction of forces and torques indicates the action of the leg. Note also that there is no one-to-one correspondence between a given torque and any one force component. Sample numbers are n = 9 steps for 0°, n = 21 steps for +45°, n = 20 steps for -45°, pooled across animals.

Table 4.2: Dynamic parameters for level (0°) and incline (±45°) walking.[a]

dynamic parameter	-45°	0°	+45°	positive trend
F_x (mN)	1.8 ± 0.48	-0.9 ± 0.12	-2.12 ± 0.51	← *
F_y (mN)	1.01 ± 0.29	-0.22 ± 0.10	-0.46 ± 0.28	← *
F_z (mN)	-1.15 ± 0.25	-2.56 ± 0.48	-2.97 ± 0.46	←
τ_{ThC} (μNm)	15.22 ± 6.09	-9.79 ± 3.27	-23.94 ± 7.87	← *
τ_{CTr} (μNm)	-32.33 ± 5.85	-41.14 ± 7.98	-43.37 ± 6.62	←
τ_{FTi} (μNm)	-29.61 ± 5.77	-2.84 ± 3.53	5.53 ± 4.66	→ *

[a]Values are mean ± s.d. (n = 9 steps for 0°, n = 20 steps for -45°, n = 21 steps for +45°, pooled across animals). Forces (F) and torques (τ) are net values averaged over each stance phase. See Figure 4.1B for force and torque conventions. Arrows indicate systematic, positive trends of parameter means with increasing (rightward) or decreasing (leftward) inclination. Asterisks mark substantial changes with sign reversal.

changes in mechanical demands on inclines, particularly at the ThC and FTi joints. The changes in dynamics are consistent with the animal's need to counteract the effects of gravity by accelerating the body more strongly during uphill walking and decelerating it during downhill walking.

4.4.3 Timing and magnitude of muscle activity is adjusted on inclines

The torques at the ThC and FTi joints indicated that muscle activity at these joints is adjusted in an inclination-dependent manner. However, as net torques represent the net magnitude and direction of all forces acting at the joint, it is not clear how a given net torque relates to the activity of any particular muscle. Therefore, we recorded EMGs of the protractor and retractor coxae muscles, which rotate the leg forward and backward around the ThC joint, respectively (Figure 4.1C).

During swing, the pattern of muscle activity was similar across walking conditions and directly reflected the forward movement of the leg. In all conditions, the protractor was active throughout swing, whereas the retractor was silent (Figure 4.4A,B). Persisting protractor activity throughout swing is to be expected even during downhill walking, because the strong passive forces associated with the small mass of insect legs prevents leg inertia to complete swing movements (Hooper et al. 2009). While the timing of protractor activity did not change across condtions, the magnitude of protractor activity tended to increase with increasing inclination (Figure 4.4B, top). The increase in magnitude was correlated with an increased likelihood of occurrence of large amplitude (LA) muscle spikes during swing, which were individually identifiably based on amplitude (Figure 4.4A and supplementary Figure 4.7A). The likelihood of occurrence of LA spikes during swing was not dependent on walking speed, but correlated with an

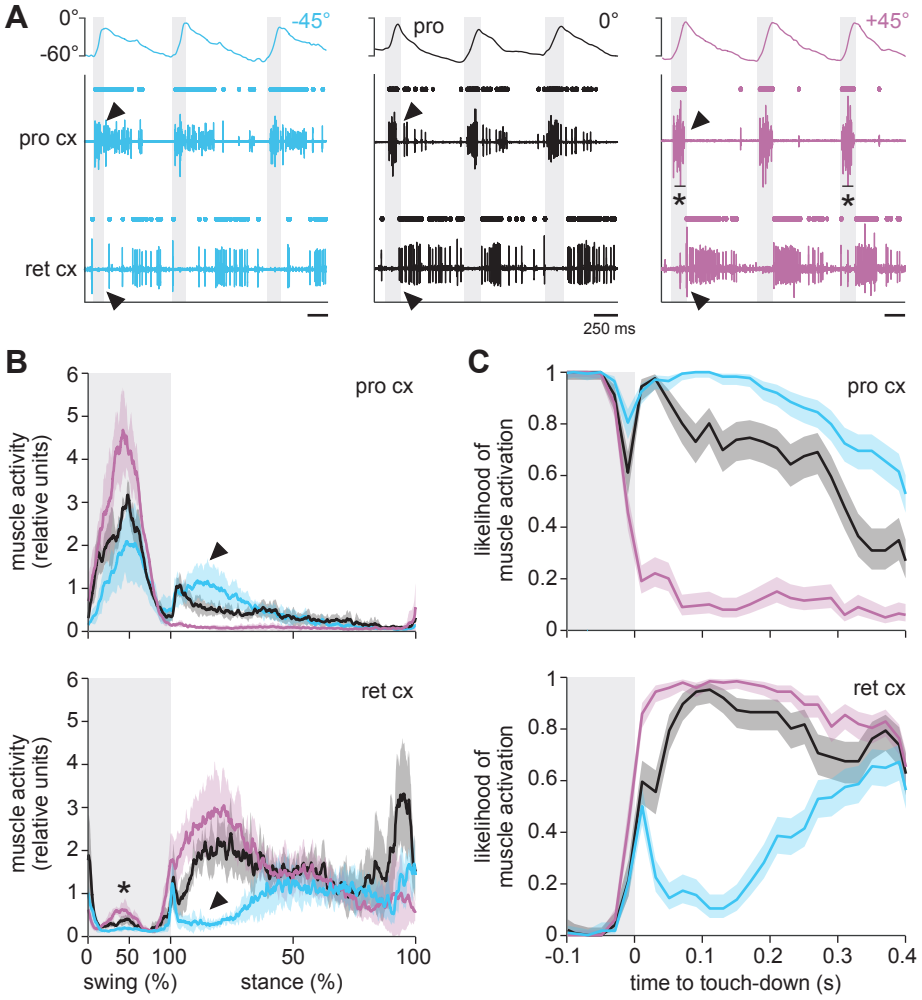

Figure 4.4: Muscle activity at the thorax-coxa joint during level and incline walking
(**A**) Example EMG patterns for the hind leg protractor coxae (pro cx) and retractor coxae (ret cx) muscles during level walking (black), uphill walking (magenta) and downhill walking (blue). Dots above EMG traces mark muscle spikes detected based on amplitude. Traces on top show the protraction angle of the leg. Light gray areas mark swing phases. Asterisks mark cross-talk from large amplitude protractor spikes (truncated). Arrows mark inclination-dependent changes in muscle activity at the beginning of stance. (**B**) Average rectified and smoothed EMG traces of the protractor and retractor muscles normalized to the swing and stance phase of level walking (black), uphill walking (magenta) and downhill walking (blue). The magnitude of muscle activity is normalized to the mean magnitude for level walking (relative units, see Methods). Lines show means of animal means, error bands show 95% confidence intervals of animal means (N = 5). Arrows mark inclination-dependent changes in muscle activity at the beginning of stance. The asterisk marks protractor cross-talk during swing. (**C**) Likelihood of muscle activation relative to leg touch-down (n = 126 steps for 0°, n = 199 steps for +45°, n = 174 steps for -45°, pooled across N = 5 animals). Error bands show binomial 95% confidence intervals (Wilson score intervals). Protractor cross-talk during swing was edited out manually (see Methods).

increase in angular velocity at the ThC joint (supplementary Figure 4.7B). Recruitment of the LA units might thus have allowed for the slight increase in step length during uphill walking without changes in swing durations (see Figure 4.2B).

During stance, the pattern of muscle activity was strongly dependent on the inclination of the walkway and did no directly reflect the backward movement of the leg. The protractor was strongly active during downhill walking, less active during level walking, and essentially silent during uphill walking (Figure 4.4A,B, arrowheads top). Inclination-dependent changes of protractor activity occurred primarily in the first 50% of stance (Figure 4.4B, top). Close inspection revealed that this activity was not a continuation of the burst during swing, but a separate burst starting with the touch-down of the leg (Figure 4.4B,C, top). Conversely to protractor activity, retractor activity during stance generally increased with increasing inclination (Figure 4.4A,B, arrowheads bottom). The muscle was strongly active during level and uphill walking, starting with the touch-down of the leg. During downhill walking, the retractor was sometimes also shortly active with the touch-down of the leg, but its main activity was reduced and delayed in all steps (approx. 300 ms; Figure 4.4B,C, bottom). Similar to protractor activity, inclination-dependent changes in retractor activity occurred primarily in the first 50% of stance (Figure 4.4B, bottom). The changes in protractor and retractor activity during stance generally agreed with the net torque at the ThC joint. That is, the net protraction torque during downhill walking was correlated with strong protractor and weak retractor activity; the increasing net retraction torque from level to uphill walking was correlated with decreasing protractor and increasing retractor activity.

Taken together, these results demonstrate that both timing and magnitude of antagonistic muscle activity at the ThC joint are adjusted to altered mechanical demands during incline walking.

Because the characteristic adjustments in muscle activity occurred primarily in the first half of stance immediately after the touch-down of the leg, we wondered whether they are a reflexive response to altered mechanical demands, or whether they already occur in anticipation of the incline as reported for mammals (Gottschall and Nichols 2011). To investigate this question, we recorded protractor and retractor activity in a stick insect transitioning from level to either downhill or uphill walking (Figure 4.5). Figure 4.5B shows that the characteristic adjustments in muscle activity observed during steady-state incline walking occurred as soon as the hind leg stepped on the incline. That is, with the first step of the hind leg on the -45° incline, protractor activity increased during early stance, whereas retractor activity was delayed (Figure 4.5B, arrowheads left). Conversely, with the first step of the hind leg on the +45° incline, protractor activity decreased during early stance, whereas retractor activity increased (Figure 4.5B, arrow-

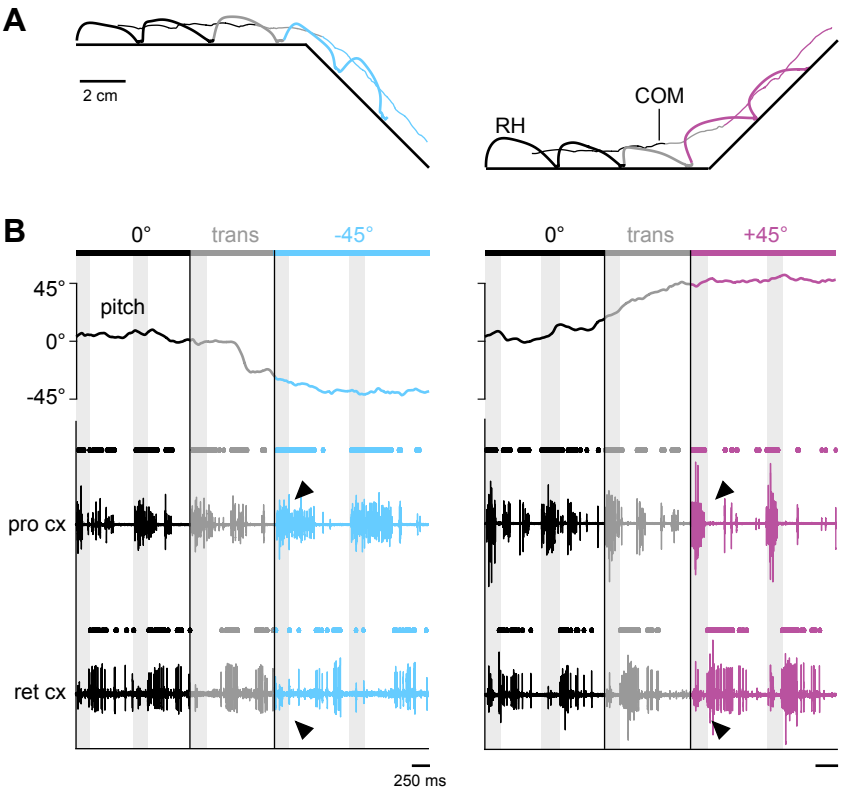

Figure 4.5: Muscle activity at the transition from level to incline walking
(**A**,**B**) Example transitions from level to downhill walking (left) and level to uphill walking (right). Walking direction is from left to right. Lines in **A** show side-view trajectories of the center of mass (COM) and the tibia-tarsus joint of the right hind (RH) leg. EMG patterns in **B** show activity of the hind leg protractor coxae (pro cx) and retractor coxae (ret cx) muscles. Dots above EMG traces mark muscle spikes detected based on amplitude (protractor cross-talk during swing was edited out manually, see Methods). Light gray regions mark swing phases. The body pitch angle is expressed relative to level ground. Transition (trans) steps, in which the body pitch angle is adjusted as front and middle legs already encounter the incline, are colored in dark gray. Steps before the transition are colored in black. Steps after the transition are colored in blue (downhill) or magenta (uphill). Arrows mark characteristic, inclination-dependent changes in muscle activity at the beginning of stance.

heads right). These adjustments were not present in the steps preceding the transition (Figure 4.5B, black traces), suggesting that muscle activity was adjusted to the current mechanical demand on a step-by-step basis rather than in anticipation of the incline.

4.5 Discussion

To investigate how leg muscle activity is adjusted to changing mechanical demand during walking, we combined electromyography with 3D motion capture and ground reaction force measurements in stick insects walking freely on level ground and up and down inclines ($\pm 45°$). Kinematics changed comparatively little across walking conditions (Figure 4.2), although leg forces and joint torques revealed substantial changes in mechanical demand (Figure 4.3). At the thorax-coxa joint, the altered mechanical

demand was met by characteristic adjustments in timing and magnitude of antagonistic muscle activity, which occurred primarily in the first half of stance (Figure 4.4) and with the first step of the leg on the incline (Figure 4.5).

4.5.1 Inclination-dependent changes in kinematics, dynamics and muscle activity

Stick insects tended to walk slower on inclines, but step cycle parameters (stance and swing phase durations) and postural parameters (body height, body pitch, foot placement, joint angles) changed comparatively little (Figure 4.2). This is generally consistent with previous observations in insects (Mendes et al. 2014; Seidl and Wehner 2008; Weihmann and Blickhan 2009). For example, ants walking on $\pm 60^{\circ}$ inclines do not adjust the touch-down and lift-off positions of their legs (Seidl and Wehner 2008). Similarly, fruit flies walking vertically or upside-down show only minor adjustments in leg placement (Mendes et al. 2014). The situation is quite different in larger vertebrates. For example, cats and humans require substantial kinematic adjustments for stable walking on inclines, including changes in body tilt, foot placement, and inter-joint coordination (Carlson-Kuhta et al. 1998; Gregor et al. 2006; Lay et al. 2006; Leroux et al. 2002; Smith et al. 1998).

In contrast to kinematics, hind leg forces and joint torques varied substantially across walking conditions (Figure 4.3). The largest changes concerned the anterior-posterior and medio-lateral directions, in which the hind leg reversed from pushing backward and outward during level and uphill walking to pushing forward and pulling inward during downhill walking (Table 4.2, asterisks). This sign reversal is consistent with the animal's need to control the descent of the body during downhill walking and was also described in ants (Wöhrl et al. 2017), cats (Gregor et al. 2006), and humans (Lay et al. 2006). In stick insects, the sign reversal was primarily reflected in changes in torques at the ThC and FTi joints. At these joints, torques were directed toward retraction and extension during uphill walking, but toward protraction and flexion during downhill walking. This result was not predicted from kinematics, because the leg was retracted and extended similarly in all conditions. It indicates that the ThC and FTi joints stabilized the leg during downhill walking, supporting our previous hypothesis that these two leg joints may serve a stabilizing function (Dallmann et al. 2016).

The inclination-dependent changes in antagonistic muscle activity at the ThC joint corroborate this hypothesis (Figure 4.4). Strictly reciprocal activity of the protractor and retractor muscles reflecting the swing and stance phases of the leg was only present during uphill walking. In contrast, during level and downhill walking, the protractor muscle was active during the first half of stance. This resulted in times of co-activation

and likely considerable co-contraction with the retractor muscle given the long activation and deactivation time constants of insect muscle (Guschlbauer et al. 2007; Hooper et al. 2007; Zakotnik et al. 2006). The co-activation of antagonistic muscles indicates that the ThC joint was actively stiffened to stabilize the leg depending on the current mechanical demand. This finding extends earlier observations in locusts and cockroaches reporting co-activation of antagonistic muscles at the ThC and FTi joints in the early stance phase of level walking (Duch and Pflüger 1995; Krauthamer and Fourtner 1978; Larsen et al. 1995). Moreover, it is consistent with the finding that antagonistic muscles at these joints show no co-activation in tethered animals walking on a slippery surface (Rosenbaum et al. 2010)—a situation in which legs do not have to be stabilized against gravity-induced collapse.

Although the changes in protractor and retractor activity generally agreed with the net torques at the ThC joint during stance, it is noteworthy that the relation was non-linear. For example, the torque at the ThC joint reversed in sign during downhill walking, but protractor and retractor activity did not completely reverse. Rather, protractor activity occurred in the first half of stance and the main retractor activity was delayed. This non-linear relation could be related to the contraction properties of insect muscle (Hooper and Weaver 2000), passive forces of muscles and skeletal structures (e.g., Ache and Matheson 2013; Hooper et al. 2009; Zakotnik et al. 2006), and mechanical coupling with other legs (e.g., Dallmann et al. 2017). Regardless of such effects, the point remains that the changing mechanical demand at the ThC joint was actively accounted for by adjustments in timing and magnitude of protractor and retractor muscle activity.

4.5.2 Potential control of incline walking

Which mechanisms adjust leg muscle activity at the ThC joint during walking? In previous studies, descending inputs from the brain have been implicated in mediating distinct kinematic patterns for turning (Gruhn et al. 2016; Martin et al. 2015) and obstacle climbing (Schütz and Dürr 2011; Watson et al. 2002a; Watson et al. 2002b). In our experiments, stick insects showed little change in kinematics across walking conditions, indicating that the same kinematic pattern was used (Figure 4.2). In addition, protractor and retractor activity was adjusted primarily during the first half of stance after the touch-down of the leg (Figure 4.4), and with the first step of the leg on the incline (Figure 4.5). Together, these findings could indicate that stick insects did not use distinct, inclination-specific motor programs, but instead adjusted leg muscle activity on a step-by-step basis using afferent inputs from leg proprioceptors.

One possibility is that muscle activity was adjusted based on load feedback from

leg campaniform sensilla (Burrows and Pflüger 1988; Pearson 1972; Zill et al. 2012). These mechanoreceptors are located close to the leg joints and detect load as strain in the cuticle (Pringle 1938; Zill et al. 2004). Indeed, our torque calculations show that the mechanical loads acting at the ThC and FTi joints differed substantially across walking conditions, suggesting that inputs from campaniform sensilla on the trochanter (Hofmann and Bässler 1982; Schmitz 1993) and tibia (Zill et al. 2011) should differ too. For example, the resisted retraction torques during level and uphill walking should initially excite campaniform sensilla on the anterior side of the trochanter, whereas the resisted protraction torques during downhill walking should initially excite campaniform sensilla on the posterior side (Schmitz 1993). In part, the muscle activity patterns observed in the present study could be explained assuming that the anterior group provides positive feedback to the retractor (resulting in retractor activity during the stance phase of level and uphill walking), whereas the posterior group provides positive feedback to the protractor (resulting in protractor activity during the stance phase of downhill walking). Load feedback from both groups of campaniform sensilla is known to affect muscle activity at the ThC joint (Akay et al. 2004; Akay et al. 2007; Schmitz 1993). However, their involvement in positive feedback pathways, as was shown for campaniform sensilla on the dorsal trochanter (Zill et al. 2012), remains to be determined. In addition, load feedback cannot directly account for altered recruitment of protractor units during swing (supplementary Figure 4.7). This is because campaniform sensilla are only excited during stance, when leg muscle contractions are resisted (Zill et al. 2012). Therefore, it seems unlikely that load reflexes alone are sufficient to account for the adaptive changes in muscle activity observed in the present study.

Another possibility is that muscle activity was adjusted based on leg proprioceptors signaling leg position and movement. We found that kinematics changed comparatively little across walking conditions, which might suggest that kinematic parameters are being controlled. In a kinematic control scheme, muscle activation could depend on the mismatch between the actual and a desired, referent kinematic pattern. Any mismatch due to altered mechanical conditions could be determined based on signals from leg proprioceptors. For example, hair plates monitor the movement range of the leg (Bässler 1977; Cruse et al. 1984; Markl 1962; Schmitz 1986; Theunissen et al. 2014; Wendler 1964; Wong and Pearson 1976) and chordotonal organs monitor the current position and movement of individual leg segments (Burns 1974; Field and Matheson 1998; Hofmann et al. 1985; Zill 1985). The few changes in kinematics observed in the present study, such as the magnitude of the extension angle (Figure 4.2E), do not contradict this idea. They could reflect that local control of joint angles does not always succeed completely, for example due to mechanical coupling with other legs. They could also

indicate that a higher-level kinematic parameter is being controlled. This conclusion is supported by previous studies showing that walking stick insects compensate for perturbations of body height and body tilt (Cruse 1976a; Cruse et al. 1993; Diederich et al. 2002).

In summary, we suggest that stick insects do not use distinct, inclination-specific motor programs during walking, but instead adjust leg muscle activity on a step-by-step basis so as to minimize changes in kinematics under different mechanical demands. Future work extending our measurements to other muscles, legs and more extreme inclinations will help to further probe this idea. For example, based on our torque calculations, we expect antagonistic muscle activity at the FTi joint to be adjusted similarly to that at the ThC joint. In addition, the reliable, characteristic changes in muscle activity described here might be suitable to evaluate the effects of sensory manipulations and determine which leg proprioceptors provide the critical sensory information for control.

4.6 Supplementary information

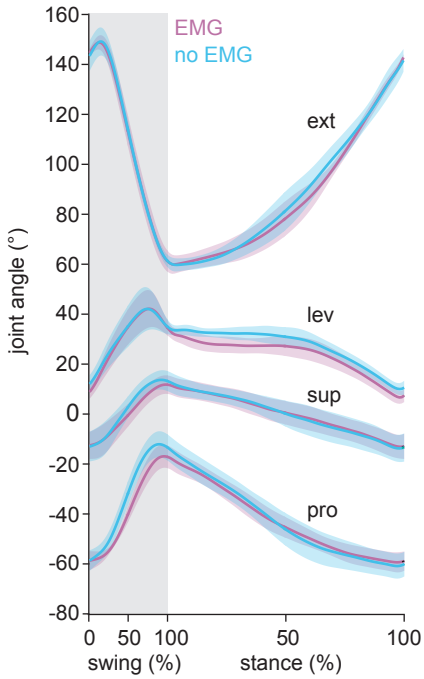

Figure 4.6: Effects of the EMG backpack on hind leg kinematics
Joint angles of the hind leg during level walking normalized to swing and stance duration. Lines show means of animal means, error bands show 95% confidence intervals of animal means (N = 5). Magenta lines show data with EMG backpack attached and electrodes implanted (n $>$ 15 steps per animal). Blue lines show data recorded from the same animals prior to backpack attachment and electrode implantation (n = 10 steps per animal).

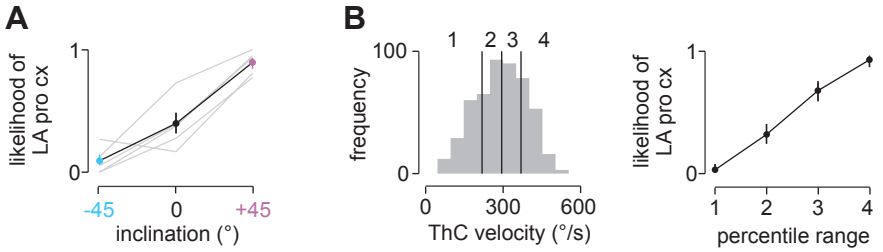

Figure 4.7: Occurrence of large amplitude protractor coxae muscle spikes
(**A**) Likelihood of occurrence of large amplitude (LA) protractor coxae (pro cx) muscle spikes during swing as a function of inclination (n = 126 steps for 0°, n = 199 steps for +45°, n = 174 steps for -45°, pooled across N = 5 animals). Error bars show binomial 95% confidence intervals (Wilson score intervals). Gray lines show likelihood per animal. (**B**) Histogram of the average velocity of the ThC joint during swing pooled across all steps (left) and likelihood of occurrence of LA protractor spikes as a function of the percentile range (right). Sample numbers as in **A**. Error bars show Wilson score intervals. Note that the ThC velocity is the first derivative of the angle describing the rotation of the leg plane around the slanted ThC joint axis, not the derivative of the protraction or supination angle (see Figure 4.1B).

4.7 References

Ache, J. M. and Matheson, T. (2013). Passive joint forces are tuned to limb use in insects and drive movements without motor activity. *Curr. Biol.* 23, 1418–1426.

Akay, T., Haehn, S., Schmitz, J., and Büschges, A. (2004). Signals from load sensors underlie interjoint coordination during stepping movements of the stick insect leg. *J. Neurophysiol.* 92, 42–51.

Akay, T., Ludwar, B. C., Göritz, M. L., Schmitz, J., and Büschges, A. (2007). Segment specificity of load signal processing depends on walking direction in the stick insect leg muscle control system. *J. Neurosci.* 27, 3285–3294.

Bässler, U. (1977). Sensory control of leg movement in the stick insect *Carausius morosus*. *Biol. Cybern.* 25, 61–72.

Bässler, U. (1983). *Neural Basis of Elementary Behavior in Stick Insects*. Berlin: Springer.

Bates, D., Mächler, M., Bolker, B., and Walker, S. (2015). Fitting linear mixed-effects models using lme4. *J. Stat. Softw.* 67, 1–48.

Botev, Z. I., Grotowski, J. F., and Kroese, D. P. (2010). Kernel density estimation via diffusion. *Ann. Stat.* 38, 2916–2957.

Burns, M. D. (1974). Structure and physiology of the locust femoral chordotonal organ. *J. Insect Physiol.* 20, 1319–1339.

Burrows, M. and Pflüger, H. J. (1988). Positive feedback loops from proprioceptors involved in leg movements of the locust. *J. Comp. Physiol. A* 163, 425–440.

Büschges, A. and Gruhn, M. (2007). Mechanosensory feedback in walking: from joint control to locomotor patterns. *Adv. In Insect Phys.* 34, 193–230.

Carlson-Kuhta, P., Trank, T. V., and Smith, J. L. (1998). Forms of forward quadrupedal locomotion. II. A comparison of posture, hindlimb kinematics, and motor patterns for upslope and level walking. *J. Neurophysiol.* 79, 1687–1701.

Cruse, H. (1976a). The control of body position in the stick insect (*Carausius morosus*), when walking over uneven surfaces. *Biol. Cybern.* 24, 25–33.

Cruse, H. (1976b). The function of the legs in the free walking stick insect, *Carausius morosus*. *J. Comp. Physiol. A* 112, 235–262.

Cruse, H. (1979). The control of the anterior extreme position of the hindleg of a walking insect, *Carausius morosus*. *Physiol. Entomol.* 4, 121–124.

Cruse, H., Dean, J., and Suilmann, M. (1984). The contributions of diverse sense organs to the control of leg movement by a walking insect. *J. Comp. Physiol. A* 154, 695–705.

Cruse, H., Schmitz, J., Braun, U., and Schweins, A. (1993). Control of body height in a stick insect walking on a treadwheel. *J. Exp. Biol.* 181, 141–155.

Dallmann, C. J., Dürr, V., and Schmitz, J. (2016). Joint torques in a freely walking insect reveal distinct functions of leg joints in propulsion and posture control. *Proc. R. Soc. B* 283, 20151708.

Dallmann, C. J., Hoinville, T., Dürr, V., and Schmitz, J. (2017). A load-based mechanism for inter-leg coordination in insects. *Proc. R. Soc. B* 284, 20171755.

Dean, J. and Wendler, G. (1983). Stick insect locomotion on a walking wheel: interleg coordination of leg position. *J. Exp. Biol.* 103, 75–94.

Diederich, B., Schumm, M., and Cruse, H. (2002). Stick insects walking along inclined surfaces. *Integr. Comp. Biol.* 42, 165–173.

Donelan, J. M., McVea, D. A., and Pearson, K. G. (2009). Force regulation of ankle extensor muscle activity in freely walking cats. *J. Neurophysiol.* 101, 360–371.

Duch, C. and Pflüger, H. J. (1995). Motor patterns for horizontal and upside down walking and vertical climbing in the locust. *J. Exp. Biol.* 198, 1963–1976.

Dürr, V., Theunissen, L. M., Dallmann, C. J., Hoinville, T., and Schmitz, J. (2018). Motor flexibility in insects: adaptive coordination of limbs in locomotion and near-range exploration. *Behav. Ecol. Sociobiol.* 72, 15.

Field, L. H. and Matheson, T. (1998). Chordotonal organs of insects. *Adv. In Insect Phys.* 27, 1–228.

Goldammer, J., Büschges, A., and Schmidt, J. (2012). Motoneurons, DUM cells, and sensory neurons in an insect thoracic ganglion: a tracing study in the stick insect *Carausius morosus*. *J. Comp. Neurol.* 520, 230–257.

Goldman, D. I., Chen, T. S., Dudek, D. M., and Full, R. J. (2006). Dynamics of rapid vertical climbing in cockroaches reveals a template. *J. Exp. Biol.* 209, 2990–3000.

Gottschall, J. S. and Nichols, T. R. (2011). Neuromuscular strategies for the transitions between level and hill surfaces during walking. *Phil. Trans. R. Soc. B* 366, 1565–1579.

Graham, D. (1985). Pattern and control of walking in insects. *Adv. In Insect Phys.* 18, 32–140.

Gregor, R. J., Smith, D. W., and Prilutsky, B. I. (2006). Mechanics of slope walking in the cat: quantification of muscle load, length change, and ankle extensor EMG patterns. *J. Neurophysiol.* 95, 1397–1409.

Gruhn, M., Rosenbaum, P., Bockemühl, T., and Büschges, A. (2016). Body side-specific control of motor activity during turning in a walking animal. *eLife* 5, e13799.

Guschlbauer, C., Scharstein, H., and Büschges, A. (2007). The extensor tibiae muscle of the stick insect: biomechanical properties of an insect walking leg muscle. *J. Exp. Biol.* 210, 1092–1108.

Hofmann, T. and Bässler, U. (1982). Anatomy and physiology of trochanteral campaniform sensilla in the stick insect, *Cuniculina impigra*. *Physiol. Entomol.* 7, 413–426.

Hofmann, T., Koch, U. T., and Bässler, U. (1985). Physiology of the femoral chordotonal organ in the stick insect, *Cuniculina impigra*. *J. Exp. Biol.* 114, 207–223.

Hooper, S. L. and Büschges, A., eds. (2017). *Neurobiology of Motor Control: Fundamental Concepts and New Directions*. Wiley.

Hooper, S. L., Guschlbauer, C., Blümel, M., Rosenbaum, P., Gruhn, M., Akay, T., and Büschges, A. (2009). Neural control of unloaded leg posture and of leg swing in stick insect, cockroach, and mouse differs from that in larger animals. *J. Neurosci.* 29, 4109–4119.

Hooper, S. L., Guschlbauer, C., Uckermann, G. von, and Büschges, A. (2007). Slow temporal filtering may largely explain the transformation of stick insect (*Carausius morosus*) extensor motor neuron activity into muscle movement. *J. Neurophysiol.* 98, 1718–1732.

Krauthamer, V. and Fourtner, C. R. (1978). Locomotory activity in the extensor and flexor tibiae of the cockroach, *Periplaneta americana*. *J. Insect Physiol.* 24, 813–819.

Larsen, G. S., Frazier, S. F., Fish, S. E., and Zill, S. N. (1995). Effects of load inversion in cockroach walking. *J. Comp. Physiol. A* 176, 229–238.

Lay, A. N., Hass, C. J., and Gregor, R. J. (2006). The effects of sloped surfaces on locomotion: a kinematic and kinetic analysis. *J. Biomech.* 39, 1621–1628.

Lay, A. N., Hass, C. J., Nichols, R. T., and Gregor, R. J. (2007). The effects of sloped surfaces on locomotion: an electromyographic analysis. *J. Biomech.* 40, 1276–1285.

Leroux, A., Fung, J., and Barbeau, H. (2002). Postural adaptation to walking on inclined surfaces: I. Normal strategies. *Gait Posture* 15, 64–74.

Markl, H. (1962). Borstenfelder an den Gelenken als Schweresinnesorgane bei Ameisen und anderen Hymenopteren. *Z. Vgl. Physiol.* 45, 475–569.

Martin, J. P., Guo, P., Mu, L., Harley, C. M., and Ritzmann, R. E. (2015). Central-complex control of movement in the freely walking cockroach. *Curr. Biol.* 25, 2795–2803.

Mendes, C. S., Rajendren, S. V., Bartos, I., Márka, S., and Mann, R. S. (2014). Kinematic responses to changes in walking orientation and gravitational load in *Drosophila melanogaster*. *PLoS One* 9, e109204.

Orlovsky, G. N., Deliagina, T. G., and Grillner, S. (1999). *Neuronal Control of Locomotion: From Mollusc to Man*. Oxford: Oxford University Press.

Pearson, K. G. (1972). Central programming and reflex control of walking in the cockroach. *J. Exp. Biol.* 56, 173–193.

Pearson, K. G. (1995). Proprioceptive regulation of locomotion. *Curr. Opin. Neurobiol.* 5, 786–791.

Pringle, J. W. S. (1938). Proprioception in insects. II. The action of the campaniform sensilla on the legs. *J. Exp. Biol.* 15, 114–131.

Prochazka, A. (1996). Proprioceptive feedback and movement regulation. *Handbook of Physiology, Exercise: Regulation and Integration of Multiple Systems*. Ed. by Rowell, L. B. and Shepherd, J. T. American Physiological Society, 89–127.

Rosenbaum, P., Wosnitza, A., Büschges, A., and Gruhn, M. (2010). Activity patterns and timing of muscle activity in the forward walking and backward walking stick insect *Carausius morosus*. *J. Neurophysiol.* 104, 1681–1695.

Schmitz, J. (1986). Properties of the feedback system controlling the coxa-trochanter joint in the stick insect *Carausius morosus*. *Biol. Cybern.* 55, 35–42.

Schmitz, J. (1993). Load-compensating reactions in the proximal leg joints of stick insects during standing and walking. *J. Exp. Biol.* 33, 15–33.

Schütz, C. and Dürr, V. (2011). Active tactile exploration for adaptive locomotion in the stick insect. *Phil. Trans. R. Soc. B* 366, 2996–3005.

Seidl, T. and Wehner, R. (2008). Walking on inclines: how do desert ants monitor slope and step length. *Front. Zool.* 5, 8.

Smith, J. L., Carlson-Kuhta, P., and Trank, T. V. (1998). Forms of forward quadrupedal locomotion. III. A comparison of posture, hindlimb kinematics, and motor patterns for downslope and level walking. *J. Neurophysiol.* 79, 1702–1716.

Spirito, C. P. and Mushrush, D. L. (1979). Interlimb coordination during slow walking in the cockroach. I. Effects of substrate alterations. *J. Exp. Biol.* 79, 233–243.

Theunissen, L. M. and Dürr, V. (2013). Insects use two distinct classes of steps during unrestrained locomotion. *PLoS One* 8, e85321.

Theunissen, L. M., Vikram, S., and Dürr, V. (2014). Spatial co-ordination of foot contacts in unrestrained climbing insects. *J. Exp. Biol.* 217, 3242–3253.

Tuthill, J. C. and Wilson, R. I. (2016). Mechanosensation and adaptive motor control in insects. *Curr. Biol.* 27, R1022–R1038.

Watson, J. T., Ritzmann, R. E., and Pollack, A. J. (2002a). Control of climbing behavior in the cockroach, *Blaberus discoidalis*. II. Motor activities associated with joint movement. *J. Comp. Physiol. A.* 188, 55–69.

Watson, J. T., Ritzmann, R. E., Zill, S. N., and Pollack, A. J. (2002b). Control of climbing behavior in the cockroach, *Blaberus discoidalis*. I. Kinematics. *J. Comp. Physiol. A.* 188, 39–53.

Weihmann, T. and Blickhan, R. (2009). Comparing inclined locomotion in a ground-living and a climbing ant species: sagittal plane kinematics. *J. Comp. Physiol. A* 195, 1011–1020.

Wendler, G. (1964). Laufen und Stehen der Stabheuschrecke *Carausius morosus*: Sinnesborstenfelder in den Beingelenken als Glieder von Regelkreisen. *Z. Vgl. Physiol.* 48, 198–250.

Wöhrl, T., Reinhardt, L., and Blickhan, R. (2017). Propulsion in hexapod locomotion: how do desert ants traverse slopes? *J. Exp. Biol.* 220, 1618–1625.

Wong, R. K. and Pearson, K. G. (1976). Properties of the trochanteral hair plate and its function in the control of walking in the cockroach. *J. Exp. Biol.* 64, 233–249.

Zakotnik, J., Matheson, T., and Dürr, V. (2006). Co-contraction and passive forces facilitate load compensation of aimed limb movements. *J. Neurosci.* 26, 4995–5007.

Zill, S. N. (1985). Plasticity and proprioception in insects. I. Responses and cellular properties of individual receptors of the locust metathoracic femoral chordotonal organ. *J. Exp. Biol.* 116, 435–461.

Zill, S. N., Büschges, A., and Schmitz, J. (2011). Encoding of force increases and decreases by tibial campaniform sensilla in the stick insect, *Carausius morosus*. *J. Comp. Physiol. A* 197, 851–867.

Zill, S. N., Schmitz, J., and Büschges, A. (2004). Load sensing and control of posture and locomotion. *Arthropod Struct. Dev.* 33, 273–286.

Zill, S. N., Schmitz, J., Chaudhry, S., and Büschges, A. (2012). Force encoding in stick insect legs delineates a reference frame for motor control. *J. Neurophysiol.* 108, 1453–1472.

Chapter 5

General discussion

In this thesis, I used a biomechanics approach (Figure 1.4) to study sensorimotor control of insect walking. Due to their accessible nervous and musculoskeletal systems, insects have served as important model systems for studying walking control (see Chapter 1). However, it has been difficult to understand the specific mechanisms at work during natural locomotion—when the body mechanically interacts with the environment. One reason is that the comparatively small size of insect legs has hampered a detailed understanding of the mechanical output at the leg joints (joint kinematics, joint torques) and its relation to leg muscle activity during natural locomotion. Chapters 2-4 tackled this issue by providing the first combination of 3D motion capture, ground reaction force measurements and electromyography in a freely walking insect. I chose to study the stick insect *Carausius morosus*, because its comparatively large size and well-studied anatomy and physiology offer several advantage for detailed biomechanical analyses. Below, I first review the main findings and their significance for walking control (Section 5.1). I then consider limitations of the biomechanics approach and speculate about future directions (Sections 5.2 and 5.3).

5.1 Significance of main findings for walking control

Several previous studies on freely walking insects examined kinematics of leg joints (e.g., Bender et al. 2010; Kram et al. 1997; Theunissen et al. 2015), ground reaction forces of single legs (e.g., Cruse 1976b; Full and Tu 1991; Harris and Ghiradella 1980;

Reinhardt and Blickhan 2014b), or leg muscle activity (e.g., Delcomyn and Usherwood 1973; Duch and Pflüger 1995; Watson and Ritzmann 1998). However, no previous study has combined all measurements and analyses in a single animal. The results of the present thesis demonstrate that in combination these biomechanical techniques can provide valuable new insights into sensorimotor control.

5.1.1 Joint torques during level walking

In Chapter 2, I combined 3D motion capture and ground reaction force measurements to determine the kinematics and torques of all main stick insect leg joints during level walking. The time courses of joint torques had not been determined in detail, neither in stick insects (Bartling and Schmitz 2000; Cruse 1976b) nor in any other insect. As a consequence, little was known about how insect leg joints interact to propel and stabilize the body and how individual leg segments are loaded mechanically during the stance phase. In stick insects, all legs were retracted and flexed/extended around the thorax-coxa (ThC) and femur-tibia (FTi) joints as expected for propulsion. However, the torques at these joints were often directed opposite to joint movements (Figures 2.2, 2.3 and 2.4), indicating that the joints might serve a stabilizing rather than a propulsive function. Unexpectedly, much of the propulsion resulted from strong torques at the coxa-trochanter (CTr) joint, which pressed the leg down on the ground. CTr torques contributed to controlling propulsion because the leg plane was not orthogonal to the ground but either supinated or pronated. This way, CTr torques toward depression resulted in downward as well as forward or backward directed leg forces. The ThC and FTi joints appeared to stabilize the leg in these situations and "steer" the power provided by the CTr joint to control both body height and propulsion. Because this mechanism is not predicted from kinematics, it had been overlooked in the past.

As discussed in Chapter 2, one interesting new conclusion is that the propulsive mechanism in stick insects conceptually parallels propulsive mechanisms in other insects, indicating a common motor control principle. For example, walking cockroaches also control propulsion by depression of their legs (Noah et al. 2004a; Watson and Ritzmann 1998), and a functional division into "power" and "steering" units was also described in jumping (Sutton and Burrows 2008; Sutton and Burrows 2010) and flying (Balint and Dickinson 2001; Walker et al. 2014) insects.

In addition, the torque patterns provided two novel hypotheses with respect to walking control. First, the torques at the CTr joint were comparatively strong (Figures 2.2, 2.3 and 2.4) and showed low step-to-step variability (Figure 2.5). These findings indicated that feedback from load-sensitive campaniform sensilla near the joint might be particularly useful for controlling the stance phase. This hypothesis was tested in

Chapter 3 (below). Second, the putative stabilizing torques at the ThC and FTi joints suggested that walking under natural load conditions might require a more flexible activation of leg muscles than currently envisaged based on findings from tethered insects. For example, antagonistic leg muscles show largely reciprocal activity in tethered stick insects walking with their body weight supported above a slippery surface (Rosenbaum et al. 2010). In free walking, however, the need to stabilize the body might require substantial adjustments in timing and magnitude of leg muscle activity to meet the current mechanical demand acting on the body. This hypothesis was tested in Chapter 4 (below).

5.1.2 Inter-leg coordination based on local load feedback

In Chapter 3, I combined 3D motion capture, ground reaction force measurements, electromyography and simulation data to show that feedback from campaniform sensilla near the CTr joint can aid in the control of the stance phase, as hypothesized in Chapter 2. In a previous study, Zill et al. (2012) showed how two groups of campaniform sensilla on the dorsal trochanter respond to imposed upward and downward bending of the leg (i.e., torques at the CTr joint). In Chapter 3, I first used this knowledge to infer how the two groups of campaniform sensilla should respond to the torques at the CTr joint measured during walking. I concluded that the decrease in torque toward the end of stance—the unloading of the leg—is sufficiently strong to reverse the activation of the two groups (Figures 3.2 and 3.6). Zill et al. (2012) further showed that in active animals an increase in load excites one of the two groups, which in turn activates the leg depressor (stance) muscle and inhibits the leg levator (swing) muscle. Conversely, a decrease in load excites the other group, which in turn activates the levator muscle and inhibits the depressor muscle (Zill et al. 2017a). In agreement with these motor effects, I showed that the unloading of the leg coincided with a switch from stance to swing muscle activity during walking (Figures 3.3 and 3.4). This suggested that load feedback from the two groups of campaniform sensilla promoted the stance-to-swing transition. Finally, a mechanical simulation revealed that the unloading of a leg can be specifically ascribed to the touch-down and load acceptance of the posterior neighboring leg (Figure 3.5). Together, these findings indicate that when a leg touches down on the ground during walking, it effectively takes over body load from the neighboring leg in front, which in turn can reliably detect the unloading and start it's stance-to-swing transition. This way, neighboring legs can be coordinated in a back-to-front sequence.

As discussed in Chapter 3, these findings have several implications for walking control. Most importantly, they strongly suggest that inter-leg coordination does not have to be mediated entirely by neural signals between legs, but can emerge from me-

chanical signals between legs through the ground. This idea is not new (e.g., Aoi et al. 2012; Ekeberg and Pearson 2005; Owaki et al. 2013; Zill et al. 2009). In fact, it has been around for so long that one might conclude that it had been thoroughly tested already. With respect to insects, several studies even implicated that campaniform sensilla on the trochanter mediate the required load feedback (Bässler 1977; Macmillan and Kien 1983; Noah et al. 2004a; Wendler 1965). However, experimental evidence for load-based inter-leg coordination from freely moving animals has been surprisingly scarce. Accordingly, Chapter 3 builds upon previous results in several ways. First, the joint torque calculations showed which specific groups of campaniform sensilla on the trochanter are suited to encode the unloading of the leg on a step-by-step basis. By comparing torques measured during walking with those applied in reduced preparations (Zill et al. 2012), the actions of campaniform sensilla could be inferred without having to record their activity (which is technically challenging, see Chapter 3). Second, relating leg muscle activity directly to changes in joint torques showed that muscle activity changes as predicted based on local load feedback from campaniform sensilla. Finally, simulating the load transfer among legs revealed that load is transferred specifically between ipsilateral neighboring legs. This is critical, because load must be transferred effectively between specific legs to be exploitable for coordination. The simulation was necessary because more than two legs were in ground contact at all times so that load transfer among legs could not be intuitively inferred like in bipeds. Collectively, these and previous findings now provide good evidence that inter-leg coordination can emerge from mechanical interactions of legs through the ground (although demonstrating a causal contribution of campaniform sensilla remains an issue, see Section 5.2 below).

The findings of Chapter 3 are also interesting with respect to the "leg coordination rules" introduced by Cruse (1990). Originally, the leg coordination rules were derived from behavioral studies on stick insects and crayfish. They describe how the movement of a leg during walking depends on the states of its neighboring legs. For example, a leg's stance-to-swing transition is suppressed while the posterior neighboring leg is in swing (rule 1), but promoted as soon as the latter has touched down (rule 2) (Cruse 1990; Cruse et al. 1998; Dürr et al. 2004; Schilling et al. 2013). Little is known about how such information is mediated between legs in the central nervous system (Borgmann and Büschges 2015). The load-based coordination mechanism described in Chapter 3 could readily be a neuromechanical implementation of rules 1 and 2. For example, while the hind leg is in swing, the load on the middle leg will be high. Local load feedback can then reinforce ongoing stance muscle activity in the middle leg and suppress the leg's stance-to-swing transition (rule 1). When the hind leg touches down on the ground, load

of the middle leg effectively decreases due to mechanical coupling. The altered local load feedback can then promote the stance-to-swing transition of the middle leg (rule 2).

These findings are not only relevant for stick insects. As discussed in Chapter 3, other insects including cockroaches (Zill et al. 1999), locusts (Hustert et al. 1981) and flies (Gnatzy et al. 1987; Merritt and Murphey 1992) bear campaniform sensilla similar to those on the stick insect trochanter (mutually perpendicular orientations in the plane of leg movement). Therefore, load-based coordination might be used across insects to similar advantage.

Finally, the coordination mechanism might be useful for the control of multi-legged robots. Because the mechanism is decentralized and based on mechanical interactions of legs through the ground, it might provide a fast, computationally inexpensive and inherently adaptive control concept. Recent experiments on a minimalistic four-legged robot support this idea (Owaki et al. 2013; Owaki and Ishiguro 2017). In these experiments, local load feedback from sensors on the foot was sufficient to couple otherwise uncoupled leg oscillators and generate different stepping patterns. The findings of Chapter 3 indicate that local load feedback can also be exploited in more complex leg designs. In addition, having load sensors on the proximal part of the leg rather than on the foot might be beneficial for real-world applications, in which damage to sensors on the foot is likely more common.

5.1.3 Mechanics and muscle activity during incline walking

While Chapters 2 and 3 focussed on level walking, Chapter 4 extended the measurements to uphill (+45°) and downhill (-45°) walking. The rationale for comparing different walking conditions was that inclination-dependent changes in leg muscle activity, leg kinematics and leg dynamics (forces, torques) might help understand how the nervous system accounts for different mechanical demands during walking. In cats and humans, these kinds of analyses have been used to infer whether a distinct motor program is used on inclines (Lay et al. 2006; Lay et al. 2007), or to what extent movement- and load-related afferent inputs from the leg can account for adjustments in leg muscle activity (Donelan et al. 2009; Gregor et al. 2006). In insects, previous studies examined inclination-dependent changes in leg muscle activity (cockroach: Larsen et al. 1995; locust: Duch and Pflüger 1995), leg kinematics (fruit fly: Mendes et al. 2014; ant: Seidl and Wehner 2008; cockroach: Spirito and Mushrush 1979), or leg forces (ant: Wöhrl et al. 2017; cockroach: Goldman et al. 2006; stick insect: Cruse 1976b). However, no study had combined all measurements in a single animal. As a consequence, changes in parameters such as joint torques, which are closely related to load feedback (see Chapter 3), were unknown. In Chapter 4, I combined 3D motion capture, ground re-

action force measurements and electromyography in stick insect hind legs, which are critical to propel the body and stabilize it above ground during level walking (see Chapter 2). I found that kinematics including leg joint angles and body height varied little across walking conditions (Figure 4.2). At the same time, dynamics revealed substantial changes in mechanical demand (Figure 4.3). During downhill walking, for example, horizontal leg forces and torques at the ThC and FTi joints reversed in sign. At the ThC joint, the altered mechanical demand was met by adjustments in timing and magnitude of protractor and retractor muscle activity (Figure 4.4). Adjustments occurred primarily in the first half of stance, immediately after the touch-down of the leg. When insects transitioned from level to incline walking, the characteristic adjustments in muscle activity were present in the first step of the hind leg on the incline, but not in the steps preceding the transition (Figure 4.5). These findings confirm that walking under natural load conditions requires a highly flexible activation of leg muscles at the ThC joint, as hypothesized in Chapter 2. Because changes in leg muscle activity were determined together with changes in kinematic and dynamic parameters, the findings also provide new insights into the underlying control.

As discussed in Chapter 4, one interpretation is that stick insects do not use distinct, inclination-specific motor programs during walking, but instead adjust leg muscle activity on a step-by-step basis so as to minimize changes in kinematics under different mechanical demands. This interpretation is based on two findings. First, protractor and retractor activity was adjusted primarily during the first half of stance and with the first step of the leg on the incline, suggesting a reactive, step-by-step control mechanism. Second, kinematics changed comparatively little across walking conditions, suggesting that kinematic parameters are being controlled. In a kinematic control scheme, muscle activation could depend on the mismatch between the actual and a desired, referent kinematic pattern. Any mismatch due to altered mechanical conditions could be determined based on signals from leg proprioceptors, such as hair plates and chordotonal organs. In support of a kinematic control scheme, previous studies showed that walking stick insects compensate for perturbations of body height and body tilt (Cruse 1976a; Cruse et al. 1993; Diederich et al. 2002). Whether such a control scheme could be implemented entirely in the thoracic nerve cord or whether it would require input from the brain remains an open question. However, incline walking does not seem to require descending inputs from the brain that mediate distinct kinematic patterns, as suggested for turning (Gruhn et al. 2016; Martin et al. 2015) and obstacle climbing (Schütz and Dürr 2011; Watson et al. 2002a; Watson et al. 2002b). The torque calculations also suggest that load feedback from campaniform sensilla on the trochanter (Hofmann and Bässler 1982; Schmitz 1993) could contribute to control, because the mechanical loads acting at

the ThC joint differed substantially across walking conditions. However, based on previously described reflex effects of these campaniform sensilla (Akay et al. 2004; Akay et al. 2007; Schmitz 1993), simple load reflexes appeared to be insufficient to account for the observed changes in leg muscle activity.

5.2 The challenge of causality

The findings of the present thesis illustrate that detailed biomechanical analyses are a powerful complementary tool for identifying behaviorally-relevant sensory signals and control mechanisms during walking. However, in interpreting these findings, it is important to keep in mind that any inferences about control are indirect. The coordination mechanism studied in Chapter 3 is a good example. The results indicate that the unloading of the leg toward the end of stance is sufficiently strong to reverse the activation of two groups of campaniform sensilla on the dorsal trochanter. The changes in muscle activity that follow the onset of unloading and later lead to the leg's stance-to-swing transition agree with the known motor effects of these campaniform sensilla. Collectively, these and previous findings suggest that load feedback from campaniform sensilla promoted the stance-to-swing transition. However, the findings do not provide direct, causal evidence. Unfortunately, providing such causal evidence in a sensorimotor control task like walking, which relies on the interaction of many control components (Figure 1.1), is challenging.

With respect to the coordination mechanism studied in Chapter 3, one might naively assume that ablation of the campaniform sensilla in question should provide causal evidence. Figure 5.1 shows an example of such an ablation for one of the animals tested in Chapter 3. The results indicate that ablations will not have an obvious, qualitative effect during walking that is easy to interpret. After the ablation, the leg still lifts into swing, and the change from leg depressor (stance) to leg levator (swing) muscle activity still occurs around the onset of unloading (Figure 5.1D), as seen in intact animals. On second thought, this is not surprising. The time of unloading is correlated with the touch-down of the ipsilateral posterior leg, an event that is likely signaled between legs via neural pathways (Borgmann et al. 2009; Brunn and Dean 1994; Dean 1989; Laurent and Burrows 1989). In addition, recall that insect legs are equipped with several types of mechanoreceptors (Sections 1.3.4 and 1.5.2). Many of them will be co-activated during natural movements and potentially signal complementary information (Bräunig and Hustert 1985; Cruse et al. 1984). Depressor and levator muscle activity, for example, may be influenced by feedback from campaniform sensilla on the femur, tibia and tarsus (Zill et al. 2011; Zill et al. 2015; Zill et al. 2017b), hair plates

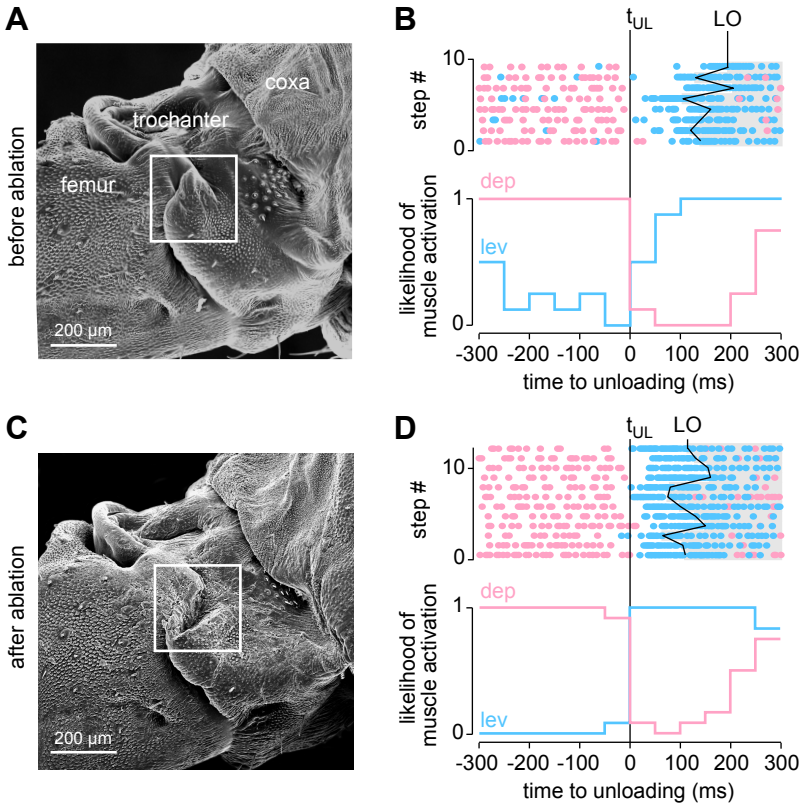

Figure 5.1: Effects of campaniform sensilla ablation on muscle activities
(**A**,**C**) Dorsal trochanter of two stick insect right middle legs before (**A**) and after (**C**) ablation of campaniform sensilla groups G3 and G4 (white box) with a razor blade. (**B**,**D**) Activity of the levator (light blue) and depressor (light red) trochanteris muscles of a right middle leg before (**B**) and after (**D**) campaniform sensilla ablation. Dots indicate muscle spikes detected based on EMG amplitude. t_{UL}, onset of unloading; LO, lift-off of the leg. See Figure 3.3 and Chapter 3 for details. **B**–**D** are from one of the animals tested in Chapter 3.

at the coxa-trochanter joint (Schmitz 1986; Wendler 1964), strand receptors in the coxa (Schöwerling 1992), and the femoral chordotonal organ (Bucher et al. 2003; Hess and Büschges 1999) (Figure 1.6). All of the above likely confound the effects of specific sensory ablations in freely walking animals and complicate the interpretation of small variations in muscle activity like those seen in the example recordings in Figure 5.1. In other words, demonstrating a causal contribution of a sensory mechanism by means of ablation is difficult if the mechanism is not necessary and can be compensated for.

Because ablation of individual mechanoreceptors usually has little or no effect on walking (reviewed in Delcomyn 1985), other approaches have been used to probe causality. One approach is to eliminate feedback from other mechanoreceptors. For example, Noah et al. (2004b) denervated the cockroach hind leg in the femur, thereby eliminating feedback from distal leg mechanoreceptors. The authors showed that muscle activity in the stump was coordinated when the leg was pressed against the substrate, suggesting the feedback from proximal mechanoreceptors is sufficient. Similar results

were obtained in other insects when distal parts of a leg were replaced by a prosthesis (Macmillan and Kien 1983; Wendler 1965). Although it is tempting to conclude that campaniform sensilla like the ones on the trochanter mediate this coordination, the interpretation is again complicated by the many other proximal mechanoreceptors remaining intact, for example strand receptors or chordotonal organs associated with the coxa. It would be worthwhile to test whether ablation of campaniform sensilla has a clear effect in these animals.

Another approach is to stimulate mechanoreceptors artificially. The rationale is that incorrectly timed or artificially strong sensory input provides a stimulus that the nervous system cannot ignore. The resulting behavioral effects should then indicate how the specific sensory input is used. Early investigations included continuous mechanical and intermittent electrical stimulation of mechanoreceptors (reviewed in Delcomyn 1985). In a classic experiment, Bässler (1977) placed a small clamp on the stick insect trochanter. With the clamp on, the leg moved to a posterior position during walking but did not lift into swing, presumably because campaniform sensilla on the trochanter continuously signaled that the leg is under load. Unfortunately, many of these early investigations suffered from stimulating more than a single type of leg mechanoreceptor. Bässler (1977) tackled this issue by demonstrating that the leg was able to step normally with the clamp after ablation of the campaniform sensilla. To my knowledge, this is the only causal evidence that campaniform sensilla contribute to timing the stance-to-swing transition. It would be worthwhile to revisit Bässler's classic experiment and confirm and extend his results with the biomechanical techniques used in this thesis.

A limitation of surgical ablation and electrical stimulation is that these methods can only be applied to a few accessible mechanoreceptors. New genetic tools might help to address this limitation (reviewed in Tuthill and Wilson 2016a). For example, the fruit fly *Drosophila* can be genetically engineered so that specific neurons can be silenced or activated by light and other methods (reviewed in Waddell et al. 2015). A recent study identified fly mutants that permit manipulations of different types of leg mechanoreceptors: tactile hairs, hair plates, chordotonal organs and campaniform sensilla (Tuthill and Wilson 2016b). These sorts of mutants are already being used to study the role of leg mechanoreceptors in walking control by silencing them (e.g., Mendes et al. 2013; Mendes et al. 2014). In the future, genetic tools should permit manipulations of leg mechanoreceptors during walking that cannot be easily manipulated using the traditional approaches mentioned above. Genome-editing strategies like CRISPR/Cas9 might permit the use of these tools also in larger insects (Chen et al. 2016), which are more amenable to detailed biomechanical analyses.

Despite these advances, it is questionable whether the contribution of sensory

feedback can be fully understood using experimental approaches alone. The complexity of walking control will likely require complementary approaches including simulations and robotics (e.g., Buschmann et al. 2015; Dürr et al. 2004; Pearson et al. 2006). With respect to the load-based coordination mechanism presented in Chapter 3, simulation and robotic studies have demonstrated that feedback from load sensors on the legs is in principle sufficient to coordinate neighboring legs and generate different stepping patterns (Aoi et al. 2012; Ekeberg and Pearson 2005; Owaki et al. 2013; Owaki and Ishiguro 2017). Modeling campaniform sensilla as strain gauges on simulated or robotic insect-like legs may provide further insights into their function during walking.

All of the above considerations emphasize the broader point that insights from multiple approaches and different species will be required to address the challenge of causality in a complex sensorimotor control task such as walking.

5.3 Future biomechanical experiments

Having established a setup for simultaneously analyzing joint kinematics, joint torques and muscle activity in stick insects walking freely on level ground and up and down inclines clears the way for valuable future experiments. One interesting experiment would be to probe the load-based coordination mechanism studied in Chapter 3 in different walking conditions. The mechanism is based on strong and reliable changes in torques at the CTr joint. Are torques at the CTr joint only suitable for load-based coordination during level walking? Preliminary example data suggest that the mechanism could also work on $\pm 45^{\circ}$ inclines (Figure 5.2). At least two prerequisites are met in middle legs: torques at the CTr joint are sufficiently high and decrease rapidly soon after the touch-down of the ipsilateral posterior leg, independent of the inclination of the walkway. Repeating the full experiment presented in Chapter 3 including electromyography and mechanical simulation on different inclines would not solve the challenge of causality discussed above, but it would indicate the robustness of the mechanism and thereby help to understand its potential relevance.

Another interesting experiment would be to study load-dependent changes in muscle activity when insects transition from level to incline walking in detail. The example recordings shown in Chapter 4 (Figure 4.5) indicate that muscle activity is adjusted with the first step of the leg on the incline, but not in anticipation. A quantitative comparison of steps before, during and after the transition would reveal whether muscle activity is adjusted directly or in a gradual fashion. A useful extension in this context would be to record the activity of other leg muscles. For example, the results of Chapters 2 and 4 suggest that the FTi joint could serve a stabilizing function similar to the ThC joint. Is

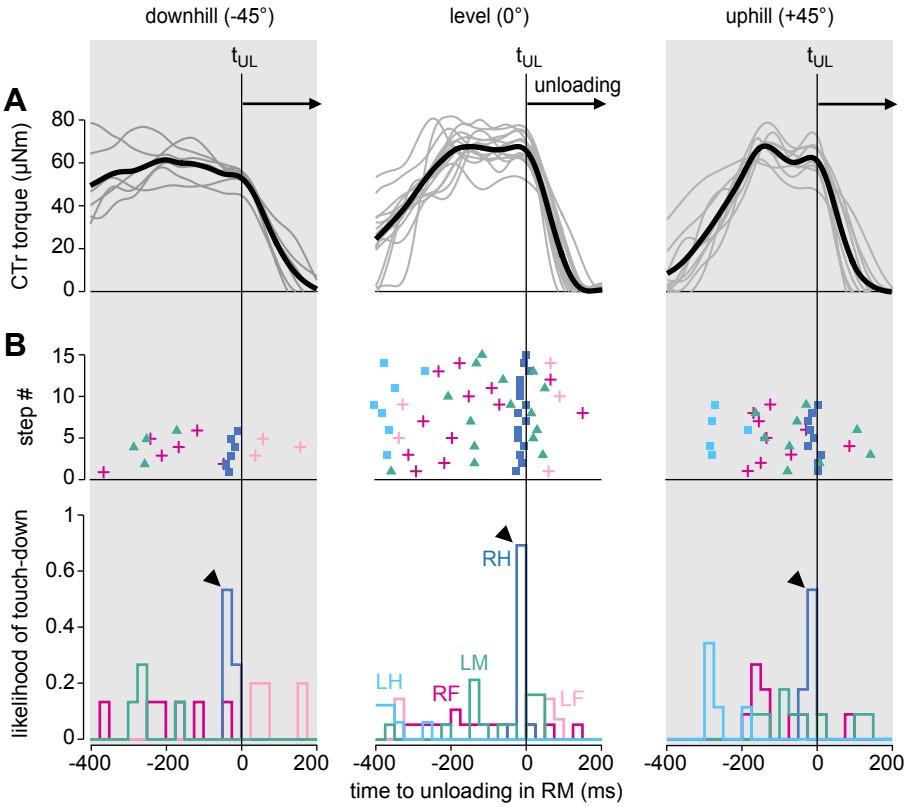

Figure 5.2: Leg unloading is correlated with the touch-down of the posterior neighboring leg during level and incline walking
(**A**) Torque at the CTr joint of the right middle (RM) leg relative to the onset of unloading, t_{UL}, during level (0°) and uphill/downhill (±45°) walking. Bold black lines show the grand mean of all steps, gray lines show individual steps. Torques decrease rapidly toward the end of stance in all conditions. Note that steps in the downhill condition have longer stance phases than steps in the other conditions in this example dataset. (**B**) Touch-down events of all legs (top) and likelihood of touch-down per leg (bottom) relative to t_{UL}. Touch-downs of the right hind (RH) leg reliably precede t_{UL} in the middle leg with short latency in all conditions (arrowheads). RF, right front leg; LF, left front leg; LM, left middle leg; LH, left hind leg. See also Figures 3.2 and 3.3. Example data are from animals tested in Chapter 4.

activity of the flexor and extensor tibiae muscles adjusted similarly to that of the protractor and retractor coxae muscles? Does it support the idea of a kinematic control strategy? How are changes in muscle activity in different legs correlated with different mechanical demands to propel and stabilize the body? The setup established in this thesis could be used to address these questions. As noted in Section 1.3.3, one potential complication when recording activity of the flexor muscle is that its multi-terminal innervation might require multiple recording sites (see also Page et al. 2008). Moreover, pilot recordings of the extensor muscle showed substantial cross-talk from the flexor muscle. However, if the cross-talk can be edited out during post-processing, extensor muscle recordings would allow to study the specific roles of the slow and the fast motor neuron in adjusting motor output to changing mechanical demands during walking.

In designing these and other experiments, it might be beneficial to revisit the meth-

ods used in this thesis. For example, the tethered EMG backpack used in Chapters 3 and 4 was appropriate for recording muscle activity during walking. However, the pilot experiments on the transition from level to incline walking indicated that it could restrict the animal in more complex scenarios like obstacle climbing. For these scenarios, a wireless telemetry backpack might be more appropriate (Sato and Maharbiz 2010), although it will likely be heavier than the lightweight 50 mg (approx. 5% body weight) backpack used here. Experiments focusing on control tasks other than the stance phase of walking might also benefit from re-examining the anatomically complex ThC joint and considering inertial and gravitational effects for torque calculations (Section 2.6.1). The ThC joint might not be approximated well with a single degree of freedom in tasks requiring more mobility, such as climbing (Schütz and Dürr 2011; Watson et al. 2002b). Including inertial and gravitational effects would allow studying joint torques when ground reaction force information is not available, such as during swing or other targeting movements (e.g., Zakotnik et al. 2006).

5.4 Concluding remarks

Walking is a complex sensorimotor control task that we are just beginning to understand in detail. As outlined in Chapter 1, a major challenge is to understand how sensory feedback from different types of leg mechanoreceptors, descending inputs from the brain, signals from pattern generating circuits in the lower central nervous system, and properties of the musculoskeletal system interact during natural locomotion—when the body mechanically interacts with the environment. The present thesis demonstrates that detailed biomechanical analyses of freely walking insects are a powerful complementary tool to study sensorimotor control of walking. Combining 3D motion capture, ground reaction force measurements and electromyography in freely walking stick insects revealed a previously unknown mechanism to control propulsion (Chapter 2), showed how inter-leg coordination can emerge from local load feedback and mechanical coupling of legs through the ground (Chapter 3), and suggested a reactive mechanism for adjusting leg muscle activity to changing mechanical demands during walking (Chapter 4). Due to their comparatively large size and well-studied anatomy and physiology, stick insects are an attractive model system for these biomechanical analyses. However, with ever advancing methods for markerless tracking (Mathis et al. 2018), miniaturizations of force plates (Reinhardt and Blickhan 2014a), and new techniques for monitoring muscle activity (Lindsay et al. 2017), the biomechanical analyses presented in this thesis for stick insects might soon be feasible in other insects, including smaller insects like ants

and fruit flies. Detailed biomechanical analyses in other insects will help determine to what extent the control mechanisms proposed in Chapters 2-4 for stick insects can be generalized. In turn, a better understanding of how insects control natural locomotion may inspire the design of agile robots that are capable of walking in the real world, including the Teutoburg Forest.

5.5 References

Akay, T., Haehn, S., Schmitz, J., and Büschges, A. (2004). Signals from load sensors underlie interjoint coordination during stepping movements of the stick insect leg. *J. Neurophysiol.* 92, 42–51.

Akay, T., Ludwar, B. C., Göritz, M. L., Schmitz, J., and Büschges, A. (2007). Segment specificity of load signal processing depends on walking direction in the stick insect leg muscle control system. *J. Neurosci.* 27, 3285–3294.

Aoi, S., Ogihara, N., Funato, T., and Tsuchiya, K. (2012). Sensory regulation of stance-to-swing transition in generation of adaptive human walking: a simulation study. *Rob. Auton. Syst.* 60, 685–691.

Balint, C. N. and Dickinson, M. H. (2001). The correlation between wing kinematics and steering muscle activity in the blowfly *Calliphora vicina*. *J. Exp. Biol.* 204, 4213–4226.

Bartling, C. and Schmitz, J. (2000). Reaction to disturbances of a walking leg during stance. *J. Exp. Biol.* 203, 1211–1223.

Bässler, U. (1977). Sensory control of leg movement in the stick insect *Carausius morosus*. *Biol. Cybern.* 25, 61–72.

Bender, J. A., Simpson, E. M., and Ritzmann, R. E. (2010). Computer-assisted 3D kinematic analysis of all leg joints in walking insects. *PLoS One* 5, e13617.

Borgmann, A., Hooper, S. L., and Büschges, A. (2009). Sensory feedback induced by front-leg stepping entrains the activity of central pattern generators in caudal segments of the stick insect walking system. *J. Neurosci.* 29, 2972–2983.

Borgmann, A. and Büschges, A. (2015). Insect motor control: methodological advances, descending control and inter-leg coordination on the move. *Curr. Opin. Neurobiol.* 33, 8–15.

Bräunig, P. and Hustert, R. (1985). Actions and interactions of proprioceptors of the locust hind leg coxo-trochanteral joint. I. Afferent responses in relation to joint position and movement. *J. Comp. Physiol. A.* 157, 73–82.

Brunn, D. E. and Dean, J. (1994). Intersegmental and local interneurons in the metathorax of the stick insect *Carausius morosus* that monitor middle leg position. *J. Neurophysiol.* 72, 1208–1219.

Bucher, D., Akay, T., DiCaprio, R. A., and Büschges, A. (2003). Interjoint coordination in the stick insect leg-control system: the role of positional signaling. *J. Neurophysiol.* 89, 1245–1255.

Buschmann, T., Ewald, A., Twickel, A. von, and Büschges, A. (2015). Controlling legs for locomotion - insights from robotics and neurobiology. *Bioinspir. Biomim.* 10, 041001.

Chen, L., Wang, G., Zhu, Y.-N., Xiang, H., and Wang, W. (2016). Advances and perspectives in the application of CRISPR/Cas9 in insects. *Zool. Res.* 37, 136–143.

Cruse, H. (1976a). The control of body position in the stick insect (*Carausius morosus*), when walking over uneven surfaces. *Biol. Cybern.* 24, 25–33.

Cruse, H. (1976b). The function of the legs in the free walking stick insect, *Carausius morosus*. *J. Comp. Physiol. A* 112, 235–262.

Cruse, H. (1990). What mechanisms coordinate leg movement in walking arthropods? *Trends Neurosci.* 13, 15–21.

Cruse, H., Dean, J., and Suilmann, M. (1984). The contributions of diverse sense organs to the control of leg movement by a walking insect. *J. Comp. Physiol. A* 154, 695–705.

Cruse, H., Kindermann, T., Schumm, M., Dean, J., and Schmitz, J. (1998). Walknet - a biologically inspired network to control six-legged walking. *Neural Netw.* 11, 1435–1447.

Cruse, H., Schmitz, J., Braun, U., and Schweins, A. (1993). Control of body height in a stick insect walking on a treadwheel. *J. Exp. Biol.* 181, 141–155.

Dean, J. (1989). Leg coordination in the stick insect *Carausius morosus*: effects of cutting throacic connectives. *J. Exp. Biol.* 145, 103–131.

Delcomyn, F. (1985). Factors regulating insect walking. *Annu. Rev. Entomol.* 30, 239–256.

Delcomyn, F. and Usherwood, P. N. R. (1973). Motor activity during walking in the cockroach *Periplaneta americana*. I. Free walking. *J. Exp. Biol.* 59, 629–642.

Diederich, B., Schumm, M., and Cruse, H. (2002). Stick insects walking along inclined surfaces. *Integr. Comp. Biol.* 42, 165–173.

Donelan, J. M., McVea, D. A., and Pearson, K. G. (2009). Force regulation of ankle extensor muscle activity in freely walking cats. *J. Neurophysiol.* 101, 360–371.

Duch, C. and Pflüger, H. J. (1995). Motor patterns for horizontal and upside down walking and vertical climbing in the locust. *J. Exp. Biol.* 198, 1963–1976.

Dürr, V., Schmitz, J., and Cruse, H. (2004). Behaviour-based modelling of hexapod locomotion: linking biology and technical application. *Arthropod Struct. Dev.* 33, 237–250.

Ekeberg, Ö. and Pearson, K. G. (2005). Computer simulation of stepping in the hind legs of the cat: an examination of mechanisms regulating the stance-to-swing transition. *J. Neurophysiol.* 94, 4256–4268.

Full, R. J. and Tu, M. S. (1991). Mechanics of a rapid running insect: two-, four-, and six-legged locomotion. *J. Exp. Biol.* 156, 215–231.

Gnatzy, W., Grünert, U., and Bender, M. (1987). Campaniform sensilla of *Calliphora vicina* (Insecta, Diptera). I. Topography. *Zoomorphology* 106, 312–319.

Goldman, D. I., Chen, T. S., Dudek, D. M., and Full, R. J. (2006). Dynamics of rapid vertical climbing in cockroaches reveals a template. *J. Exp. Biol.* 209, 2990–3000.

Gregor, R. J., Smith, D. W., and Prilutsky, B. I. (2006). Mechanics of slope walking in the cat: quantification of muscle load, length change, and ankle extensor EMG patterns. *J. Neurophysiol.* 95, 1397–1409.

Gruhn, M., Rosenbaum, P., Bockemühl, T., and Büschges, A. (2016). Body side-specific control of motor activity during turning in a walking animal. *eLife* 5, e13799.

Harris, J. and Ghiradella, H. (1980). The forces exerted on the substrate by walking and stationary crickets. *J. Exp. Biol.* 85, 263–279.

Hess, D. and Büschges, A. (1999). Role of proprioceptive signals from an insect femur-tibia joint in patterning motoneuronal activity of an adjacent leg joint. *J. Neurophysiol.* 81, 1856–1865.

Hofmann, T. and Bässler, U. (1982). Anatomy and physiology of trochanteral campaniform sensilla in the stick insect, *Cuniculina impigra*. *Physiol. Entomol.* 7, 413–426.

Hustert, R., Pflüger, H. J., and Bräunig, P. (1981). Distribution and specific central projections of mechanoreceptors in the thorax and proximal leg joints of locusts. III. The external mechanoreceptors: the campaniform sensilla. *Cell Tissue Res.* 216, 97–111.

Kram, R., Wong, B., and Full, R. J. (1997). Three-dimensional kinematics and limb kinetic energy of running cockroaches. *J. Exp. Biol.* 200, 1919–1929.

Larsen, G. S., Frazier, S. F., Fish, S. E., and Zill, S. N. (1995). Effects of load inversion in cockroach walking. *J. Comp. Physiol. A* 176, 229–238.

Laurent, G. and Burrows, M. (1989). Intersegmental interneurons can control the gain of reflexes in adjacent segments of the locust by their action on nonspiking local interneurons. *J. Neurosci.* 9, 3030–3039.

Lay, A. N., Hass, C. J., and Gregor, R. J. (2006). The effects of sloped surfaces on locomotion: a kinematic and kinetic analysis. *J. Biomech.* 39, 1621–1628.

Lay, A. N., Hass, C. J., Nichols, R. T., and Gregor, R. J. (2007). The effects of sloped surfaces on locomotion: an electromyographic analysis. *J. Biomech.* 40, 1276–1285.

Lindsay, T., Sustar, A., and Dickinson, M. (2017). The function and organization of the motor system controlling flight maneuvers in flies. *Curr. Biol.* 27, 345–358.

Macmillan, D. L. and Kien, J. (1983). Intra- and intersegmental pathways active during walking in the locust. *Proc. R. Soc. B* 218, 287–308.

Martin, J. P., Guo, P., Mu, L., Harley, C. M., and Ritzmann, R. E. (2015). Central-complex control of movement in the freely walking cockroach. *Curr. Biol.* 25, 2795–2803.

Mathis, A., Mamidanna, P., Abe, T., Cury, K. M., Murthy, V. N., Mathis, M. W., and Bethge, M. (2018). Markerless tracking of user-defined features with deep learning. *arXiv* 1804.03142.

Mendes, C. S., Bartos, I., Akay, T., Márka, S., and Mann, R. S. (2013). Quantification of gait parameters in freely walking wild type and sensory deprived *Drosophila melanogaster*. *eLife* 2, e00231.

Mendes, C. S., Rajendren, S. V., Bartos, I., Márka, S., and Mann, R. S. (2014). Kinematic responses to changes in walking orientation and gravitational load in *Drosophila melanogaster*. *PLoS One* 9, e109204.

Merritt, D. J. and Murphey, R. K. (1992). Projections of leg proprioceptors within the CNS of the fly *Phormia* in relation to the generalized insect ganglion. *J. Comp. Neurol.* 322, 16–34.

Noah, J. A., Quimby, L., Frazier, S. F., and Zill, S. N. (2004a). Sensing the effect of body load in legs: responses of tibial campaniform sensilla to forces applied to the thorax in freely standing cockroaches. *J. Comp. Physiol. A* 190, 201–215.

Noah, J. A., Quimby, L., Frazier, S. F., and Zill, S. N. (2004b). Walking on a 'peg leg': extensor muscle activities and sensory feedback after distal leg denervation in cockroaches. *J. Comp. Physiol. A* 190, 217–231.

Owaki, D., Kano, T., Nagasawa, K., Tero, A., and Ishiguro, A. (2013). Simple robot suggests physical interlimb communication is essential for quadruped walking. *J. R. Soc. Interface* 10, 20120669.

Owaki, D. and Ishiguro, A. (2017). A quadruped robot exhibiting spontaneous gait transitions from walking to trotting to galloping. *Sci. Rep.* 7, 277.

Page, K. L., Zakotnik, J., Dürr, V., and Matheson, T. (2008). Motor control of aimed limb movements in an insect. *J. Neurophysiol.* 99, 484–499.

Pearson, K. G., Ekeberg, Ö., and Büschges, A. (2006). Assessing sensory function in locomotor systems using neuro-mechanical simulations. *Trends Neurosci.* 29, 625–631.

Reinhardt, L. and Blickhan, R. (2014a). Ultra-miniature force plate for measuring triaxial forces in the micronewton range. *J. Exp. Biol.* 217, 704–710.

Reinhardt, L. and Blickhan, R. (2014b). Level locomotion in wood ants: evidence for grounded running. *J. Exp. Biol.* 217, 2358–2370.

Rosenbaum, P., Wosnitza, A., Büschges, A., and Gruhn, M. (2010). Activity patterns and timing of muscle activity in the forward walking and backward walking stick insect *Carausius morosus*. *J. Neurophysiol.* 104, 1681–1695.

Sato, H. and Maharbiz, M. M. (2010). Recent developments in the remote radio control of insect flight. *Front. Neurosci.* 4, 199.

Schilling, M., Hoinville, T., Schmitz, J., and Cruse, H. (2013). Walknet, a bio-inspired controller for hexapod walking. *Biol. Cybern.* 107, 397–419.

Schmitz, J. (1986). Properties of the feedback system controlling the coxa-trochanter joint in the stick insect *Carausius morosus*. *Biol. Cybern.* 55, 35–42.

Schmitz, J. (1993). Load-compensating reactions in the proximal leg joints of stick insects during standing and walking. *J. Exp. Biol.* 33, 15–33.

Schöwerling, H. (1992). Untersuchungen zur Reflexaktivierung der Levator-Trochanteris Muskeln der Stabheuschrecke *Carausius mororsus*, Br. Thesis. Bielefeld University.

Schütz, C. and Dürr, V. (2011). Active tactile exploration for adaptive locomotion in the stick insect. *Phil. Trans. R. Soc. B* 366, 2996–3005.

Seidl, T. and Wehner, R. (2008). Walking on inclines: how do desert ants monitor slope and step length. *Front. Zool.* 5, 8.

Spirito, C. P. and Mushrush, D. L. (1979). Interlimb coordination during slow walking in the cockroach. I. Effects of substrate alterations. *J. Exp. Biol.* 79, 233–243.

Sutton, G. P. and Burrows, M. (2008). The mechanics of elevation control in locust jumping. *J. Comp. Physiol. A* 194, 557–563.

Sutton, G. P. and Burrows, M. (2010). The mechanics of azimuth control in jumping by froghopper insects. *J. Exp. Biol.* 213, 1406–1416.

Theunissen, L. M., Bekemeier, H. H., and Dürr, V. (2015). Comparative whole-body kinematics of closely related insect species with different body morphology. *J. Exp. Biol.* 218, 340–352.

Tuthill, J. C. and Wilson, R. I. (2016a). Mechanosensation and adaptive motor control in insects. *Curr. Biol.* 27, R1022–R1038.

Tuthill, J. C. and Wilson, R. I. (2016b). Parallel transformation of tactile signals in central circuits of *Drosophila*. *Cell* 164, 1046–1059.

Waddell, S., Owald, D., Lin, S., and Waddell, S. (2015). Light, heat, action: neural control of fruit fly behaviour. *Phil. Trans. R. Soc. B* 370, 20140211.

Walker, S., Schwyn, D. A., Mokso, R., Wicklein, M., Müller, T., Doube, M., Stampanoni, M., Krapp, H. G., and Taylor, G. K. (2014). In vivo time-resolved microtomography reveals the mechanics of the blowfly flight motor. *PLoS Biol.* 12, e1001823.

Watson, J. T. and Ritzmann, R. E. (1998). Leg kinematics and muscle activity during treadmill running in the cockroch, *Blaberus discoidalis*: I. Slow running. *J. Comp. Physiol. A* 182, 11–22.

Watson, J. T., Ritzmann, R. E., and Pollack, A. J. (2002a). Control of climbing behavior in the cockroach, *Blaberus discoidalis*. II. Motor activities associated with joint movement. *J. Comp. Physiol. A.* 188, 55–69.

Watson, J. T., Ritzmann, R. E., Zill, S. N., and Pollack, A. J. (2002b). Control of climbing behavior in the cockroach, *Blaberus discoidalis*. I. Kinematics. *J. Comp. Physiol. A.* 188, 39–53.

Wendler, G. (1964). Laufen und Stehen der Stabheuschrecke *Carausius morosus*: Sinnesborstenfelder in den Beingelenken als Glieder von Regelkreisen. *Z. Vgl. Physiol.* 48, 198–250.

Wendler, G. (1965). The co-ordination of walking movements in arthropods. *Symp. Soc. Exp. Biol.* 20, 229–249.

Wöhrl, T., Reinhardt, L., and Blickhan, R. (2017). Propulsion in hexapod locomotion: how do desert ants traverse slopes? *J. Exp. Biol.* 220, 1618–1625.

Zakotnik, J., Matheson, T., and Dürr, V. (2006). Co-contraction and passive forces facilitate load compensation of aimed limb movements. *J. Neurosci.* 26, 4995–5007.

Zill, S. N., Büschges, A., and Schmitz, J. (2011). Encoding of force increases and decreases by tibial campaniform sensilla in the stick insect, *Carausius morosus*. *J. Comp. Physiol. A* 197, 851–867.

Zill, S. N., Chaudhry, S. S., Dallmann, C. J., Hoinville, T., Schmitz, J., and Büschges, A. (2017a). Generation and utilization of sensory signals encoding force decreases in insect legs. *Proceedings of the 47th Annual Meeting of the Society for Neuroscience*. Washington, D.C.

Zill, S. N., Chaudhry, S., Büschges, A., and Schmitz, J. (2015). Force feedback reinforces muscle synergies in insect legs. *Arthropod Struct. Dev.* 44, 541–553.

Zill, S. N., Keller, B. R., and Duke, E. R. (2009). Sensory signals of unloading in one leg follow stance onset in another leg: transfer of load and emergent coordination in cockroach walking. *J. Neurophysiol.* 101, 2297–2304.

Zill, S. N., Neff, D., Chaudhry, S., Exter, A., Schmitz, J., and Büschges, A. (2017b). Effects of force detecting sense organs on muscle synergies are correlated with their response properties. *Arthropod Struct. Dev.* 46, 564–578.

Zill, S. N., Ridgel, A. L., DiCaprio, R. A., and Frazier, S. F. (1999). Load signalling by cockroach trochanteral campaniform sensilla. *Brain Res.* 822, 271–275.

Zill, S. N., Schmitz, J., Chaudhry, S., and Büschges, A. (2012). Force encoding in stick insect legs delineates a reference frame for motor control. *J. Neurophysiol.* 108, 1453–1472.

Erklärung

Hiermit versichere ich, dass ich die vorliegende Dissertation selbstständig angefertigt, keine Textabschnitte von Dritten oder eigener Prüfungsarbeiten ohne Kennzeichnung übernommen und alle von mir benutzten Hilfsmittel und Quellen in meiner Arbeit angegeben habe. Dritte haben weder unmittelbar noch mittelbar geldwerte Leistungen von mir für Vermittlungstätigkeiten oder für Arbeiten erhalten, die im Zusammenhang mit dem Inhalt der vorgelegten Dissertation stehen. Ich habe die Dissertation noch nicht als Prüfungsarbeit für eine staatliche oder andere wissenschaftliche Prüfung eingereicht. Ebenso habe ich die Arbeit zuvor weder im Inland noch im Ausland in gleicher oder ähnlicher Form bei einer anderen Hochschule als Dissertation eingereicht. Die geltende Promotionsordnung der Fakultät ist mir bekannt.

Chris J. Dallmann